5-2013

Safety Aware Platooning of Automated Electric Transport Vehicles

Spencer Scott Jackson
Utah State University

SAFETY AWARE PLATOONING OF AUTOMATED ELECTRIC TRANSPORT VEHICLES

by

Spencer Scott Jackson

A thesis submitted in partial fulfillment
of the requirements for the degree

of

MASTER OF SCIENCE

in

Electrical Engineering

Approved:

Dr. Chris Winstead Major Professor	Dr. Don Cripps Committee Member
Dr. YangQuan Chen Committee Member	Dr. Kevin Heaslip Committee Member

Dr. Mark R. McLellan
Vice President for Research and
Dean of the School of Graduate Studies

UTAH STATE UNIVERSITY
Logan, Utah

2013

Abstract

Safety Aware Platooning of Automated Electric Transport Vehicles

by

Spencer Scott Jackson, Master of Science

Utah State University, 2013

Major Professor: Dr. Chris Winstead
Department: Electrical and Computer Engineering

Automated Electric Transport (AET) is a promising variation of highway automation, a topic of interest for decades. Whereas previously researched schemes have been largely developed around the internal combustion engine vehicle, AET will use purely electric vechicles. In the thesis, several models of electric vehicles are developed and applied to platooning situations. These models will be created with the goal of evaluating how platooning safety can be increased, especially with regard to the emergency brake scenario. The results provide insight to the effects of variance in a homogeneous vehicle system. The models will also be used by other researchers in the project for system-level analysis.

(139 pages)

Public Abstract

Safety Aware Platooning of Automated Electric Transport Vehicles

by

Spencer Scott Jackson, Master of Science

Utah State University, 2013

Major Professor: Dr. Chris Winstead
Department: Electrical and Computer Engineering

Safety is a paramount concern when considering implementation of an automated highway where computers control the vehicles. Even with computer-fast reaction time there is inevitably some delay and if vehicles do not follow at safe distances, emergency braking maneuvers can cause dangerous collisions. This research investigates situations that might make automated vehicles have dangerous collisions and what standards the system design must hold to keep passengers safe.

To my brilliant wife, and our two new sons...

Acknowledgments

I would like to give thanks to Dr. Chris Winstead who effectively served as a foster advisor when Dr. Ren left, and Drs. Y. Chen, Heaslip, and Cripps for their contributions. To Dr. Ren I owe joining the Automated Electric Transport project in the first place. I must also mention Dr. Scott Budge who did not remain on my committee but did offer helpful advice at an early point of my research.

I would also like to acknowledge the AET group, previous and current, for all their interesting ideas, discussions, presentations, and information shared: Drs. A. Chen and Gerdes, Dan Stuart, Megan Emmons, Sarawut Janswan, Pooja Kavathekar, Derek Freckleton, Seungkyu Ryu, David Cornelio, Jacob Vanfleet, and especially James Fishelson for sparking my curiosity to make a Matlab model that generates H-Δv curves.

Of course, special acknowledgments go to those who had a special part in completing my thesis, Rachel, Parker, and Porter....

Spencer Scott Jackson

Contents

List of Tables

List of Figures

Acronyms

ABS	Automatic Braking System
AET	Automated Electric Transport
DC	Direct Current
EMF	Electro-Motive Force
EV	Electric Vehicle
H-Δv curve	Difference in Velocity versus Initial Headway Curve
ICE	Internal Combustion Engine
KAIST	Korea Advanced Institute of Science and Technology
OLEV	On-Line Electric Vehicle
PAH	Preceding vehicle Acceleration with Headway
PATH	Partners for Advanced Transport and Highways
PI	Proportional and Integral
PID	Proportional, Intregral, and Derivative
RC	Resistor and Capacitor
SARTRE	SAfe Road TRains for the Environment
UHZ	Unsafe Headway Zone
USU	Utah State University
VMT	Vehicle Mile Travelled
WAD	Whiplash-Associated-Disorders

Chapter 1

Introduction

1.1 Highway Automation

As highway congestion increases in high-volume commuter areas, delays and accidents caused by human errors create frustrating costs to the individual, the environment, and to the local economy. Emissions from vehicles can have negative influence on local air conditions affecting both physical and mental health of residents and the environment as a whole. Dependence on foreign oil is detrimental to national economics. Various competing technologies are developing to reduce vehicle fossil fuel consumption and emissions including fuel cells, hybrid vehicles, fully electric vehicles (EVs), and others. These address the problems with internal combustion engine (ICE) vehicles' use of oil and emissions but do not offer any relief from traffic congestion. Various alternative forms of transportation and public transit are in development and use to help relieve delays, but these do not offer the performance and convenience of traditional automobiles. Unfortunately, highways create a sort of prisoner's dilemma: if everyone uses public transit, congestion is less and service gets better, but those who drive private vehicles get the benefit of convenience and often shorter travel time. If everyone drives private vehicles, congestion occurs and delays increase for all. In contrast, highway automation offers relief from both congestion and inconvenience by removing human errors from highway driving. This brings benefits of safety, energy efficiency, highway capacity, and convenience.

To most vehicle owners, an appealing factor for developing self-driving cars is freeing commuters from the menial task of driving, allowing drivers to become passengers, free to read, nap, enjoy media, or whatever they choose. Less obvious reasons include traffic congestion relief, benefits to the environment, and perhaps most importantly, safety.

1.1.1 Automation Benefits

In stopped traffic, ICEs idle, getting literally zero miles per gallon. Every ounce of emissions enters the atmosphere, wasted. Hybrid vehicles, such as the Toyota Prius, reduce this wasteful polluting through using electric motors during "stop-go" situations and rely on the addition of the combustion motor when higher torque is necessary. Even these high efficiency vehicles are not zero emissions as are pure EVs. When EVs are powered through clean energy generating mediums such as solar, wind, or nuclear power, they truly produce zero emissions. Automation of EVs has additional benefit of reducing the congestion that leads to inefficient stop-go behavior and could reduce total energy consumption of the highway system through careful vehicle and traffic control.

Traffic congestion is traditionally remedied through the addition of lanes. This method is effective but becomes difficult and expensive when urban areas are developed with insufficient space for expansion. Automation uses the existing space more efficiently, increasing density so more vehicles can travel on each lane. A major cause of inefficient use of lanes is delays due to accidents. Even minor incidents during rush hour traffic can cause delays that last for hours before traffic resumes normal flow. Hitchcock points out that over ninety percent of accidents on highways are the result of human error [1]. Even a reduction of incidents by half through automation would have great benefits to highway performance.

Finally, safety is one of the greatest motivating factors. While vehicle manufacturers continue to improve safety of vehicles such that accidents are not lethal, the sheer number of vehicles on the road and daily incidents make the automobile one of the leading killers in the United States [2]. Safety is improving: the number of deaths per vehicle mile traveled (VMT) has been steadily dropping for the past half-century. It was reported approximately forty thousand people died annually from vehicle collisions in 2007 [3], and the number dropped to around thirty-four-thousand in 2009 [4]. Currently, a fatality only occurs approximately once per two million VMT, and an injury every fifty thousand VMT. Freeways are actually safer than most other high-traffic roads [5]. By removing the human factor to driving, automation has great potential to increase safety.

Safety is the highest priority in highway automation design due to the potential for fatalities in event of a system failure. It is impossible to estimate the true cost of a loss of life. If the system is not safer than current roadways it is unlikely to be supported by users. In an automated highway the primary collision to be concerned with is the rear-end collision, since lane maneuvers can be very carefully controlled. The safe spacing for the vehicles in various maneuvers is determined by braking abilities of the vehicles, which limit the controllers. A vehicle able to brake instantaneously at any deceleration could be perfectly safe at any following distance. If the vehicle characteristics are set, safety is a trade-off with capacity, such that if the cars are following closely any delay or error is more likely to cause collision. Ultimately the "safest" system would have the vehicles following extremely far apart, which would reduce the capacity to unacceptable levels. The main objective is to improve both capacity and safety. Difficulty lies in control of the vehicle. Considering highway drivers currently do not follow at safe distances, safety alone is easy to improve upon, but at high capacity it is a challenging problem.

1.1.2 Connectivity and Automation

Part of the solution to the difficulty is through communication between vehicles. In traditional car following models the amount of time for perception and reaction are generally defined by some stochastic distribution. This has some application to automated vehicles, but the distributions have much less variance as computers and sensors are relatively fast and do not get distracted. If vehicles are connected through wireless communication, they can act cooperatively, such that the perception time is simply the time required for a vehicle to send a brake signal over the wireless network. By communicating a maneuver in advance cars can act synchronously such that both perception and reaction time for following vehicles are effectively zero. This allows vehicles to follow very closely, for large capacity gains.

Automation does not necessarily have high connectivity. The Google Car was able to travel thousands of miles with little or no human intervention based entirely on sensing and control. This sort of "free-agent" system design is robust since each vehicle is able to act independently; error does not propagate to other vehicles. Some current luxury vehicles

feature sensing-based intelligent cruise control, which is a stride toward automation. While it is clearly not a requirement for automation, inter-vehicle communication can have large benefits to capacity and safety. It does however impose certain issues. Security of the network must be maintained and consistently high data rates must be maintained if very high performance requires good communication. While these issues are important, they are only touched on by this research.

1.2 Platooning

One way to organize automated vehicles on the highway is in platoons — linear groups of consecutive vehicles acting in unison and traveling in close-following formation. This strategy puts vehicles within a platoon following very closely. This small intra-platoon separation allows for drafting which increases efficiency by reducing aerodynamic drag on following vehicles in the platoon. Platoons follow each other at a larger inter-platoon distance. This is illustrated in Figure 1.1. In this way platoons act like trains, but each car in the platoon is able to have a unique destination. Kanaris et al. [6] finds that while maintaining the same safety level, platooning has significantly higher capacities than highways using free agent systems whether free-agent vehicles had intercommunication or not. Platooning requires high connectivity and automation to be safe because intra-platoon following distances are so short.

Platooning was researched in depth by the National Automated Highway System Consortium (NAHSC) led by the Partners for Advanced Transit and Highways (PATH) group at University of California, Berkeley. Their thorough work of over 1000 publications and reports through the 1990s and early 2000s was toward retrofitting existing vehicles and developing strategies to implement automated highway platooning. PATH was able to achieve a real life platooning demo in 1997 [7–9] but they had some limitations due to the use of ICE

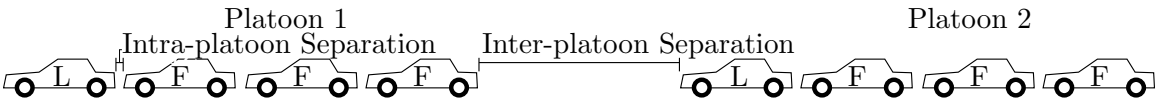

Fig. 1.1: Two platoons. L indicates the lead vehicle of the platoon, F a follower.

vehicless. The largest difficulty of the ICE vehicle is the rate limits and other nonlinearities in the engine and brakes. One such rate limit arises because of the inability of internal combustion engines (ICEs) to provide instantaneous torque. Generally the engine must rev to a higher speed when torque is needed, making a slower response to a step input. Similarly the hydraulic brakes introduce a pure time delay that make string stability degrade as platoon size grows. String stability requires that spacing errors decrease as they propagate down the platoon.

Many current groups are also researching platooning such as Safe Road Trains for the Environment (SARTRE), which forms platoons of intercommunicating vehicles using a manually driven cargo truck with a certified driver as the lead vehicle [10]. A similar work is Rheinisch-Westflische Technische University Aachen's project KONVOI, which focuses mainly on whole platoons of cargo trucks [11]. The Korea Advanced Institute of Science and Technology (KAIST) On-Line Electric Vehicles (OLEV) project is also currently researching related topics [12], though that group is focused primarily on electrification. In each of these projects, the vehicles are at least partly controlled by a computer rather than a driver. Excepting of OLEV these groups are using ICE vehicles.

Some promising improvements can be made by using EVs for platooning. Electrical motors have primary time constants of an order of magnitude smaller than a typical combustion engine. Brake by wire technology can offer higher performance to hydraulic brake systems or electromechanical brakes (EMBs) and regenerative braking can yield other performance improvements still [13]. Other technologies developed since PATH's work in the computing, sensing, and communication fields have direct benefits for automated platooning. It is expected that the progress in technology will make highway automation even more viable and achievable.

1.3 Automated Electric Transport

The automated highway scheme currently under investigation at Utah State University (USU) is known as automated electric transport (AET). In this variation of automation, vehicles are charged wirelessly through electromagnetic induction from coils in the road.

This power strategy, under research at the USU Energy Dynamics Laboratory, reduces the need for large, bulky batteries required in long range electric vehicles. AET vehicles have a large enough battery system for the user to get from origin to the highway (within twenty miles for most of the American population). Once on the AET highway the vehicle will be completely powered and even recharged through wireless power transfer while traveling. This allows lighter, more efficient vehicles and greater flexibility in vehicle form.

When contemplating the AET concept it quickly becomes clear that there are a great many details in implementing such a complex system. Many important design decisions are yet to be decided. The role of this work is to create models to demonstrate the effects of various design decisions on safety. These models can be incorporated into the work of other researchers or used independently to help designers understand and fulfill the requirements for a safe system.

1.4 Thesis Overview

First a series of simple kinematic models are developed and used to show the critical factors for vehicle and communication system selection. Next, the models are used for Monte Carlo analysis to determine the probability of unsafe impact with respect to following distance. Physical modeling is then used to determine what parameters of vehicle design and condition most contribute to variation in braking. The model is then extended to a full platoon of vehicles. Finally, the full platoon model is used to test several different controllers in emergency situations to determine which is safest.

Chapter 2

The Emergency Brake Scenario

A primary concern with platooning is how vehicles are kept from running into one another. This natural concern keeps drivers following at the distances seen in current highway systems. Brake lights warn surrounding drivers to slow down, reducing the time required to perceive the need to brake. There is still a delay inherent to drivers, who must see the signal and react to it. The car itself also has a delay, as it takes some time to reduce speed. In addition, different vehicles have different braking abilities, imposing additional requirements for spacing. Insufficient following distances to account for these delays result in rear-end collisions.

A computer has much quicker reaction time than humans, so an automated vehicle is able to follow at much smaller distances, but the principles are largely the same. The most extreme instance of this (requiring the longest separation) is the complete stop of a platoon with the leader braking at maximum ability — the emergency brake scenario. It becomes the main consideration in controller design for each maneuver and in overall system design.

The ideal distance between vehicles is dictated by the reaction time and braking ability. Reaction time includes sensing and communication time, computation time, and actuation delay. Braking ability can be compromised by tire wear, road conditions, brake actuator time constants, vehicle normal force (load), drag forces, and other influences.

There are many ways that the emergency brake scenario can be initiated. One way is the "brake-on" failure, where the leader's brakes unexpectedly lock or a computer error sends a maximum brake signal. The vehicle systems should be designed to be robust against these failures. A more familiar cause would be an obstacle on the road when swerving is not possible. Again, the system could be designed to reduce the number of these instances through using barriers and banning open cargo loads which could result in extraneousness

objects on the road.

The probability of these events, even in current highway systems, seems low but does exist, so such possibilities must be considered in system design. A thorough analysis of the likelihood of these faults is beyond the scope of this work, but must be conducted in order to perform an accurate cost analysis of the system.

2.1 Difference in Velocity and Initial Headway

Two important factors in this investigation are the initial headway (H) between vehicles when an emergency is initiated and the difference in velocity (Δv) between the vehicles when a collision occurs, sometimes called closing speed in the literature. Any emergency brake scenario begins when vehicles are separated at some distance. This initial headway reflects the steady state following distance and is inversely related to the system capacity. In any collision, the vehicles have some difference in their traveling velocity at the instant the impact occurs. This Δv is proportional to the severity of the impact and therefore a metric of safety. Δv is also a function of H.

2.1.1 Difference in Velocity

It will be shown below in Section 2.8.2 that safe platooning is very difficult to achieve (if not impossible) if no collisions can be tolerated in emergency situations. It may seem counter-intuitive to plan collisions into the system design, but it can yield large benefits in system performance without creating additional danger to passengers. This is because the danger of a collision is proportional to Δv of the colliding vehicles, rather than the absolute velocity.

Consider a vehicle colliding into a parked vehicle at $2^{\mathrm{m}}/_{\mathrm{s}}$ (< 4.5mph). There might be some concern about damage to the bumpers and paint but the damage will be minimal and almost no fear of injury would exist. On the opposite end of the spectrum, a head on collision of two vehicles traveling at $20^{\mathrm{m}}/_{\mathrm{s}}$ would be very concerning. Probability of injury or death is very high. This is a high Δv situation because the relative velocity is double each vehicle's speed. Next consider a rear end collision between two vehicles traveling at

30m/s and 32m/s. Even though these are relatively high speeds, the Δv is the same as the parked car incident, so only the bumpers are likely to suffer if only a single impact occurs. Therefore a large Δv in colliding vehicles generates a large impact force and severe injuries and vehicle damage can result. Small Δv can have little consequence even if the absolute velocity of the vehicles is great.

Hereon it is assumed that there exists some Δv_{safe} such that any collision occurring with $\Delta v < \Delta v_{safe}$ is acceptable due to very low risk of injury. This is an assumption made in other works [1, 14, 15] and suggested by medical studies (i.e. [16, 17]). Hitchcock [14] used real incident record data from California to analyze the relationship of injury severity with Δv and a threshold Δv was observed where no data existed below. The threshold was determined by Hitchcock to be 3.3m/s. In the work that follows a more conservative 2.5m/s is used. An additional argument that collisions under Δv_{safe} are acceptable is that these collisions only occur under rare emergency situations. In normal operation, no collisions occur. If failures occur but Δv is low, collisions are unlikely to be dangerous.

2.1.2 Headway

In highway emergency brake scenarios, for any two particular vehicles in succession, Δv of an impact is a function of headway. Consider two vehicles following at a matched speed with delay in braking. If the vehicles are following at an initial headway (H) of 0m, they are touching bumpers and have effectively already collided. If an emergency brake scenario occurs, Δv is zero meters per second. At this extreme the forces generated are not likely to be great between the two vehicles, despite the delay or difference in braking ability. If instead the vehicles initially follow at H of one meter, the delay is enough that the follower will not even begin braking before the collision occurs, and Δv will become more significant. Thus, against intuition, it is actually safer to follow with very little headway than at a somewhat small headway where the preceding vehicle could decelerate more before impact occurs. At the opposite end, if H is sufficiently large both vehicles can come to a complete stop without any collision despite delays.

A curve can be generated to show what the Δv at impact would be with respect to the

initial headway. Called an H-Δv curve hereafter, this curve describes the danger of following at certain headways. The curve changes according to the vehicles' braking differences and delays, but in general it follows an arch shape, dictating that the safest headways are very close or very far. Figure 2.1 shows an example H-Δv curve.

Any two vehicles in succession have a unique H-Δv curve based on the system and vehicles' performance characteristics. Therefore modeling the platoon emergency braking scenario can be simplified to only a leader and single follower. In this context, the "lead" vehicle is not necessarily the leader of the platoon. These could represent any vehicle in the system and its immediate follower, including the last vehicle in a platoon and the leader of the following platoon (who becomes, in this context, the follower). If there are two platoons of 10 vehicles involved in the emergency brake scenario 19 such interactions occur. With this in mind it is apparent that in an automated highway with potentially thousands of vehicles, very low probabilities of dangerous impacts must be achieved.

2.2 Shaping the H-Δv Curve

There are three main sections that compose the H-Δv curve of an emergency brake scenario. The first is when the lead vehicle begins decelerating and the follower is still traveling at the same velocity. This rapid rise in Δv is the result of pure time delay in the reaction of the following vehicle. The second section is where both vehicles are braking at their maximum capability a_{min} (note that the deceleration is notated as a negative acceleration). If the leader has lower a_{min} (better brakes) then the second segment will slope upwards, Δv continuing to increase if the follower is at increased initial headway and therefore closer is safer. In the opposite situation the segment slopes downward since the follower has the lower a_{min} and the more headway provided the more the follower will reduce velocity (and therefore Δv), so further is safer. The third and final section is caused by the leader reaching a complete stop while the follower continues decelerating. Here Δv quickly decreases with additional headway. In the event that the follower has lower a_{min} and reaches a complete stop first then the second section reaches the x-axis and in the third section Δv will be negative which is considered inconsequential since no impact can occur.

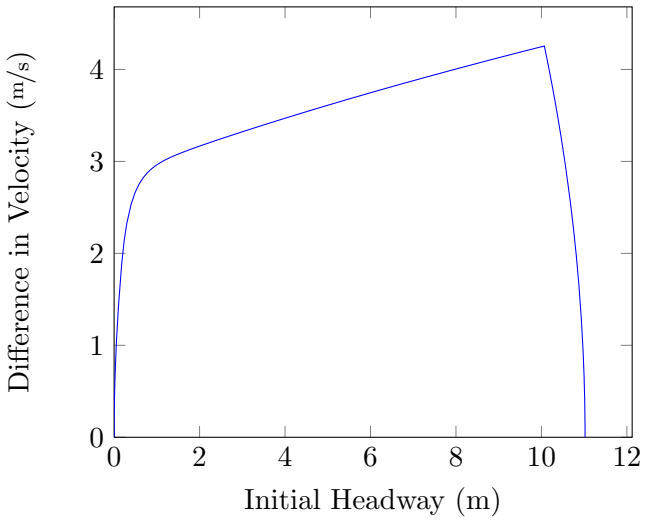

Fig. 2.1: H-Δv curve.

Therefore the H-Δv curve is only shown and considered in the first quadrant.

2.2.1 Simple Equations

Simple equations can be developed for the H-Δv curve to aid in understanding the three segments. These equations are similar to the model developed in Section 2.3 and later used for the analysis but are very simple. Assume the vehicles are able to achieve infinite jerk so

$$a = a^*$$

where a^* is the desired acceleration. The first section is created by the leader braking at maximum capability and the leader still traveling at initial velocity.

$$a_l = a_{minl},$$

$$a_f = 0,$$

where a_{minl} is negative to reflect deceleration. In the balance of this text, the subscripts l and f indicate leader and follower, respectively. This makes the velocities and positions:

$$v_l = v_0 + a_{minl}t,$$

$$
\begin{aligned}
v_f &= v_0, \\
x_l &= x_{0l} + v_0 t + \frac{1}{2} a_{minl} t^2, \\
x_f &= x_{0f} + v_0 t.
\end{aligned}
$$

The headway (H) and Δv then are then

$$
\begin{aligned}
\Delta v &= v_f - v_l = -a_{minl} t, \\
H &= x_f - x_l = x_{0f} - x_{0l} - \frac{1}{2} a_{minl} t^2.
\end{aligned}
$$

The vehicles are treated as points and the initial positions taken to be equal such that $x_{0l} = x_{0f}$ and

$$H = -\frac{1}{2} a_{minl} t^2.$$

This then is the parametrically defined H-Δv curve. With equations this simple, the parameter t can be removed to find Δv as a function of H:

$$\Delta v_1(H) = -a_{minl} \sqrt{-\frac{2H}{a_{minl}}} = \sqrt{-2H a_{minl}}.$$

Continuing the same development for the next two segments of the curve.

$$
\begin{aligned}
a_l &= a_{minl} \\
a_f &= a_{minf} \\
v_l &= v_0 + a_{minl} t \\
v_f &= v_0 + a_{minf} \left(t - t_{del}\right) \\
x_l &= x_0 + v_0 t + \frac{1}{2} a_{minl} t^2 \\
x_f &= x_0 + v_0 t + \frac{1}{2} a_{minf} t^2 - a_{minf} t_{del} t + \frac{1}{2} a_{minf} t_{del}^2 \\
\Delta v &= a_{minf} \left(t - t_{del}\right) - a_{minl} t \\
H &= \frac{1}{2} a_{minf} t^2 - a_{minf} t_{del} t + \frac{1}{2} a_{minf} t_{del}^2 - \frac{1}{2} a_{minl} t^2
\end{aligned}
$$

$$\Delta v_2(H) = \sqrt{\left(a_{minf} - a_{minl}\right)\left(2H - a_{minf}t_{del}\right) + a_{minf}^2 t_{del}^2}$$

$$\begin{aligned}
a_l &= 0 \\
a_f &= a_{minf} \\
v_l &= 0 \\
v_f &= v_0 + a_{minf}\left(t - t_{del}\right) \\
x_l &= x_0 - \frac{v_0^2}{2a_{minl}} \\
x_f &= x_0 + v_0 t + \frac{1}{2}a_{minf}t^2 - a_{minf}t_{del}t + \frac{1}{2}a_{minf}t_{del}^2 \\
\Delta v &= v_0 + a_{minf}\left(t - t_{del}\right) \\
H &= v_0 t + \frac{1}{2}a_{minf}t^2 - a_{minf}t_{del}t + \frac{1}{2}a_{minf}t_{del}^2 + \frac{v_0^2}{2a_{minl}} \\
\Delta v_3(H) &= \sqrt{2a_{minf}H - \frac{a_{minf}}{a_{minl}}v_0^2 - 2a_{minf}v_0 t_{del} + v_0^2}
\end{aligned}$$

The intersection points occur when the follower begins braking after the delay, $t = t_{del}$, and when the leader has reached a complete stop, $t = t_{stopl} = \frac{v_0}{a_{minl}}$ which correspond to $H_1 = -\frac{1}{2}a_{minl}t_{del}^2$ and $H_2 = \frac{a_{minf}}{2a_{minl}}v_0^2 + \frac{a_{minf}}{a_{minl}}v_0 t_{del} + \frac{1}{2}a_{minf}t_{del}^2 - \frac{v_0^2}{2a_{minl}}$, respectively. Both vehicles are stopped at $H_3 = -\frac{v_0^2}{2a_{minf}} + v_0 t_{del} + \frac{v_0^2}{2a_{minl}}$. The resulting piecewise function is

$$\Delta v(H) = \begin{cases} \sqrt{-2Ha_{minl}}, & H = (0, H_1] \\ \sqrt{\left(a_{minf} - a_{minl}\right)\left(2H - a_{minf}t_{del}\right) + a_{minf}^2 t_{del}^2}, & H = (H_1, H_2] \\ \sqrt{2a_{minf}H - \frac{a_{minf}}{a_{minl}}v_0^2 - 2a_{minf}v_0 t_{del} + v_0^2}, & H = (H_2, H_3] \\ 0, & \text{Otherwise.} \end{cases} \tag{2.1}$$

Let it again be noted that a_{min} is negative to represent deceleration, so $\Delta v \in \mathbb{R}$ for the domain of $H \in [0, \infty)$.

These equations are an abstraction of the cyber-physical systems that would compose

an AET vehicle. Abstraction is used in order to maintain independence from specific technologies that are likely to change and develop with time. This achieves a model that is useful to represent any system that might be developed, using current or future technology. This technique of model abstraction is used for all the models presented in this chapter.

2.2.2 Implications of Equation 2.1

One will notice in (2.1) that the first segment is only influenced by the leader braking ability. This factor could be controlled though derating leader braking which is a very important concept since it could have large benefits to platooning safety by significantly lowering the H-Δv curve. However, this and related schema assume that the leader has full control of braking ability. In the event that an obstacle is collided with or there is a tire or brake hardware failure, braking control would definitely be compromised and the vehicle would not be able to maintain the derated acceleration. More research is required for this strategy but is not within the scope of this work. Even derating only lessens the slope of the first section by increasing a_{minl}. This steeply rising section is unavoidable unless braking is perfectly coordinated. This leads to the concept of brake synchronization where a leader would send a brake signal to the followers indicating an advanced time for all to brake. This has safety implications of requiring greater headway for the platoon to stop due to the time required for a communication to travel to the end of the platoon.

The amount of time taken for the follower's brakes to begin acting dictates the length of the first segment. So while the sharp rise is somewhat unavoidable the overall effect can be reduced through minimizing the amount of delay between vehicles. Again this is an argument in the favor of coordinated braking. The primary time constant of the brake actuator (not reflected in these equations) affects the transition between the first two periods and will be discussed in Section 2.3.

The second segment of the curve occurs while both vehicles are braking. Thus, it is a function of both vehicles' a_{min}. The difference dictates the slope of the equation, thus if vehicles are matched the second segment remains level. This again leads to the idea of derating such that $a_{minl} > a_{minf}$ and segment two has negative slope. This, combined with

a very small t_{del}, could create a very small H-Δv curve and a very safe system. Derating has the negative effect that the leader would take more time to stop making the second segment longer, but if the slope is negative or small the benefits could outweigh this cost. Figure 2.2 shows three curves with varying relationships between a_{minf} and a_{minl}.

The third segment begins when the leader has reached a complete stop. The rapidity of the fall of Δv is a function of a_{minf}. In this segment the initial velocity plays a role, as it dictates how long is required for the leader to stop.

These equations are interesting for generating ideas to improve the emergency brake scenario, but for detailed analysis, it is useful to include more factors.

2.3 The First Order Model

A few more terms are useful to look at but quickly add to the complexity of the model. The braking of each vehicle is modeled simply as a deceleration curve of a first order system with delay. This approximates the traditional hydraulic actuated calipers on disc or drum brakes used on today's vehicles. These have some delay for the hydraulic pump to build pressure and for the calipers to close on the disc, then the building of caliper pressure on the disc increases the braking force (and thus deceleration) in approximately a first order response [18]. In the model the actuator delay (d) and time constant (τ) is separately assignable for both leader and follower (indicated by subscript l and f, respectively). Factors such as aerodynamic and tire drag are lumped into the minimum acceleration term, a_{min}.

The leader begins braking at $t = 0$ seconds and immediately sends a "brake" signal to the follower. The signal is delayed by some communication delay, T, which lumps computation time and other pure time delays. The follower receives and immediately begins braking. The remaining model input parameters are the initial velocities of each vehicle. These are all reflected in the block diagram in Figure 2.3. Thus the lumped t_{del} from Section 2.2.1 is being split to differentiate a communication delay T and an actuation delay d.

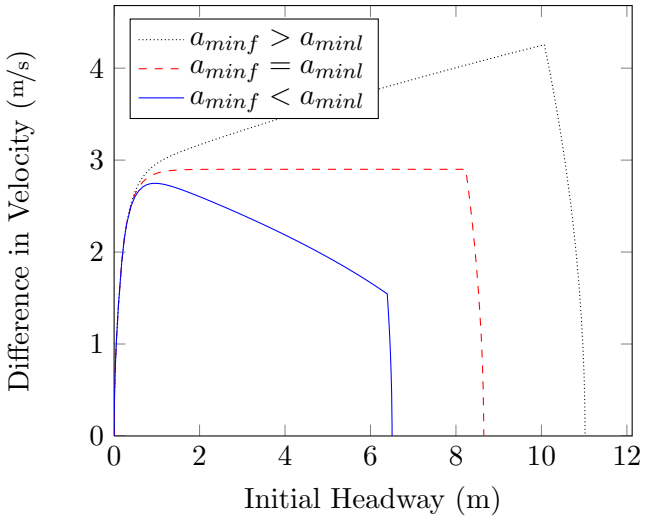

Fig. 2.2: H-Δv curves for different a_{minf}.

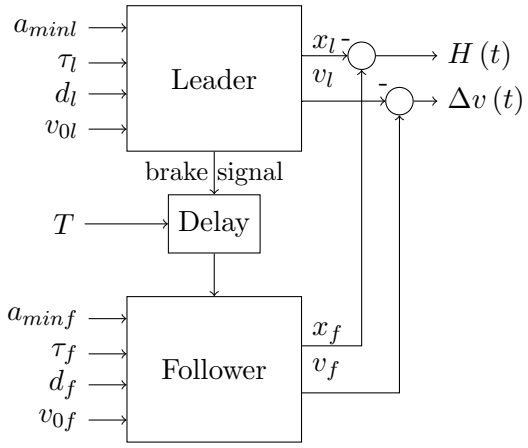

Fig. 2.3: Block diagram of simple model.

The model is therefore defining the jerk or third derivative of position for each vehicle.

$$\dot{a}_l = \begin{cases} 0, & t < d_l \\ \frac{a_{minl} - a_l}{\tau_l}, & d_l \leq t < t_{stopl} \\ 0, & t \geq t_{stopl} \end{cases}$$

$$\dot{a}_f = \begin{cases} 0, & t < T + d_f \\ \frac{a_{minf} - a_f}{\tau_f}, & T + d_f \leq t < t_{stopf} \\ 0, & t \geq t_{stopf} \end{cases}$$

This is then integrated *four* times to find the vehicles' positions at time t. The increase of order in the differential equations makes the analysis done in Section 2.2.1 much more rigorous for these equations. While the closed form solution like (2.1) is still solvable, the result is much more complex and would not provide additional insights to those already gathered from (2.1). Thus the closed form solution is not pursued here.

2.4 Matlab/Simulink Model

For further analysis, a method to rapidly generate H-Δv curves is warranted. Since the equations are somewhat difficult or awkward, a Simulink model was developed. The model follows the form of the block diagram in Figure 2.3. The model represents the state equations

$$\dot{\mathbb{X}} = \begin{bmatrix} \dddot{x} \\ \ddot{x} \\ \dot{x} \end{bmatrix} = \begin{bmatrix} \dot{a} \\ \dot{v} \\ \dot{x} \end{bmatrix} = \begin{bmatrix} \frac{a_{min} - a}{\tau} \\ a \\ v \end{bmatrix}$$

for each vehicle, with the discontinuities in $\dot{a}$ corresponding to delays and when the vehicle reaches a complete stop. The output

$$\mathbb{Y} = \begin{bmatrix} \Delta v \\ H \end{bmatrix} = \begin{bmatrix} 0 & 1 & 0 \\ 0 & 0 & 1 \end{bmatrix} (\mathbb{X}_f - \mathbb{X}_l)$$

is the parametrically defined H-Δv curve. It is saved to the Matlab workspace for further computation, visualization, or analysis.

One of the primary purposes of this work is to provide tools for other investigators in the project. This model can be used to evaluate different system strategies such as coordinated braking and brake derating. The inputs are all configurable through Matlab scripting, so large numbers of curves can be generated very quickly without starting the Simulink environment. For screenshots of the model and script examples the reader is referred to Appendix A. The model is abstract enough to cover a broad spectrum of vehicle and system design considerations, yet detailed enough to provide insight to the effects of complex behaviors such as clock jitter. When probabilistic distributions are used for input parameters, the model can become quite a powerful tool.

Some examples of factors and designs the model is being used to analyze in this and other research.

sensitivity to delay communication delay T is varied across a range

disparity in braking ability minimum acceleration of the follower a_{minf} is set below the leader

derating minimum acceleration of the leader a_{minl} is set to lower values

coordination communication delay T is set to zero

clock jitter actuation delays are adjusted a few milliseconds to make vehicles brake slightly out of sync

For this document, parameter sensitivity is focused on since it is considered to be more fundamental than these other considerations. To aid in any of these analyses it is important to identify appropriate ways to interpret the H-Δv curve data that is output from the model.

2.5 Safety Metrics

While an understanding of the H-Δv curve is useful, the curve itself is not a clear metric for system performance or safety. Several other metrics could be gathered from the H-Δv curve to determine whether the system design is "better" or not. These include the peak Δv value, the domain of unsafe headways (width of the curve), or some combination such as the area under the curve. Different metrics are useful for different analyses.

The peak Δv metric is useful to describe the most severe possible incident between two vehicles. This indicates the relative "safeness" but does not indicate what headways are unsafe, thus this metric is not related to system capacity. This metric is used for a sensitivity analysis of safety with respect to input parameters.

The domain of unsafe headways is a useful metric since it immediately shows all unsafe separations. The unsafe region lies between the safe separation regions for following within and between platoons. Though it adds complexity by using two numbers to describe the upper and lower bounds of the unsafe region, the information about the system that one can quickly gather allows for easy interpretation. Visualization is also relatively simple. This metric has units of meters but still has some information about safety due to its definition. Any collision over the threshold Δv_{safe} is unacceptable and so vehicles should avoid this "unsafe headway zone" (UHZ) at all times.

The area under the H-Δv curve could effectively indicate the relative safeness of a system or situation while also containing information about the system performance. However, this metric has units of meters-squared-per-second which seem arbitrary and unclear where an unacceptable level would lie. It is also possible for two curves to have the same area with one being very wide and short, the other being very narrow and tall. In this case the narrow curve is preferable since it would be safer to make cars avoid a small section of dangerous headways than to have risk in a large region of headways. This is not reflected in the "area" metric.

For these reasons the domain of unsafe headways is the primary metric considered here. Though it does focus mostly on capacity it does so in a conservative way that will maintain

a high safety level as long as vehicles avoid the UHZ.

2.6 The Unsafe Headway Zone

The UHZ is the region where the subsequent vehicle would have an unsafe collision if an emergency brake scenario were to occur. The H-Δv curve virtually extends from the rear bumper of each vehicle and any point of the curve over Δv_{safe} corresponds to the UHZ. Figure 2.4 illustrates this. These drawings are strictly conceptual and not to scale. In this example the follower vehicle has clearly entered the UHZ. The detailed shape of the curve will change based on those input parameters, shown in Figure 2.3, but there is little the follower can do to change those values since they correspond mainly to the condition and ability of the vehicle hardware and the system. The UHZ is always those headways between crossings of Δv_{safe} (the dashed line). The best behavior for a vehicle when in the UHZ is not discussed here, though it seems most intuitive in this case for the follower to change lanes or brake until it is at a safe headway then resume operation as the leader of a new platoon.

In a platoon, each vehicle has a UHZ behind it, and each vehicle is only subject to the UHZ of the vehicle immediately preceding it. The UHZ dictates the practical lane capacity since vehicles merging into or splitting from a platoon can neither enter the UHZ nor leave gaps between other vehicles which would put one or more at unsafe headways. This is especially important with the intra-platoon separation distance (left side of the H-Δv curve). If the UHZ is closer than one vehicle length (usually the case), a single vehicle splitting from the interior of the platoon then leaves an unsafe gap between the vehicles immediately preceding and following it. It is possible for multiple vehicles to exit in a group such that the vehicles behind them are now following at the inter-platoon distance which effectively makes a new platoon.

Figure 2.5 shows a three vehicle platoon with the H-Δv curves and UHZs of the vehicles. It is a safe following situation because each vehicle is at a safe headway (not in the UHZ) from the preceding vehicle. Note that the second H-Δv curve (dotted line) and the resulting UHZ actually extends past the figure edge. Here it is shown truncated to the end of the

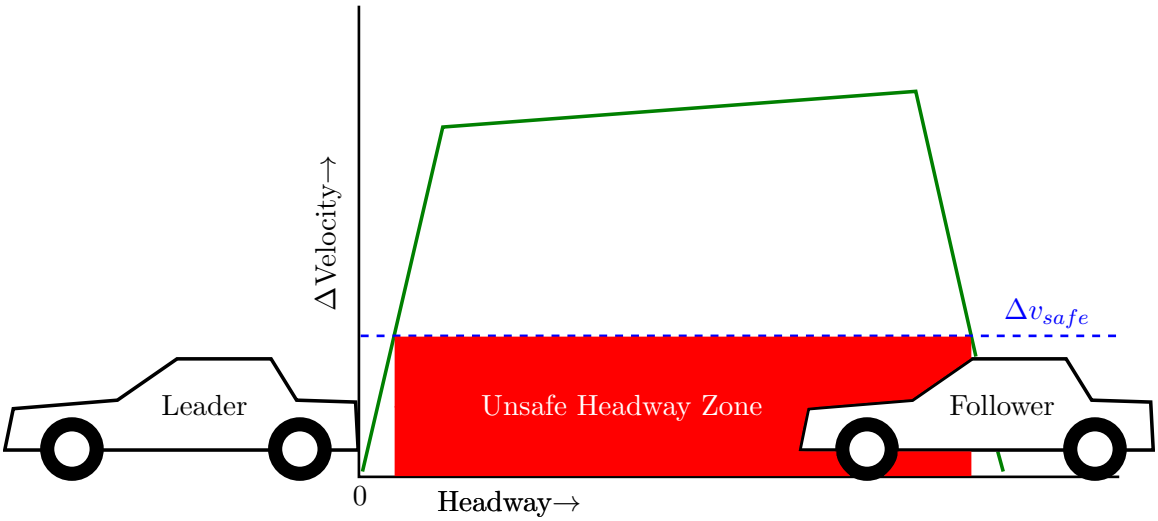

Fig. 2.4: An unsafe following situation.

previous UHZ.

If the intermediary vehicle were to split from the three car platoon suddenly the second follower would be subject to the curve associated with the leader and would lie in the UHZ as illustrated in Figure 2.6. Thus with a UHZ this size, a special design would be required for an interior vehicle to split from the platoon. One method would be a second lane where the two followers could both split then accelerate until the second follower is at a safe following distance from the lead vehicle. The second follower then would join back into the original platoon and the splitting vehicle is free to exit the system. This requires an extra lane for the distance required to complete the maneuver. This method would get complicated in larger platoons with random vehicles desiring to split from the platoon. Thus, effective capacity could be significantly compromised if the UHZ is too close to the each vehicle to allow splitting from the interior.

An easier situation is the platoon merge. Figures 2.7 and 2.8 show parts of two platoons, the last following car of one and the leader of the subsequent platoon. In Figure 2.7, the second platoon is following at a safe distance. In Figure 2.8, a new vehicle has merged into the first platoon, placing the next platoon into an UHZ. One way to avoid this is to only allow new platoons to be created when space is sufficient for a full platoon even if the platoon is not yet filled. This policy prevents platoons from being separated by only the

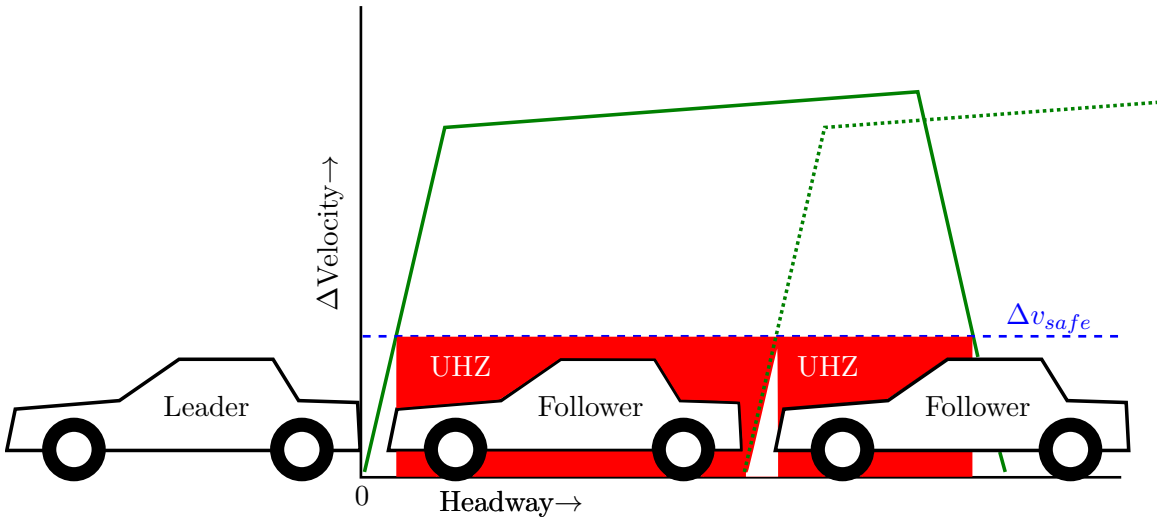

Fig. 2.5: A safe following platoon.

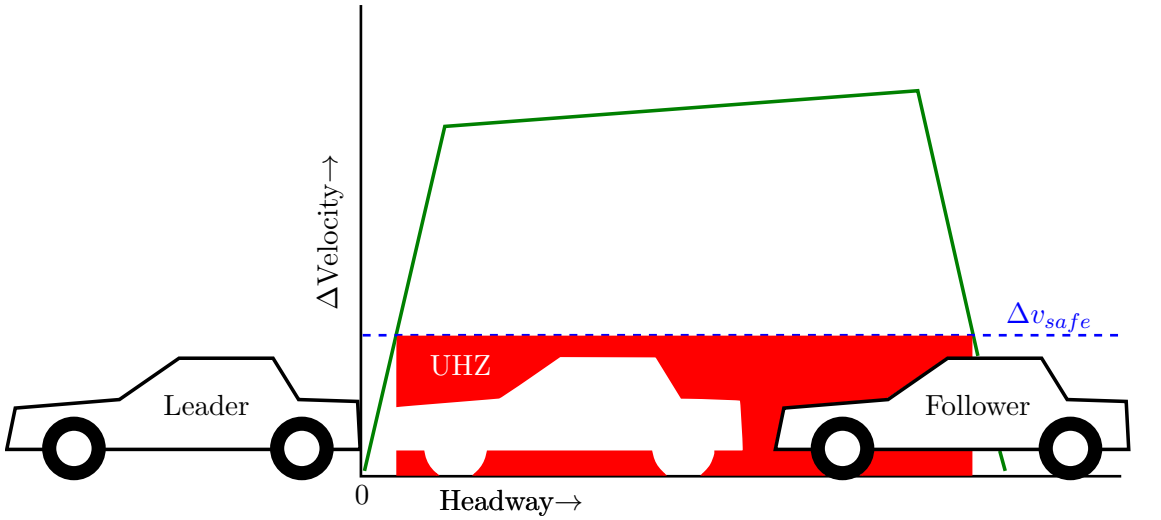

Fig. 2.6: An unsafe following situation resulting from a splitting vehicle.

upper bound of the UHZ until the preceding platoon is full. A vehicle may be required to wait for an available opening but this is the case in highway driving today. This also assumes that there is a set limit to the size of a platoon.

2.7 Sensitivity Analysis

Now that the general shape of the H-Δv curve has been developed and discussed, and appropriate metrics have been selected, it is important to look at the effects of each parameter on the UHZ. Using the Matlab model each parameter is varied to show that safety is most sensitive to the vehicles braking abilities.

2.7.1 Nominal Values

Nominal values are those that are considered normal during steady state operation. These values are based on the assumption that the system will be designed for homogeneous vehicles using high performance technology. The values are all shown in Table 2.1 with the ranges they are swept for sensitivity analysis. Only the follower values are swept because any degradation in leader performance actually improves safety of the followers in an emergency brake scenario.

For the minimum acceleration, $-10^{\mathrm{m}}/_{\mathrm{s}}$ is used as a nominal, since this range of decelerations is reachable by todays sedans equipped with ABS technology. The nominal time

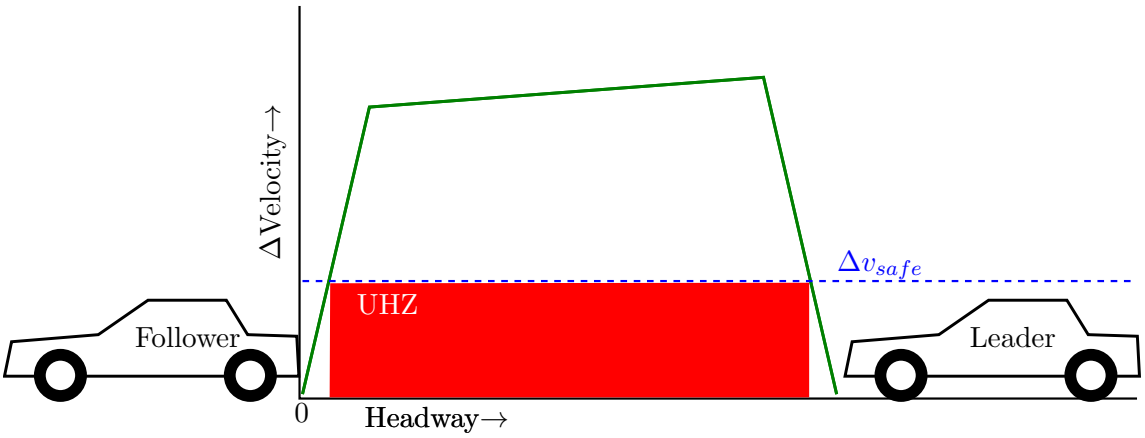

Fig. 2.7: Two platoons at a safe distance.

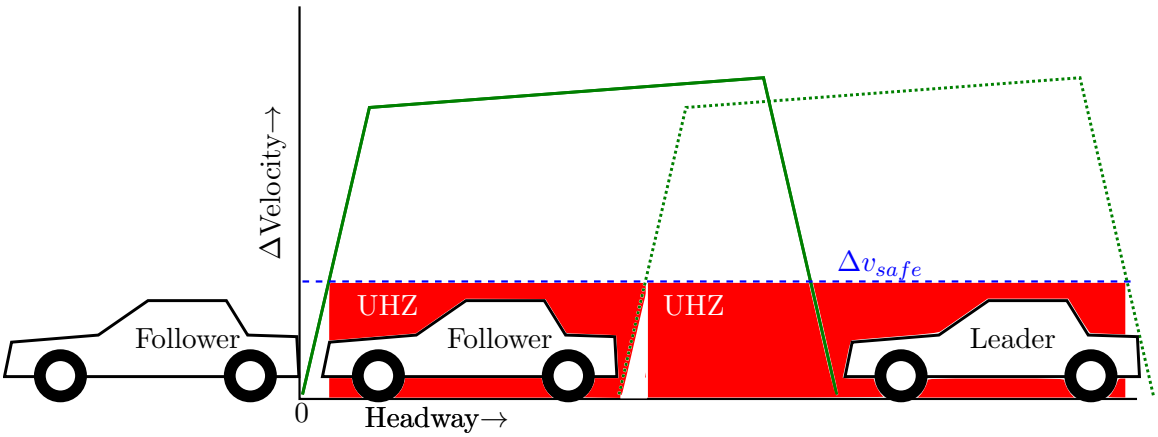

Fig. 2.8: An unsafe following situation resulting from a merging vehicle.

constant is selected due to [19,20]. They find the brake systems they retrofit for automation have time constants of $10 - 100$ms with pure time delays in a similar range. Gerdes and Hedrick suggests that a redesign of the hydraulic brakes could get actuation delay values down to 20ms [21]. Electro-mechanical brakes (EMBs) (which use dc motors rather than hydraulics) show potential for even higher performance brake systems [13]. In fact, Johansen et al. [22] modeled an EMB on a Mercedes vehicle as a first order system with pure delay of 14ms and bandwidth of $72^{\text{rad}}/_{\text{s}}$ which corresponds to a time constant of about 2ms. It was decided to use 10ms for the time constant nominal and 5ms for the nominal actuator delay. This value of actuation delay may be optimistic since computation time is included in this time. The initial velocity is simply selected at a value near current US highway speed limits.

In selecting a nominal value for the communication delay the work of PATH was considered. In Li [23] the communication architecture design is described for communication of velocity, acceleration and a time stamp for four platooned vehicles. Each cycle of the token-bus architecture takes 55ms. Later, in Hedrick et al. [24] PATH discusses a similar token-bus architecture with a 20ms cycle for up to ten vehicles in a platoon. Wireless communication technology continues to improve. The value used as a nominal here is 20ms. This is also possibly optimistic considering security is not mentioned in the work by PATH. Even with advances in technology, such small delays may not be realistically achievable

in a secure system. The analysis that follows however shows that the system is robust to variation in these delays.

2.7.2 UHZ Sensitivity Plots

The parameters were swept according to the ranges in Table 2.1 and the resulting UHZs are plotted in Figure 2.9. Since the x-axis represents different units for each parameter and the associated curve they are plotted again with respect to parameter variation percentage in Figure 2.10. Because for minimum acceleration a large percent change means greater braking capability the UHZ curve looks reversed compared to the other parameters.

It can be observed that the only factors which create unsafe zones are minimum acceleration and initial velocity. The other parameters were all varied to an order of magnitude of degraded performance showing that they must be compromised significantly to become significant factors and threaten safety. In fact with these nominals no UHZ existed until $\tau_l = 250(\text{ms})$, $d_l = 240(\text{ms})$, or $T = 260(\text{ms})$. From this it can be inferred that T, τ, and d are related since they each contribute to the total delay from leader braking to the follower braking. If this total delay exceeds $\approx 275\text{ms}$ there exists an UHZ. These facts, however, while true for single parameter variation or single faults do not necessarily hold for double faults. It is clear, however, that the total delay is more significant than any individual delay.

The natures of the minimum acceleration curve and the initial velocity curve are quite different. The minimum acceleration curve is what would typically be expected since it

Table 2.1: Nominal values and variation for sensitivity analysis.

Parameter	Units	Nominal	Sweep Range	Sweep Range (%)
a_{minf}	m/s^2	-10	-10	100
τ_l	ms	10	10	100
d_l	ms	5	5	100
v_{0l}	m/s	30	30	100
a_{minf}	m/s^2	-10	$(-15, -5)$	$(150, 50)$
τ_l	ms	10	$(1, 100)$	$(10, 1000)$
d_l	ms	5	$(0, 100)$	$(0, 2000)$
v_{0f}	m/s	30	$(25, 35)$	$(83, 117)$
T	ms	20	$(2, 200)$	$(10, 1000)$

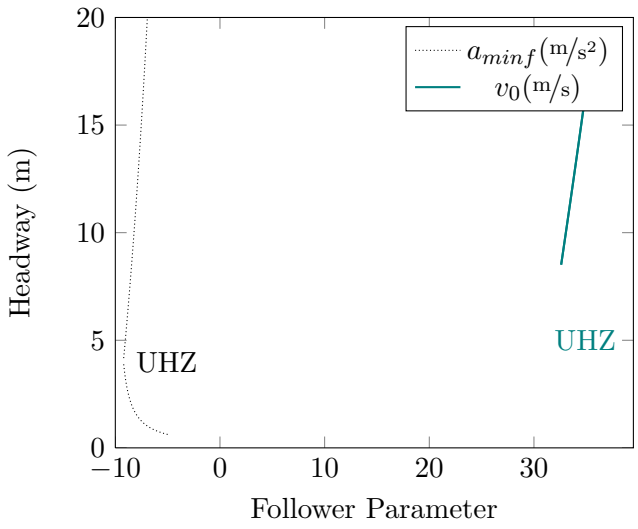

Fig. 2.9: Unsafe headway zones for varying parameters.

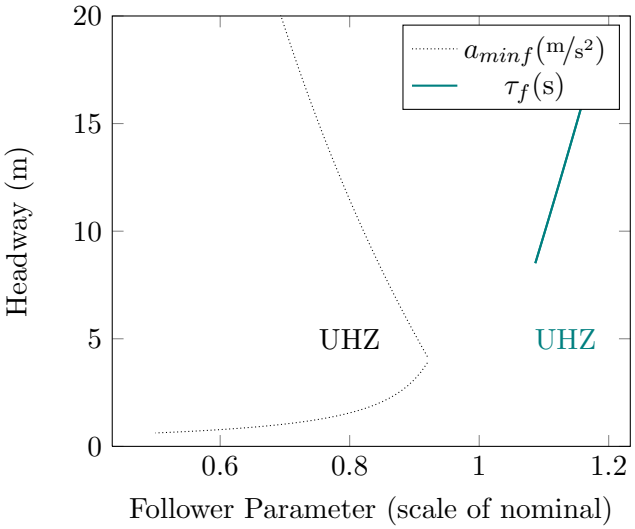

Fig. 2.10: Unsafe headway zones for varying parameters scale of nominal values.

effectively raises the H-Δv curve as a_{min} degrades and the UHZ grows wider. The initial velocity curve however has no UHZ until the difference in initial velocities is greater than the threshold Δv_{safe} such that $v_{0f} = v_{0l} + \Delta v_{safe}$. At this point the UHZ suddenly includes all headways from zero to the distance required for the follower to decelerate enough that Δv is once again below Δv_{safe} (just under 10 meters here). Any increase in v_{0f} beyond this point increases the UHZ linearly. While the v_{0f} curve seems to have greater slope and thus higher sensitivity to variation beyond that point mentioned, it is of less concern because it is the one parameter that is easily controlled by the vehicle. The controller can be designed to avoid operation at velocities over $v_l + \Delta v_{safe}$ and this problem is avoided. Degradation of a_{minf} cannot be compensated for easily by a controller since it would most likely result from a saturation nonlinearity in the vehicle physics. Therefore, disparity in the vehicles braking abilities is considered the most significant factor regarding safety in emergency braking scenarios.

As mentioned above, if a double fault occurs smaller variations can suddenly create dangerous situations. The system is reasonably robust against double faults in parameters such as time constant (τ) and communication delay (T) since these each require large degradations to become significant, but if a fault occurs degrading a_{minf} and a second fault causes delay the results become more significant. Figures 2.11 and 2.12 show the UHZ with respect to parameter variation similar to Figure 2.10, but with degraded nominals $a_{minf} = -9.5$ and -8 m/s, respectively.

In Figure 2.11, the UHZ curves for a_{minf} and v_{0f} appear nearly vertical while those of τ_f and d_f barely appear at all at the end of the ranges varied here. T shows a much larger UHZ than τ_f and d_f because of its larger nominal value and thus much more significant contribution to the total delay. As the nominal value of a_{minf} is degraded to -8 m/s^2 in Figure 2.12, the UHZ now exists even at the nominal values. This plot shows the closer relation between the delay terms T, τ_f, and d_f though again T appears more sensitive due to the larger nominal. It deserves notice that all the UHZs match at parameter variation of one which point corresponds to all parameters at nominal. Ultimately, these graphs show

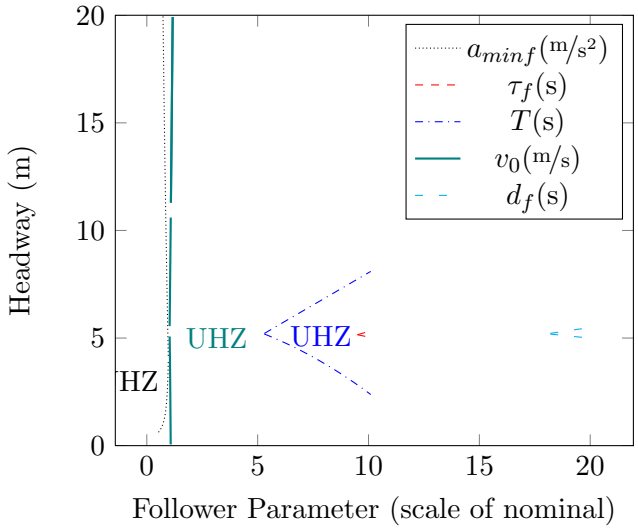

Fig. 2.11: Unsafe headway zones for varying parameters with $a_{minf} = -9.5^{\mathrm{m}/\mathrm{s}^2}$.

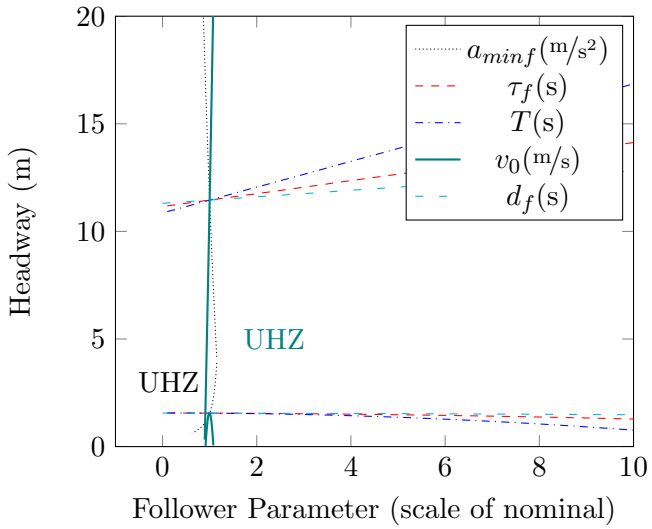

Fig. 2.12: Unsafe headway zones for varying parameters with $a_{minf} = -8^{\mathrm{m}/\mathrm{s}^2}$.

that small changes in minimum acceleration create large variations in the UHZ.

2.8 Monte Carlo Analysis

Since safety is most sensitive to variation in the vehicles' braking abilities, one way to quantify and analyze the emergency brake scenario is through Monte Carlo methods. It is assumed that the road conditions effect all vehicles approximately the same amount so the large variations come from vehicle capability dictated by condition of brake hardware and tire tread. Two main parameters are considered and analyzed: delay and braking ability.

For simplicity, only one of the delay terms are varied in the Monte Carlo analysis, that of communication delay (T). Having less effect on safety than a_{min}, T is only set to one of two deterministic levels: short, where leader and follower parameters are at nominal levels, and long, where the follower delay parameters are below the usual performance levels. The long case could correspond to a fault, or as AET research proceeds, it may be found that total delay is longer than the nominal value assumed here, and the long delay is more representative of the actual system.

The parameters safety is most sensitive to, a_{minl} and a_{minf}, are set according to stochastic distributions. The safest system will have homogeneous vehicle performance since variations cause the braking disparities which worsen the UHZ. However, even with nominally homogeneous vehicles there is variation in manufacturing and wear, as well as load and other operating conditions. Two distributions are used, the first being a "strict" distribution with all vehicles kept within a small braking variance, the other a "loose" distribution where the standard deviation is larger. This can be thought of as one system where laws and regulations are very strict, requiring regular checkups to make sure all vehicles have very consistent braking. The loose distribution system would then be one with fewer checks; perhaps no certification or registration is required etc., the result being that some vehicles on the road fall into disrepair, compromising braking, and the variance of braking is greater.

Both distributions are bounded normal distributions. The upper bound represents an evaluation of braking abilities when vehicles check into the automated highway (i.e. [25,26]) and are subsequently rejected if they do not have sufficiently low minimum acceleration.

This upper bound changes between distributions. The lower bound for both distributions is $-10^{m}/_{s^2}$, since this represents the limit of the vehicle type's ability. Both distributions have a mean value which is centered between the upper and lower bounds. This assumes as the regulations on vehicle maintenance are relaxed, the quality of the average vehicle declines. For illustration, example histograms of the two distributions are shown in Figure 2.13.

This gives four main cases of interest: strict-short, strict-long, loose-short, and loose-long. The values used for each case are summarized in Table 2.2.

The model is run 1,000 times, each run using a random outcome from one of the aforementioned distributions for minimum acceleration. Each run produces an H-Δv curve. The resulting Δv values are run through a "success" function which returns a one if over Δv_{safe}, a threshold corresponding to an acceptable impact velocity where there is effectively no risk of injury or death, a zero otherwise. The output of the success function process is a unit rect function of H that is the UHZ. The success function outputs are summed and normalized such that each headway acts as a bin containing the probability of an unsafe collision at that following distance. The simulation process is repeated 30 times for each combination of delay time and distribution and the resulting 30 probability values for each bin averaged for accuracy. The result for each case illustrates a probability curve approximating the probability of a collision over Δv_{safe} occurring with respect to headway. These curves can be interpreted to give the safe following distances correlated to vehicle parameter variations.

2.8.1 Monte Carlo Simulation Results

The plots in Figures 2.14 and 2.15 are the superimposed distributions from the simulation. To better illustrate the change in probability as parameters vary, rather than just calculating each of the four cases, two cases are presented on each plot, with intermediary plots showing a parameter sweep between them. For example in the loose distribution plots in Figure 2.14, between the loose-short and loose-long case curves are eight other loose case curves where the delay time is swept in 20ms steps from the short case to the long case.

It can be seen that the strict-short configuration is the safest since it has the lowest

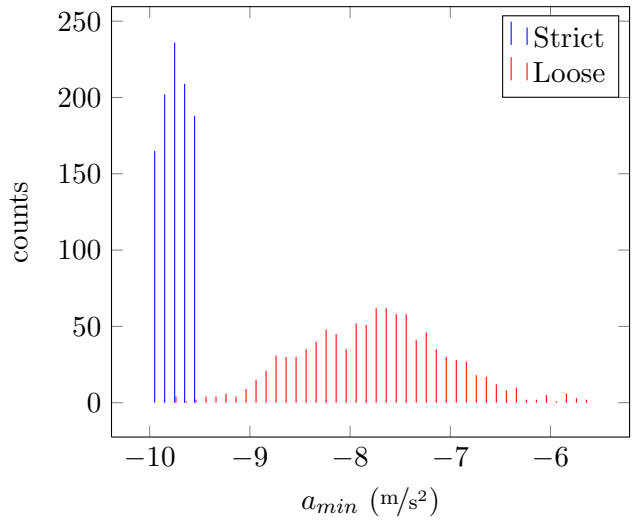

Fig. 2.13: Vehicle a_{min} histograms.

Table 2.2: Case values for Monte Carlo simulations.

Parameter	Units	Strict-Short	Strict-Long	Loose-Short	Loose-Long
T	ms	20	200	20	200
μ	m/s²	9.75	9.75	7.75	7.75
σ	m/s²	0.25	0.25	0.75	0.75
Lower Bound	m/s²	−10	−10	−10	−10
Upper Bound	m/s²	−9.5	−9.5	−5.5	−5.5

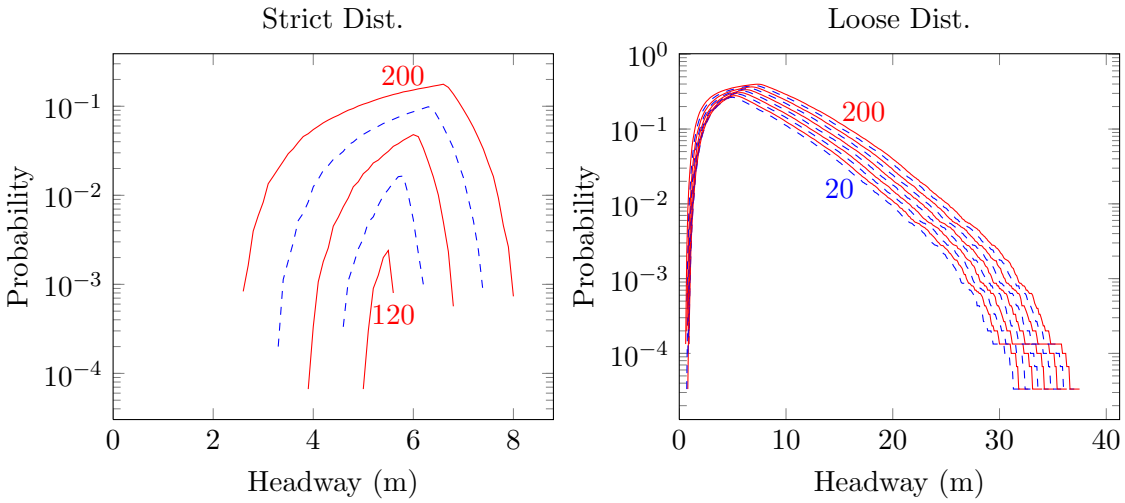

Fig. 2.14: Unsafe collision probability curves for strict and loose distribution, delay sweeping 20ms intervals.

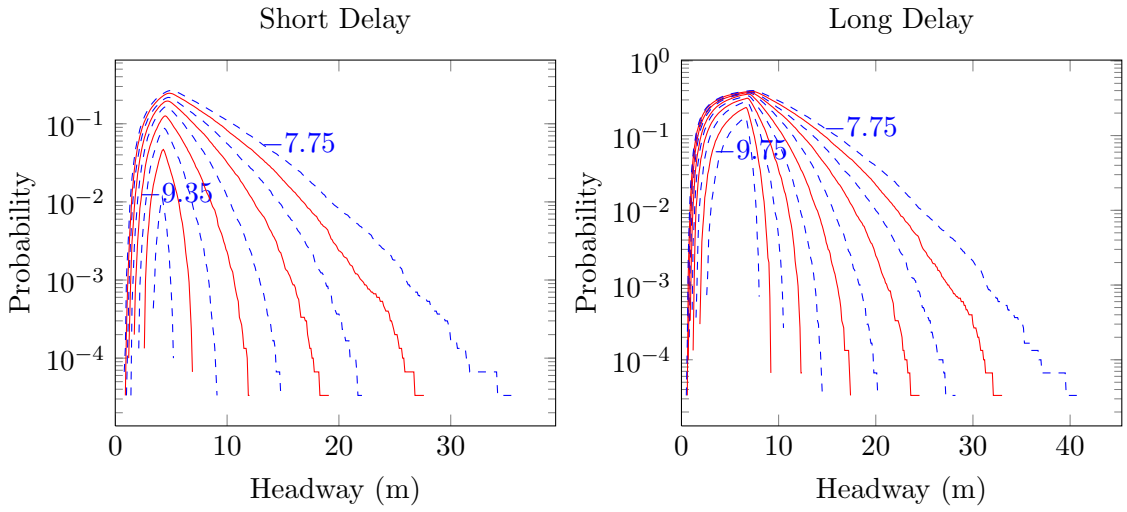

Fig. 2.15: Unsafe collision probability curves for short and long delay, distribution mean sweeping $0.2^{\mathrm{m}}/_{\mathrm{s}^2}$ intervals.

probability of collision for all headways. UHZ does not exist even, until the delay increases to more than 120ms. This is as expected since the vehicles are very closely matched. With this level of variation in a_{min}, the probability of unsafe collision never reaches 20% even at the worst point of the strict-long case. This is a manageable situation since it is fairly simple to keep vehicles out of the three to eight meter headway zone where the probability of dangerous collision is measurable.

The loose distribution's curves are not to be desired but are manageable if delay is sufficiently short. This larger zone of high probability of unsafe collision will require careful merging and splitting strategies.

While a probability of 1% seems low at first, when multiplied by the number of interactions that might occur in an incident, which could easily reach thousands on a high-capacity, automated highway, the numbers are sobering. It would be very difficult to keep platooning safe in the loose-long case since there is quite high probability of dangerous collision even at distances of one meter. In this case the highway may not use a platooning strategy, with each vehicle following at the right side of the UHZ but this creates significant losses in capacity.

It is obvious that the change to a loose distribution has significant effects on the probability of collision. This indicates that efforts to make vehicles' braking abilities matched can yield great increases in safety. There is of course a trade-off. Keeping high performance in all the vehicles requires higher design specifications, manufacturing tolerances, and maintenance requirements, which can raise the cost of production and operation.

These probabilities describe collisions in an emergency scenario. For accurate analysis of the implications on normal operational safety and performance the probability of an emergency scenario *occurring* must be obtained. There is not yet any working model that predicts the likelihood of an emergency scenario occurring in normal operation. System designers can take preemptive measures to reduce risk of emergency scenarios. For example, to prevent obstacles in the road, highways could be fenced or even enclosed. If emergency events are found to be low enough in probability, designers could decide to accept the risks of allowing vehicles to pass through or even operate in the UHZ. Significant work in this area is required for a reasonable estimate on the overall safety of the system. While neither a perfect model nor a perfectly safe system are possible, safety is a key factor for consideration in system design. Until this data can be found, it is conservative to design around the UHZ for acceptable safety limits.

2.8.2 Changing Δv_{safe}

At this point is it useful to discuss another variable: Δv_{safe}. While the value used is based on the values used in similar work, it is possible to design a vehicle with larger crumple zones such that it is able to withstand greater Δv without increased risk to occupants. Figures 2.16 and 2.17 show the probabilities that result when the success function threshold, Δv_{safe}, is changed from $2.5^{\mathrm{m}}/_{\mathrm{s}}$ to $5^{\mathrm{m}}/_{\mathrm{s}}$. The result shows that the system becomes much easier to operate. No UHZ is measured under any strict case. Not until the mean surpasses $-9.35^{\mathrm{m}}/_{\mathrm{s}^2}$ is there any UHZ. While allowing more dangerous impacts does not increase safety, the potential for increased capacity is compelling, provided vehicles can be made safe enough to withstand such impacts. This is not unreasonable since the collisions involved are strictly rear-end incidents, which are generally safer than head-on or t-bone type collisions.

Conversely if designers were to decide that no collisions are acceptable in emergency scenarios ($\Delta v_{safe} = 0^{\text{m}}/_{\text{s}}$) then the design task becomes much more difficult. Figures 2.19 and 2.18 suggest that a platooning system could not operate under requirement that no impact can occur in emergency scenarios unless vehicles are nearly perfectly matched and high performance. This is because there is near-unity probability of collision at very close headways even under the strict-short case.

Thus, it appears the value used, $v_{safe} = 2.5^{\text{m}}/_{\text{s}}$ is a good compromise between safety and system capacity, though it was selected based on literature. Designers should keep in mind that it is possible to have the benefits of allowing higher velocity impacts without endangering occupants through appropriate vehicle design.

2.9 Chapter Conclusions

One of the primary considerations in system design is safety in an emergency brake scenario. Collision severity is proportional to the difference in vehicles' velocity (Δv) at impact. This difference can be plotted as a function of initial headway (H). Vehicles can be organized into platoons for large increases in system capacity. Platooning is safe under certain conditions due to the shape of the H-Δv curve that shows low Δv at very short and very far headways. In between these safe regions lies the unsafe headway zone (UHZ) defined as the initial headways that result in an impact Δv greater than a safe threshold (Δv_{safe}). A model is developed for investigation of system design. It is most conservative to design vehicle maneuvers and the following distances such that vehicles always stay out of the UHZ. Safety is most sensitive to variation in vehicles minimum acceleration value (a_{min}) such that if the follower cannot decelerate as quickly as the lead vehicle, safety is most compromised. Using the UHZ Monte Carlo simulations can show the probability of unsafe collisions with respect to headway. These plots show that safe platooning is easily maintained if high vehicle and system performance is maintained, and safe platooning is still achievable if performance is compromised. Coordinated braking and brake derating could mitigate risks induced by performance degradation but are not investigated here. More research on the probability and causes of emergency scenarios is required to create a full

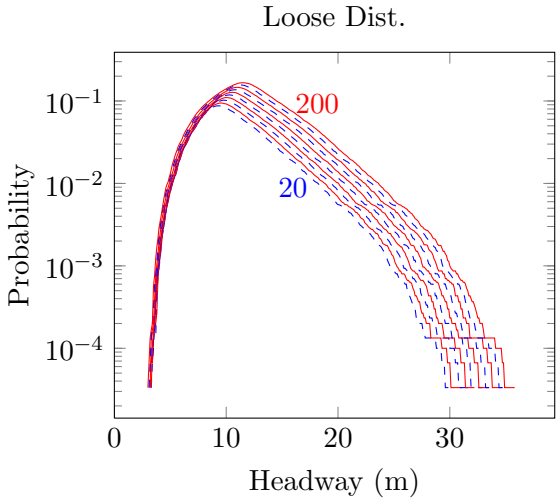

Fig. 2.16: Dangerous collision ($\Delta v_{safe} = 5^{\text{m}}/_{\text{s}}$) probability curves for strict and loose distribution, delay sweeping 20ms intervals (note: no UHZ was observed in any strict distribution curves).

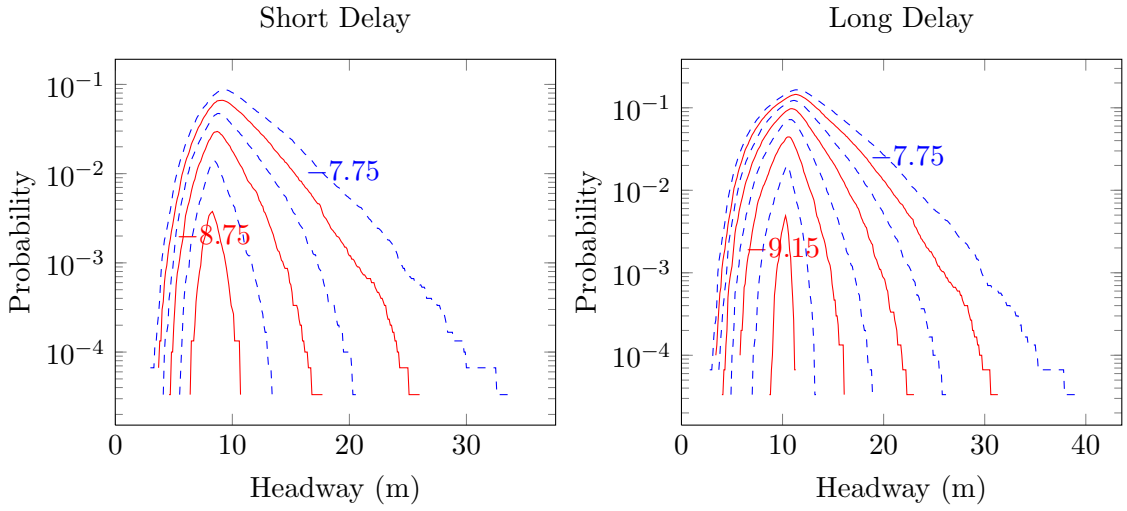

Fig. 2.17: Dangerous collision ($\Delta v_{safe} = 5^{\text{m}}/_{\text{s}}$) probability curves for short and long delay, distribution mean sweeping $0.2^{\text{m}}/_{\text{s}^2}$ intervals.

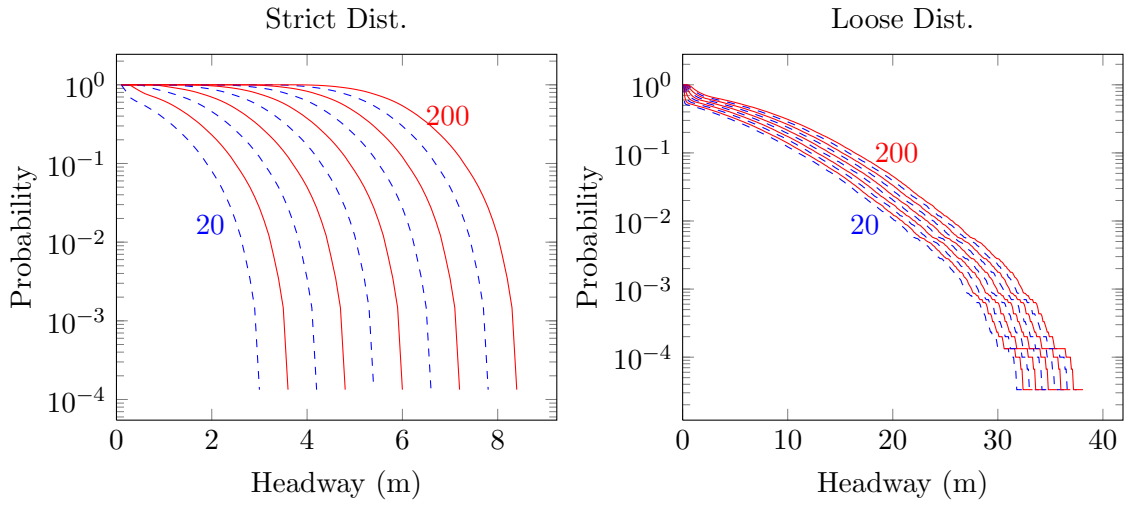

Fig. 2.18: Any collision ($\Delta v_{safe} = 0$m/s) probability curves for strict and loose distribution, delay sweeping 20ms intervals.

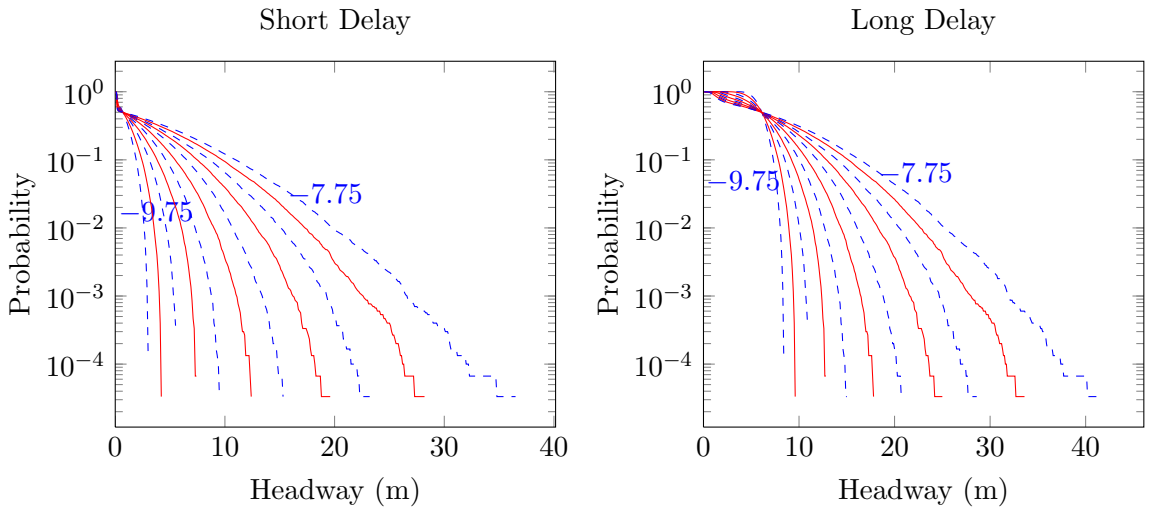

Fig. 2.19: Any collision ($\Delta v_{safe} = 0$m/s) probability curves for short and long delay, distribution mean sweeping 0.2m/s² intervals.

analysis of system safety.

Some mention is made above of constrained merge and splitting techniques. Under poorly distributed conditions, the author's suggested technique would require additional lanes such that a platoon that would add or remove members may exit into a maneuver zone, reduce speed and reconfigure. This low speed region would negatively effect throughput as well as require additional headway for special lanes, but if the system is found to be ill-behaved enough then it may be in order. This could allow special ordering for platoons to attempt the safest, most efficient configurations, and homogeneous intra-platoon destinations which would remove the need for frequent delays at the maneuver zones. More investigation of costs to traffic flow would provide additional insight to the effectiveness of such strategies.

While these values are at once sobering and hopeful, it is clear that platooning is a difficult task under highway conditions. The strict case especially seems rather optimistic that all vehicles can lie bounded within 1-σ of the mean, but insufficient data was collected to definitively say so. A study of the braking distributions of a large number of homogeneous vehicles would prove invaluable to improve the accuracy of these results.

Chapter 3

Physical Vehicle Modeling for the Emergency Brake Scenario

It has been shown that in the emergency brake scenario, safety is most sensitive to disparity between the minimum accelerations of vehicles in a platoon. If decelerations cannot be tightly controlled, capacity must suffer to maintain a constant safety threshold. While this qualitative knowledge is important, it does not indicate what might be done in vehicle and system design in order to maintain safe platooning.

This chapter builds on the previous results to provide basic guidelines in what characteristics the vehicles must have in order to achieve predictable, controllable braking. These guidelines can provide insight to what components of vehicle systems are the limiting factors to implementing an AET system with today's technology, thus indicating where additional research might prove most profitable. Additionally, this work will help system designers understand the restrictions that must be placed on a vehicle in order to make it capable for safe AET use.

To achieve this physical analysis, a model is developed of the drivetrain of the vehicle, then used to define the sensitivity of minimum acceleration to variation of several parameters.

3.1 The Physical Model

The models developed in the previous chapter use abstractions of physical systems. While capturing the behavior of the vehicles, they do not model any actual systems of the vehicles. Here the main components of the drivetrain are modeled individually in order to investigate the effects of varying parameters.

First the tire-road interaction model is developed, next the motor model, then the

dynamics of the vehicle are set forth. For simplicity, the vehicle is assumed to be a direct-drive system. A block diagram representing the model is shown in Figure 3.1.

3.1.1 The LuGre Model

The most significant nonlinear dynamic (and perhaps, most complicated) in a direct-drive EV is the tire-road interaction. This is a complex friction problem that includes Coulomb and static friction, the Stribeck effect, hysteresis, and many other phenomena. Because the dynamics occur on a microscopic scale, most practical friction models developed are empirical. Specifically for tire-road interactions, the Pacejka model, or "Magic formula" is common in the industry. This model uses many parameters to represent the tire and road condition and composition. This model is accurate and easy to solve, but is not appropriate for this analysis since the parameters must be identified from experimental data and have no physical interpretation. In contrast, brush models represent the contacting surfaces as bristles that have some elastic and adhesive characteristics corresponding to the tire characteristics. These models however, assume that the bristles are bent to some steady state position and thus do not capture transient behaviors. To include these transients, dynamic models have been developed. While not necessarily intended for tire-road interactions they have been used for such. Several examples of dynamic friction models are the Dahl, Bliman-Sorine, and LuGre models. For this analysis the LuGre model was selected. It is based on a brush model, but includes a single dynamic state representing the bristle deflection, capturing transient behavior.

While an empirical model may seem detrimental to the purpose of identifying physical parameters that need regulation, most truly physical parameters for friction are so detailed that they are useless to a designer. The LuGre model is a good abstraction of friction

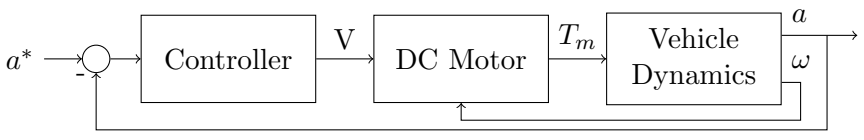

Fig. 3.1: Block diagram of physical vehicle model.

dynamics that still has a physical interpretation and thus still provides insight to the system characteristics.

The LuGre Model provides a relationship between relative velocity (v_r) and the coefficient of friction (μ). Relative velocity is the difference between the wheel rotational and linear velocity.

$$v_r = h\omega - v,$$

where h is the effective height of the wheel. Large positive v_r correspond to "spinning out" where the tire is rotating without propelling the vehicle forward (resulting in very small μ). Large negative v_r correspond to locking the brakes such that the tire is not spinning, but the car is still moving forward. Large is of course relative since the threshold where spinning or locking begins is dependent on the vehicle velocity. Most authors present curves showing μ as a function of slip.

Slip (s) is the relative velocity normalized by either the rotational or the linear velocity depending on whether accelerating or decelerating such that

$$s = \begin{cases} \frac{v-h\omega}{v}, & F_{tr} < 0 \\ 0, & F_{tr} = 0. \\ \frac{h\omega-v}{h\omega}, & F_{tr} > 0 \end{cases}$$

Notice that the cases are determined by the tractive force (F_{tr}) of the tire rather than the net acceleration of the vehicle. Static curves showing this relationship between μ and s (such as those described by the magic formula) are common in the literature. Many are taken from Harned et al. [27]. These curves by Harned et al. indicate that the greatest coefficient of friction (and thus greatest tractive force) is obtained when slip is approximately between 0.1 and 0.2, though it varies with velocity, road condition, and other factors.

Canudas de Wit and Tsiotras [28] use a desired slip of 0.15 and that is the value that will be used here.

The LuGre Model is of the form

$$\begin{aligned} g(v_r) =& \mu_c + (\mu_{st} - \mu_c)\, e^{-\sqrt{\left|\frac{v_r}{v_s}\right|}} \\ \dot{z} =& v_r - \theta \frac{\sigma_0 \left|v_r\right|}{g(v_r)} z \\ \mu =& \sigma_0 \dot{z} + \sigma_1 z + \sigma_2 v_r, \end{aligned} \tag{3.1}$$

where z is the state reflecting the average bristle deflection in the brush analogy. The other parameters can be identified through experimental data. The parameters μ_{st} and μ_c represent the Stribeck and Coulomb static friction coefficients. The $\sigma_{1,2,3}$ represent respectively the lumped spring, damper, and viscous relative damping effects of each bristle. The Stribeck velocity is v_s. The term θ is not part of the original LuGre model as presented by Canudas de Wit et al. [29] but is introduced and used by Canudas de Wit et al. [30] to represent variations in road or wheel conditions. Unity in θ represents uncompromised conditions. Wet roads correspond to approximately $\theta = 2.5$, and θ of four would be ice or snow on the road. A similar approach can represent decreasing tire tread.

This model is strictly longitudinal. Two-dimensional LuGre models have been developed to account for lateral traction, but the model used for this work does not. When vehicles turn, the lateral traction required takes away from the longitudinal tractive force available. Should an emergency occur on a curve of the highway the results from the model presented will be optimistic.

3.1.2 Actuator Modeling

A direct current (DC) motor model is used for the primary actuator of the EVs. This is one of the simplest electrical machines to model and control which accounts for its ubiquitous use in various applications. The DC motor model developed by Kenjo and Nagamori [31] is used by Waltermann [32] for the propulsive actuator in a hybrid vehicle since it captures well the dynamics of both synchronous and asynchronous electric motors.

The motor output torque is proportional to the current in the armature which has

inductance (L) and resistance (R). There is an additional term from the back electromotive force (emf), proportional to the motor's rotational velocity (ω). Therefore, the current (I) has dynamics

$$\dot{I} = \frac{V_m - K_e\omega - RI}{L},$$

where V_m is the input voltage and K_e is the back emf constant. Using the torque/current motor constant K_t the output torque is simply calculated $T_m = K_t I$.

3.1.3 Battery and Power System Modeling

The battery and power system are limited in the current and voltage available to the motor. This is represented as a saturation limit V_{max} on the voltage magnitude that is applied to the motor.

3.1.4 Quarter Vehicle Model

It is assumed that each of the four wheels behave similarly so only one is modeled and calculated. Since vertical and lateral dynamics of the vehicle are not considered, there is no differentiating between the different wheels. The vehicle is subject to the aggregate force of all four wheels, so the calculated force exerted by the single wheel is multiplied by four. The tractive force is the product of the LuGre model friction coefficient and the vehicle normal force.

$$F_{tr} = \mu F_n = \mu M g$$

Aerodynamic drag is proportional to the square of the velocity times the drag coefficient C_d. The longitudinal dynamics of the vehicle are

$$\dot{x} = v$$

$$\dot{v} = \ddot{x} = a$$

$$a = \frac{4F_{tr} - C_d v^2}{M},$$

where M is the vehicle mass.

Assuming the wheel is directly, rigidly attached to the motor the vehicle has the rotational dynamics

$$\dot{\omega} = \frac{T_m - hF_{tr} - B\omega}{J},$$

where B is the rotational damping and J is the moment of inertia.

3.1.5 Vehicle Control

The input to the vehicle is a voltage while the output is an acceleration. The vehicle controller must map these two unalike parameters such that the output is predictable and controllable. This analysis is not specifically about this physical layer of control, therefore a PI controller is implemented. While PATH and other groups made somewhat exotic nonlinear sliding mode controllers for this task they were more especially focused on the dynamics of the ICE and made simplifying assumptions about the tire-road interaction. Since the actuator in an EV is a more linear device (especially in the case of the DC motor) the vehicle will be better behaved even with a simple controller. Still, it is also anticipated that unmodeled dynamics are likely to influence the vehicle behavior so the PI controller is only loosely tuned to give the vehicle acceleration a settling time of about 30ms. In implementation, a PID controller is used, for the case that future research warrants more accurate physical layer control, but in this work the derivative gain is zero.

Above this physical layer of control lies the regulation layer. This layer of control provides the desired acceleration to the physical layer. It determines the desired vehicle behavior based on measured and communicated information. This controller will be discussed in depth in Chapter 4 below.

3.1.6 The Complete Model

The model is implemented in Simulink and can be run from a script. Specifics of model usage are described in Appendix B. The five states requiring integration in the model are few enough that the model calculations can be quickly run, but offer enough detail that the major dynamics of an AET vehicle are reflected.

This model makes some broad assumptions, foremost that the brake actuation is done by the same electric motor used for traction. Though other braking methods are common today, this is not unrealistic since direct drive vehicles are continuously under research (i.e. [33–38]). Currently direct drive brake technology is somewhat limited since the electric engines used are not usually able to provide the same levels of torque created by friction braking of disc or drum brakes. For a common compact-sedan it takes more than 240 horsepower to achieve a deceleration of $-10^{\mathrm{m}}/_{\mathrm{s}^2}$ and, if strictly regenerative braking is used, the ability to absorb the energy in the battery or other storage is necessary. Direct braking has the advantages that the torque of the motor is a fairly linear relationship to voltage rather the complicated nonlinear friction dynamics in disc brakes, also most of the energy consumed in braking can be converted to electrical energy rather than heat which is wasted. There is even potential for harvesting surplus energy generated in long downhill sections. Lastly, having lower braking capabilities could help maintain a tighter braking distribution, the advantages of which are discussed in the previous chapter. In a constrained, AET environment it is possible that vehicles, though equipped with disc brakes, would only use engine braking while automated for greater efficiency and control. Other assumptions include that the wheel is rigidly connected to the motor and that the significant dynamics are included in the model.

The PI controller is based on negative feedback. This assumes the acceleration is accurately measured. Noise in the feedback measurement is beyond the scope of this investigation. As is, the PI controller is only loosely tuned to introduce some imperfection in control. PID control (from which PI is derived) is robust against variation and common in literature (i.e. [12]).

3.2 Model Verification

In developing such a model, it is useful to seek verification to ensure proper implementation and realistic results. Since this model is simply many common models put together, verification is accomplished here in the form of reproduction of published results. Beginning with recreating the results from an IEEE paper regarding the LuGre model, the results are shown as each additional part of the model is added.

Canudas de Wit and Horowitz develop an observer to identify θ and the vehicle linear velocity v using only information from a wheel rotation sensor [39]. This is tested through varying θ while accelerating and decelerating. While the primary purpose in the article is to prove the observer, but if the actual system behaves the same with the same input, it shows a correct implementation. Canudas de Wit and Horowitz use a single wheel model that does not include the viscous damping effect in the computation of wheel rotational accelerations (such that $\sigma_2 = 0$ in (3.1)). The other difference between this and the quarter vehicle model developed above is that the tractive force is not scaled to represent four wheels. For verification, the one wheel method is also used.

A torque profile as shown in Figure 3.2 is input while θ also varies according to the other plot in Figure 3.2. The input parameter values published and used are shown in Table 3.1. The resulting friction coefficient and vehicle velocity is plotted with respect to time in Figure 3.3. Comparison to plots in Canudas de Wit and Horowitz shows that the model follows very closely to published results.

The next step is to show the effects of the DC motor model. This is accomplished simply by using the same inputs and seeing if the outputs behave accordingly. The parameters used for the motor are in Table 3.2. These values are drawn from Lovatt et al. [40], where the motor designed is for a direct-drive, solar-powered vehicle. The resulting curves are superimposed on the previous results for comparison in Figure 3.4. To make clear the effects of adding the motor, the plots is Figure 3.5 show the difference of the two curves between the previous figures.

It is apparent in the figures the low-pass filter characteristics of the motor smooth out

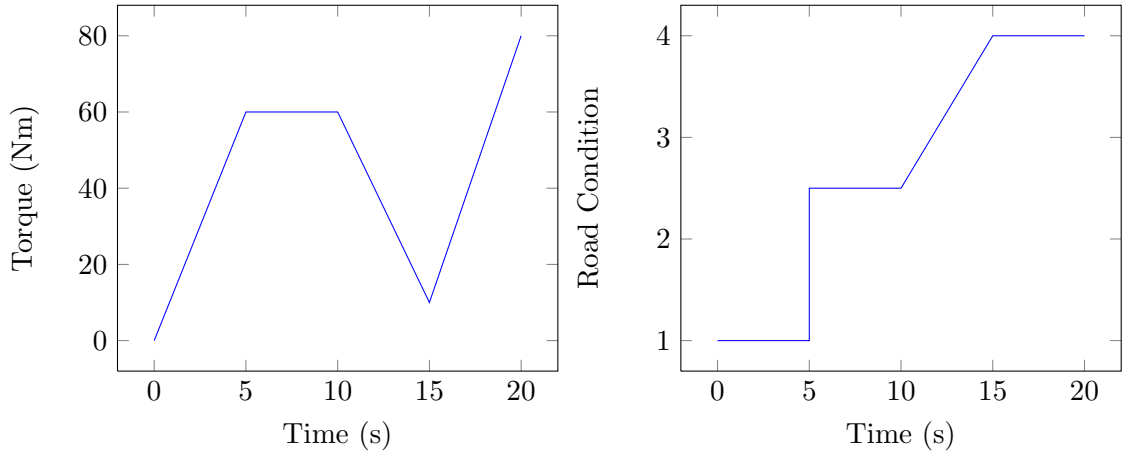

Fig. 3.2: Torque (τ) and road condition (θ) profiles for validating the LuGre model implementation.

Table 3.1: LuGre model values used for verification.

Parameter	Units	Value
μ_c	-	0.5
μ_{st}	-	0.9
σ_0	$^1/_{\mathrm{m}}$	40
σ_1	$^{\mathrm{s}}/_{\mathrm{m}}$	4.49487
σ_2	$^{\mathrm{s}}/_{\mathrm{m}}$	0.0018
v_s	$^{\mathrm{m}}/_{\mathrm{s}}$	12.5
h	m	0.25
m	Kg	5
J	Kgm^2	0.2344
B	$^{\mathrm{Kgm}^2}/_{\mathrm{s}}$	1.2285
F_n	N	14

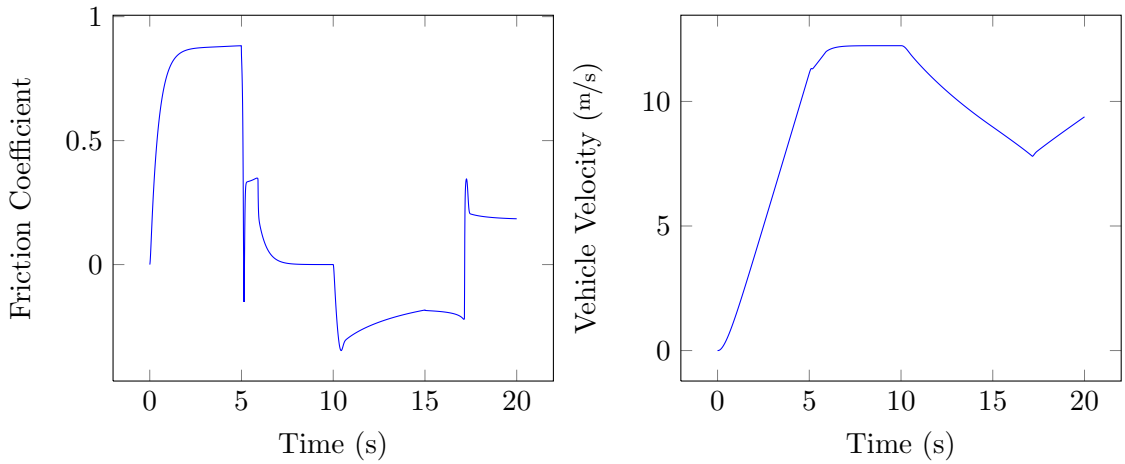

Fig. 3.3: Friction coefficient (μ) and vehicle velocity (v) output from LuGre model.

Table 3.2: Values used for verification of DC motor.

Parameter	Units	Value
L_m	μH	22
R_m	Ω	0.1
K_{emf}	$^{\text{Vs}}/_{\text{rad}}$	0.47
K_τ	$^{\text{Nm}}/_{\text{A}}$	0.49

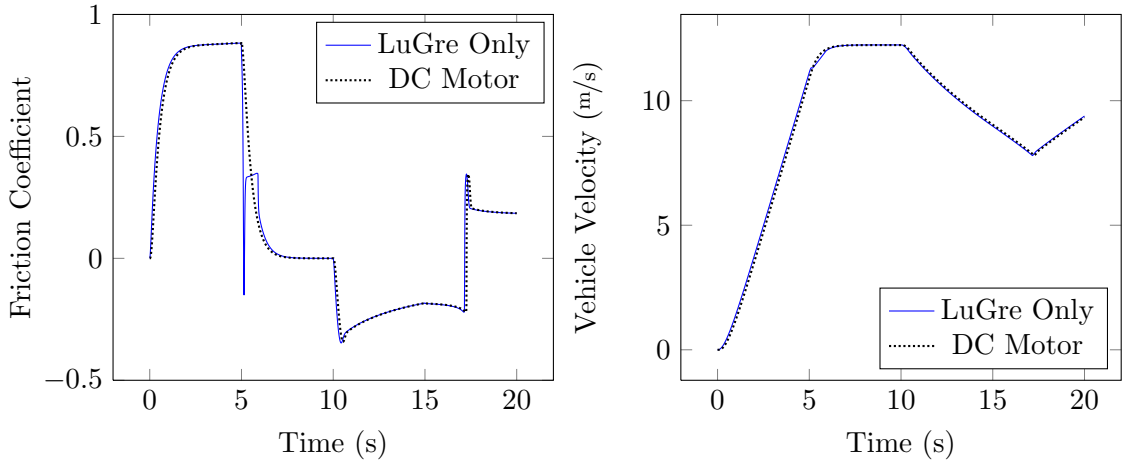

Fig. 3.4: Vehicle velocity (v) output from different model configurations.

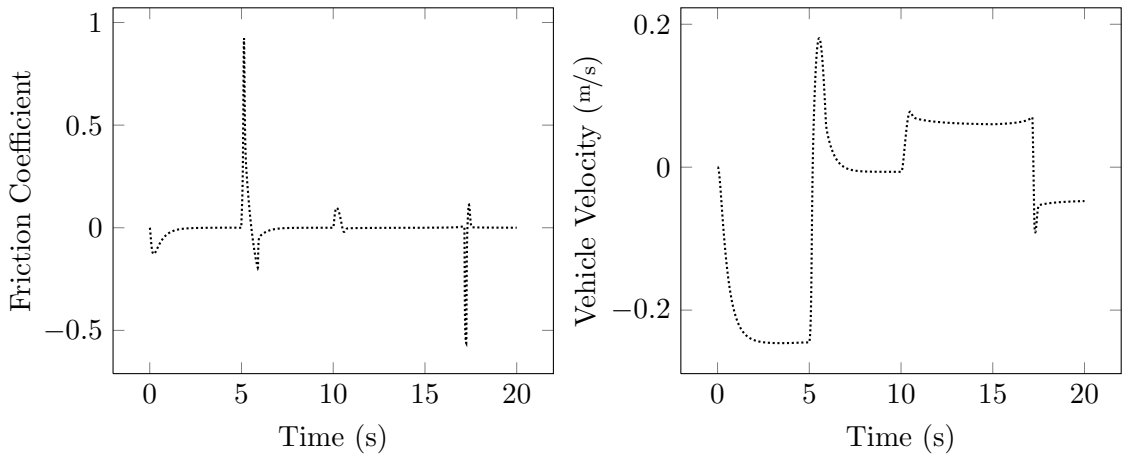

Fig. 3.5: Difference in friction coefficient (μ) and in vehicle velocity (v) output from including DC motor with model.

the changes in coefficient of friction which directly affects acceleration. Figure 3.5 shows that this smoothing does not have significant effect on the velocity and since all vehicles would be actuated through this same method it has benefits to rider comfort without greatly compromising the performance. Because of this low-pass filter characteristic, there is no need to model an automatic braking system (ABS) or other traction control. Implementation of such an ABS system shows no change in the results from the DC motor.

3.3 Parameters Subject to Variation

There are infinitely many things that can happen to any system, but many situations are so rare they need not be considered. Thus tire inflation and battery state of charge are considered, but alien abduction and black holes are not. Other physical parameters considered are tire tread condition, coefficient of aerodynamic friction, and payload (mass).

It is difficult to represent a system as complex as a vehicle, which is why simplification is so common in modeling. Representing variation in an organized manner can be especially difficult. Often the parameters are correlated in some way and since there is not a physical vehicle available where all parameters can be measured as the equipment is worn over thousands of miles, the variation must be modeled using simplifying assumptions. For example, the inflation of a tire would surely affect all the parameters in the LuGre model, but it is simplified to only a change in effective radius. This is justified through the assumption that inflation does not have a great effect on coefficient of friction, as confirmed by MacIsaac and Garrott [41]. A 50% decrease in pressure only created approximately seven percent decrease in the maximum friction coefficient. Similarly tire tread variation is represented using the model variable θ used by Canudas de Wit et al. [30] for general road or tire variations.

The aerodynamic drag coefficient is defined explicitly in the model, but variation represents either a change in the vehicle shape or surface. If vehicles are not allowed external payloads this can easily be controlled. The effects of drafting as vehicles follow very closely will have influence on this term, but the relationship is very complex.

The state of charge of the battery is significant because when batteries are in a low

state of charge the full voltage is not available. While AET vehicles have the benefit of charging while on the highway the possibility exists that an emergency situation occurs immediately after some vehicle has just entered the automated lane with a low battery.

3.4 Variation in a_{min}

Safety is most sensitive to variation in a_{min} between vehicles in a platoon, as previously found in Chapter 2. To put the physical parameter variation in context of the previous chapter, parameters were varied until the a_{min} values used for the strict and loose distributions (summarized in Table 2.2) were reached. The input to the model described in Section 3.1 was changed to have a vehicle immediately decelerate from an initial velocity of $v_0 = 30^{\mathrm{m}}/_{\mathrm{s}}$ until the vehicle has stopped. Minimum acceleration is achieved by inputing negative infinity as the controller reference. Since actual deceleration varies with respect to velocity, the value for a_{min} is taken to be the mean value of acceleration during the simulation.

The vehicle parameter values used for this analysis are drawn from Yi et al. [42] including parameters for the LuGre model. These values represent Buick LeSabres used in PATH's research which are much larger vehicles than AET vehicles are likely to be, providing more conservative results. The values are summarized in Table 3.3. The DC motor model parameters are kept at those values used for model validation shown in Table 3.2. For the parameters to be varied (θ, h, V_{max}, C_d, and m) the values in Table 3.3 are the nominal values held while each is individually degraded until the a_{min} reaches the desired value. The resulting parameter values are shown in Table 3.4. Aerodynamic drag varied in this way does not produce enough effect on a_{min} to reach the values desired and so is not shown. Reducing effective wheel radius actually improves braking, since less torque is required for the same tractive force, and increasing radius seems an unrealistic variation, so the results are not shown. Since lower tire pressure increases the contact patch between the wheel and the road, this outcome is probably accurate.

In Table 3.4 it can be seen that, similar to aerodynamic drag coefficient, the parameter for tire condition θ is a weak parameter, unable to influence a_{min} enough to cause the full range of variation explored in Chapter 2. Since this is the most difficult parameter to draw

Table 3.3: Values used in physical vehicle model.

Parameter	Symbol	Units	Value
Mass	m	kg	1707
Tire Radius	h	m	0.323
Rotational Inertia	J	Kgm^2	2.603
Rotational Damping	B	$\mathrm{Kgm}^2/\mathrm{s}$	1.2257
Aerodynamic Drag Coeff.	C_d	-	0.3693
Max Voltage	V_{max}	V	± 250
Tire Condition	θ	-	1
Coulomb Friction Coeff.	μ_c	-	0.35
Static Friction Coeff.	μ_{st}	-	0.5
Spring Factor	σ_0	$1/\mathrm{m}$	100
Damping Factor	σ_1	s/m	0.7
Viscous Friction Factor	σ_2	s/m	0.011
Stribeck Velocity	v_s	m/s	10

Table 3.4: Values used to achieve a_{min}.

Parameter	Units	-10	-9.5	-9	-7.75	-5.5
θ	-	-	1.90	2.65	11.52	-
V_{max}	V	263.5	248.7	233.9	196.9	130.8
m	kg	1619	1710	1810	2119	3028

a physical interpretation, this does not conclusively prove that tire condition is not an issue, it rather suggests that this model may not accurately represent such variation. A University of Michigan study indicates that as a vehicle's tire tread depth decreases from seven to zero millimeters at 60mph the peak coefficient of friction goes from about 0.9 to about 0.6 on wet pavements [43], however for this work the topic is left for future research.

Variation in the state of charge is able to reach such values but must make nearly 50% deviation from the nominal value to reach the extreme of $-5.5 \mathrm{m/s^2}$. Since batteries are designed to maintain as constant a voltage as possible, it seems unlikely that this extreme will be reached even in unusual operational circumstances. It is also possible that if vehicles have a low enough state of charge at check-in they could be sent to a stationary charging station until a safer state is reached.

The final parameter is vehicle mass. While, like the state of charge, the full range of -10 to $-5.5 \mathrm{m/s^2}$ requires nearly doubling the mass, it is easily conceivable for some homogeneous vehicles to have several $70-90$kg passengers with baggage that contribute significant variations to the vehicle mass. The nominal vehicle mass used is from an ICE vehicle. An AET EV is likely to be much lighter since there is no need for a large, heavy battery pack or combustion engine. This would make variation due to passenger and payload mass much higher, but has the benefit that all vehicles have better braking to begin with. If all vehicles account for the heaviest vehicle, that vehicle being only as massive as today's sedans, then the lighter vehicles can derate braking to an easily manageable level, preventing braking saturation in the heavier vehicles, while still braking quickly overall. When development of real AET vehicles proceeds, the unloaded mass and the range of passenger and payload mass that will be possible must be carefully considered in order to analyze the variation in vehicle braking ability. Smaller vehicles that allow few passengers or cargo are less prone to variation, but can also be less convenient, useful, or comfortable.

3.5 Chapter Conclusions

A quarter-vehicle model is developed, incorporating the LuGre model to represent the tire-road interaction. The complete model has only five states requiring integration.

Physical parameters such as tire condition, battery charge, and vehicle mass have direct effect on the minimum acceleration. Battery state of charge and mass have greater effect than aerodynamic drag or tire condition, though tire condition still deserves investigation. In order to achieve strict braking distribution, mass and state of charge should be controlled as much as possible. The author is of the opinion that mass will play the largest single role in braking variation of AET vehicles. In reality the most likely cause of variation in braking ability will not be a large variation of a single parameter, but a combination of soft faults that each contribute to a dangerous compromise in braking ability. As AET vehicles are developed and hardware is being specified and selected, the likelihood of performance degradation, not just complete failure, must be considered. These results reinforce that variation is inevitable, and very careful measures must be taken to control variance as much as possible and design conservatively to account for a wide range of operation.

Chapter 4

Emergency Braking of a Full Platoon

The analyses above are all focused on the interactions of two vehicles in emergency brake scenarios. The models only represent events up until the point that an impact occurs. In this chapter the analysis is extended to a full platoon of five vehicles and includes an impact model such that the entire emergency scenario can be analyzed from full speed to a complete stop regardless of whether collisions occur. This model is used to reinforce the previous results, showing that variation in minimum acceleration has significant consequences, as well as suggest that correct ordering may mitigate the effects of variation.

4.1 Modeling the Platoon

The platoon is a collection of consecutive vehicles with intercommunication to achieve cooperative control, ideally acting as a single unit. In the platoon, several instances of the model developed in Chapter 3 are used, each being one of the vehicles. Said model describes the operation of the individual vehicles yet they are interconnected through wireless communication and sensing. Modeling of the wireless interconnects follows.

4.1.1 Communication

A simple model of communication is used, incorporating a constant delay on any signals communicated between vehicles. The model infrastructure is established so that much more complex and accurate models could be implemented for future use. Each vehicle communicates its own acceleration and velocity, and whether an emergency scenario has been detected.

In emergencies, it is likely desirable for vehicles to switch a new regulation layer control strategy that only operates in emergency conditions. Ideally all vehicles switch to the

emergency control at the same time, but due to communication delay some vehicles are aware of the emergency before others. Two types of emergency signal propagation are implemented: a serial propagation, where each vehicle receives the information one delay time after the preceding vehicle receives it, and a parallel propagation, where when one vehicle indicates an emergency all vehicles receive it at the same time.

Serial propagation is based on a communication architecture where each vehicle passes information along a direct link to the one following it. This has the advantage that accurate directional wireless links can be established, making high-speed communication possible, but presents security concerns as one malicious vehicle can easily forge or tamper with communicated information.

The parallel propagation is typical in a token-bus type communication architecture where all vehicles share a channel and use time division multiplexing to determine when one may communicate. All vehicles in such a system receive the same communication, but typically disregard the information coming from vehicles that are not immediately preceding them or leading the platoon. This is the communication architecture used by PATH [23] and is the one primarily considered in the analysis below.

4.1.2 Sensing

Like communication, a framework is put in the model to allow retrofitting with other sensor models, but only a simple one is used here. Headway to the preceding vehicle is measured as well as each vehicle's own speed and acceleration. This sensing model does not include any nonlinearities or dynamics. The information in this simplistic model comes from the actual vehicle states, but it passes through the sensor system, which later can incorporate noise, quantization, and other errors.

4.2 Regulation Layer Controller

Where the task of the physical layer controller is to linearize the vehicle such that it tracks the desired acceleration, the task of the regulation layer is to tell the physical layer what desired acceleration will achieve correct behavior. This is accomplished through

a combination of the measured and communicated information. A safe acceleration is calculated that will maintain string stability. The regulation layer is named so because it regulates the vehicle motion based on the situation of the platoon. It is also given to the regulation layer controller to maintain passenger comfort.

Vehicle control has been heavily researched. One controller developed by PATH that is often referenced in literature is that of Rajamani et al. [44]. This sliding mode controller uses preceding vehicle and leader acceleration and velocity, where many previous controllers also required position information to achieve string stability [45]. Though it has been shown that the string stability of this controller erodes as communication delay is introduced, it is simple enough to implement without extensive knowledge of the vehicles or the communication channel.

The controller is of the form:

$$\begin{aligned}\ddot{x}_i^* =&(1-C_1)\ddot{x}_{i-1} + C_1\ddot{x}_l - \left(2\zeta - C_1\left(\zeta + \sqrt{\zeta^2-1}\right)\right)\omega_n\dot{\epsilon}_i \\ &- C_1\left(\zeta + \sqrt{\zeta^2-1}\right)\omega_n(\dot{x}_i - \dot{x}_l) - \omega_n^2\epsilon_i\end{aligned}$$

where x is the position, the spacing error ϵ is defined as

$$\epsilon_i = x_{i-1} - x_i - l_{i-1} + H^*, \tag{4.1}$$

l_i being the length of the i^{th} vehicle and H^* being the desired headway. Note that the vehicles move in the positive x direction. The l index is used for the leader instead of a one, for clarity.

Rajamani et al. shows this controller to be string stable under the conditions $\zeta \geq 1$ and $C_1 < 1$. The gains and the values used in the controller for this analysis are found in Table 4.1. The leader information bias is set such that the leader and preceding vehicle information are considered equally. The damping ratio is set to critical damping, and the bandwidth is set very low, five radians per second, in order to improve rider comfort. In Godbole and Lygeros [46] and others, levels of jerk above five meters per second cubed are

considered uncomfortable. Thus the bandwidth is selected such that acceleration frequencies that contain such levels of jerk are attenuated. To further promote passenger comfort, the output of the controller is limited to magnitudes of two meters per second per second or less, as also done by Godbole and Lygeros in the PATH program.

This controller is sufficient for the analysis here since the emergency brake scenario is that being investigated. This controller will be used for only a few seconds in order to better represent occurrence of the emergency brake scenario at a random time.

4.2.1 Leader Control

At this level, the control of the leader during normal operation is more a problem of automatic cruise control than platoon control. Here the leader actually uses the Rajamani controller but uses the platoon desired velocity (v^*) in place of the leader velocity. Using the Rajamani controller in this way is like having the leader follow a "ghost car" which perfectly maintains the desired speed and headway in front of the leader. The lack of acceleration or spacing error between the leader and this imaginary ghost car makes all other terms go to zero.

$$\ddot{x}_l^* = \left(\zeta + \sqrt{\zeta^2 - 1}\right) \omega_n (\dot{x}_l - v^*)$$

The platoon desired velocity comes from the coordination layer which controls overall platoon behavior and interactions between platoons. The coordination layer is not modeled as only one platoon is being represented.

Table 4.1: Gain values and interpretation for physical layer controller.

Gain	Interpretation	Value
C_1	Leader information weighting	0.5
ζ	Damping ratio	1
ω_n	Controller bandwidth	5

4.2.2 Emergency Control

The topic at hand is safe vehicle behavior during emergency scenarios, so several controllers were implemented and tested. In each controller tested, the desired acceleration of the platoon leader is changed to an exogenously determined value selected for emergency braking $a_{\text{emergency}}$. The first control scheme attempted was to not switch controllers at all, other than the leader's as just noted.

The next control method is suggested by Choi and Darbha [47], who use analytical means to determine that it is better for all vehicles to match the acceleration of the preceding vehicle rather than any combination of preceding vehicle and leader acceleration. The reasoning is should a vehicle reach a braking saturation and have a collision, the following vehicles can brake at the lesser deceleration value of the saturated vehicle, reducing probability that vehicles further back in the platoon saturate, while still maintaining safe separations. Choi and Darbha explain this as the platoon breaking into subplatoons, each being led by a vehicle with saturated braking, all other vehicles in the platoon matching the subplatoon leader's acceleration. This establishes monotonically decreasing acceleration through the platoon. Here the controller is implemented by using the Rajamani controller and changing C_1 to zero, making the leader information not considered at all. A better implementation would be to actually change the leader information used by each vehicle to be the information of the subplatoon leader, the nearest preceding vehicle that has reached braking saturation, but this increases complexity significantly as it requires a method for subplatoon leaders' information be designated as the new leader information.

Another method tried, a variation of the Choi method, has each vehicle simply try to match the acceleration of the preceding vehicle. Referred to as the preceding acceleration method hereafter, in implementation, this controller is

$$\ddot{x}_l^* = a_{\text{emergency}},$$
$$\ddot{x}_i^* = \ddot{x}_{i-1}.$$

This controller is additionally limited to output negative values so that even if an impact

occurs no vehicle is commanded to accelerate, but passenger comfort limits are not enforced in emergency scenarios.

An alternative builds upon the preceding acceleration controller to include the headway error measurement, so each vehicle seeks to also maintain the desired headway or greater in addition to the preceding vehicle's acceleration. The equations then become

$$\ddot{x}_l^* = a_{\text{emergency}},$$
$$\ddot{x}_i^* = \ddot{x}_{i-1} + \epsilon,$$

where ϵ is the spacing error as defined in (4.1). This spacing error, though increasing the probability of saturation, helps keep the vehicles from colliding. This will be referred to as the preceding acceleration with headway (PAH) controller.

The final method used is simply to have all vehicles seek to hold the same predetermined target deceleration. This means no actual coordination once the emergency scenario is initiated. This has the advantage that the entire communication channel is then free to communicate the emergency signal to other vehicles, rather than trying to communicate state information as well. The emergency braking is also more robust to certain delays since the controller is no longer dependent on communication. Headway feedback from the sensors is also used here. This controller is referred to as the uncoordinated method as all vehicles are attempting to keep the same predetermined deceleration without sharing information directly. The controller follows the equations

$$\ddot{x}_l^* = a_{\text{emergency}},$$
$$\ddot{x}_i^* = a_{\text{emergency}} + \epsilon.$$

These methods are all dependent on appropriate choice of $a_{\text{emergency}}$ but to varying degrees. Too low a value (remembering that it is negative) results in many vehicles saturating while too high a value does not stop the platoon quickly. If the minimum acceleration is desired, $a_{\text{emergency}} = -\infty^{\text{m}}/\text{s}^2$ can be used, but this creates a large probability that there will

be collisions due to variation in vehicle masses. This is where Choi's suggestion is designed to have the advantage since no vehicle is required to brake harder than the preceding one, reducing probability of collisions even if the platoon leader is braking very hard. Theoretically, this will stop the platoon with the fewest primary collisions as fast as possible. The uncoordinated method, in contrast, is the most dependent on the choice of $a_{\text{emergency}}$ since every vehicle with $a_{min} > a_{\text{emergency}}$ will saturate braking.

The value used here for the controllers is $a_{\text{emergency}} = -10 \text{m/s}^2$. This is below the nominal vehicle's ability and will saturate some vehicles, but it is still reachable by the strongest braking vehicles.

4.3 Impact Dynamics

While the vehicles are wirelessly connected through communication, sensing, and control, if an impact occurs, the vehicles have a physical connection and there are additional dynamics between the vehicles.

Collision dynamics are very complicated in the general case, but collisions between vehicles are often modeled to analyze collisions for legal purposes [48]. One simple model developed for such analysis is developed by Brach [49]. This variation of the Hunt-Crossley model is developed empirically to represent the impulse curves between vehicles colliding, specifically in front to back accidents at lower speeds. This is the collision type expected to occur in platooning emergencies. Brach describes lower speeds as those below 9m/s. This is advantageous as the general strategy of platooning safety is based upon keeping Δv low and, as indicated by Brach, other models are not accurate in low Δv calculations as will be primarily studied here.

The model describes the contact force as

$$F_{Ci} = \begin{cases} c_{dmp}(\dot{x}_i - \dot{x}_{i-1})^b (x_i - x_{i-1} - l_{i-1})^c + k(x_i - x_{i-1})^a, & x_i - x_{i-1} \leq l_i \\ 0, & x_i - x_{i-1} > l_i, \end{cases}$$

$$c_{dmp} = \begin{cases} c'_{dmp}, & t \leq t_p \\ c'_{dmp}\left(\frac{t}{t_p}\right)^d, & t > t_p, \end{cases}$$

where c'_{dmp} is a damping constant, k is a stiffness coefficient, t_p is the time of the peak force, and a, b, c, and d are constants used to match measured data. The values used are drawn from an example given in the same paper, shown here in Table 4.2.

This collision model covers the damping caused by crumple zones and also the spring-like restorative force, but the changes in vehicle length due to crumple are not accounted for. This has the largest effect in simulations where the vehicles have multiple impacts. The first crushes the crumple zone, leaving less (or no) material damping from crumple when the subsequent collisions occur. This model effectively resets the car to its undamaged state as soon as contact between the vehicles is lost.

The contact force is equal and opposite between colliding vehicles. When impacts are occurring, each vehicle has a net force from the gross preceding and following vehicle collision forces. In an n vehicle platoon the net force is calculated as

$$F_{Ci\text{net}} = \begin{cases} F_{Ci}, & i = 1 \\ F_{Ci} - F_{Ci-1}, & i = 2, 3 \ldots n-1 \\ -F_{Ci-1}, & i = n \end{cases},$$

Table 4.2: Values used for collision model.

Parameter	Units	Value
c'_{dmp}	$\mathrm{kNs/m^2}$	95.8
k	kN/m	73
t_p	s	0.07
a	-	1
b	-	1
c	-	1
d	-	3

which makes the complete longitudinal vehicle dynamics for each vehicle,

$$\dot{x} = v$$

$$\dot{v} = \ddot{x} = a$$

$$a = \frac{4F_{tr} - C_d v^2 + F_{Ci\text{net}}}{M}.$$

4.4 Simulation

A platoon of five vehicles is assembled with a desired following distance of one meter. The vehicles travel for one second of normal operation to better simulate the small errors that are likely to be present during normal operation, creating more realistic initial conditions for the emergency. After one second of travel, an emergency brake is initiated by the leader who immediately switches to the emergency controller. The emergency signal is transmitted to the following vehicles which all receive it at the same time and switch to emergency control. The details of the Simulink implementation are found in Appendix B.

4.4.1 Metrics

The emergency situation calls for all vehicles to stop as quickly as possible, while (ideally) collisions within the platoon are reduced or eliminated. Unsafe collisions however, are not acceptable. Thus several metrics of importance can be used to interpret the data: the peak collision force, vehicle acceleration, the total time to stop, the vehicle jerk, and, as discussed in Chapter 2, the Δv. These will each be used in the discussion of the results.

The peak force in the impact is a good indicator of the damages done to the vehicle. The larger the force, the deeper into the crumple zone the imposing vehicle reaches. As force rises, the chance of injury to occupants rises, though the threshold that results in injury, as well as the cost of damages done varies a great deal, so quantization of these matters is beyond the scope of this research.

The peak force gives some indication to passenger safety, but in complex pile-up collisions (as may occur in a platoon) impact forces come from forward and behind so the

net force is not as great. The net force manifests in the vehicle acceleration, thus rather than include an additional plot, acceleration is used in the discussion. Acceleration is often a key metric in analyzing passenger safety in collisions such as the analysis of whiplash-associated-disorders (WAD) by Krafft et al. [50].

The time to stop should be minimized, since the cause of emergency brake scenarios is not fully researched. If the braking is due to an object in the road, compromise in stopping time (and the resulting longer stopping distance) will have significant changes to safety.

Jerk contributes to rider comfort but also to safety. Hynes and Dickey [51] show that the magnitude of jerk changes the head accelerations that lead to WAD even if the vehicle acceleration is the same magnitude. While no threshold for safety is given, in general lesser magnitude is better. Jerk is the derivative of acceleration, so sharp corners or cusps in the acceleration curve are undesirable.

4.4.2 Five Vehicle Platoon with Random Masses

The vehicles are assigned masses from a distribution with mean at the nominal 1707kg and variance of 6400kg corresponding approximately to a strict braking distribution as found in the results of Chapter 3. The resulting masses are listed in Table 4.3. While vehicle three is less massive than the nominal, this is not unacceptable, since it is likely AET vehicles will be lighter than the Buick LeSabres of the 1990s that the nominal values are taken from. However, the overall range of 327kg seems a fairly significant amount of variation if the vehicles are of homogeneous type. The operating range of mass of AET vehicles must be determined before qualifications can be made about the reasonableness of

Table 4.3: Masses of vehicles in random-ordered platoon.

Vehicle	Mass (Kg)
1	1750.0
2	1853.7
3	1526.3
4	1776.0
5	1732.5

this variance.

For each controller implemented the acceleration and velocity of each vehicle and the headway and collision force between vehicles are plotted. The resulting curves are shown in Figure 4.1 for the Rajamani controller method, Figure 4.2 for the Choi method, and Figures 4.3, 4.4, and 4.5 for the preceding acceleration, PAH, and uncoordinated method controllers, respectively. The Δv of the initial impacts are summarized in Table 4.4 along with the peak impact forces in Table 4.5 and the time required to stop the platoon for each controller is shown in Table 4.6.

Note that because the braking is performed through the direct-drive motors, when the vehicle reaches a stop the regulation layer controller must switch to have desired acceleration zero or the vehicle will begin moving in reverse. This switching causes chatter seen at the end of the acceleration plots of Figures 4.4 and 4.5.

From Table 4.4 it is apparent that the collision between the second vehicle and the leader is not avoidable under these conditions and that Δv between said vehicles does not vary, regardless of the controller. This is simply due to the braking disparity caused by the 100kg extra mass in vehicle two. This can easily be the difference of a single passenger and exhibits the consequence of disparity in braking ability caused by mass variation. Fortunately, as designed, the vehicles are following closely enough that Δv is still less than half of $\Delta v_{safe} = 2.5^{\mathrm{m}}/_{\mathrm{s}}$ as assumed in Chapter 2.

Table 4.5 shows that even though Δv is the same, the peak force of the collision does change depending on controller. The collision with lowest Δv (between vehicles two and three under preceding acceleration control) also had greatest peak force. These results indicate the assumptions made relating Δv to safety are only somewhat accurate in multiple vehicle situations. This is possibly due to pileup effect, since vehicles behind push the others into more severe collisions.

The Rajamani and Choi controllers have practically identical output in this scenario. It is possible that the benefits described by Choi are not manifest until the platoon is larger than only five cars. With the current platoon setup both controllers perform very well, with

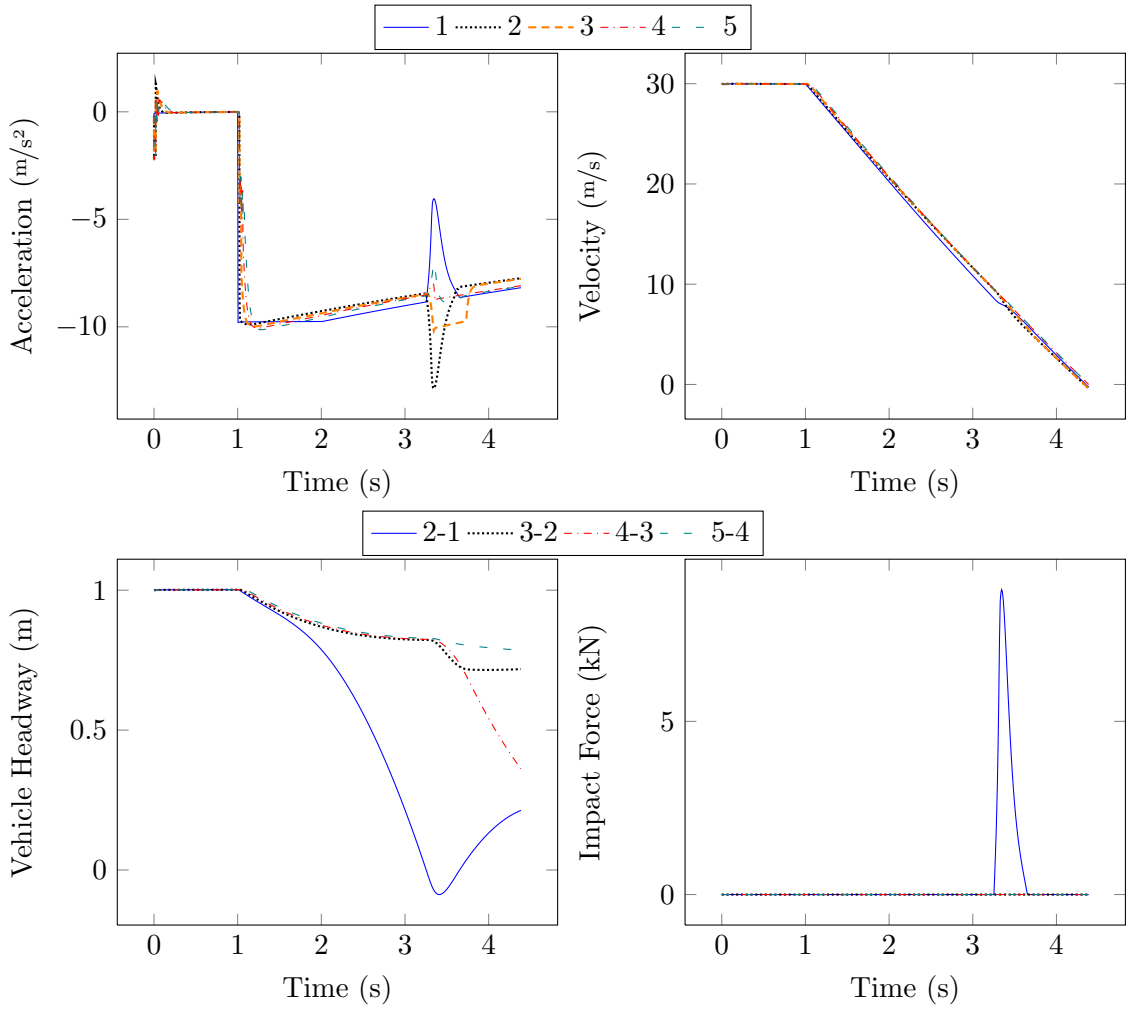

Fig. 4.1: Results of random-ordered platoon in emergency brake scenario using Rajamani controller.

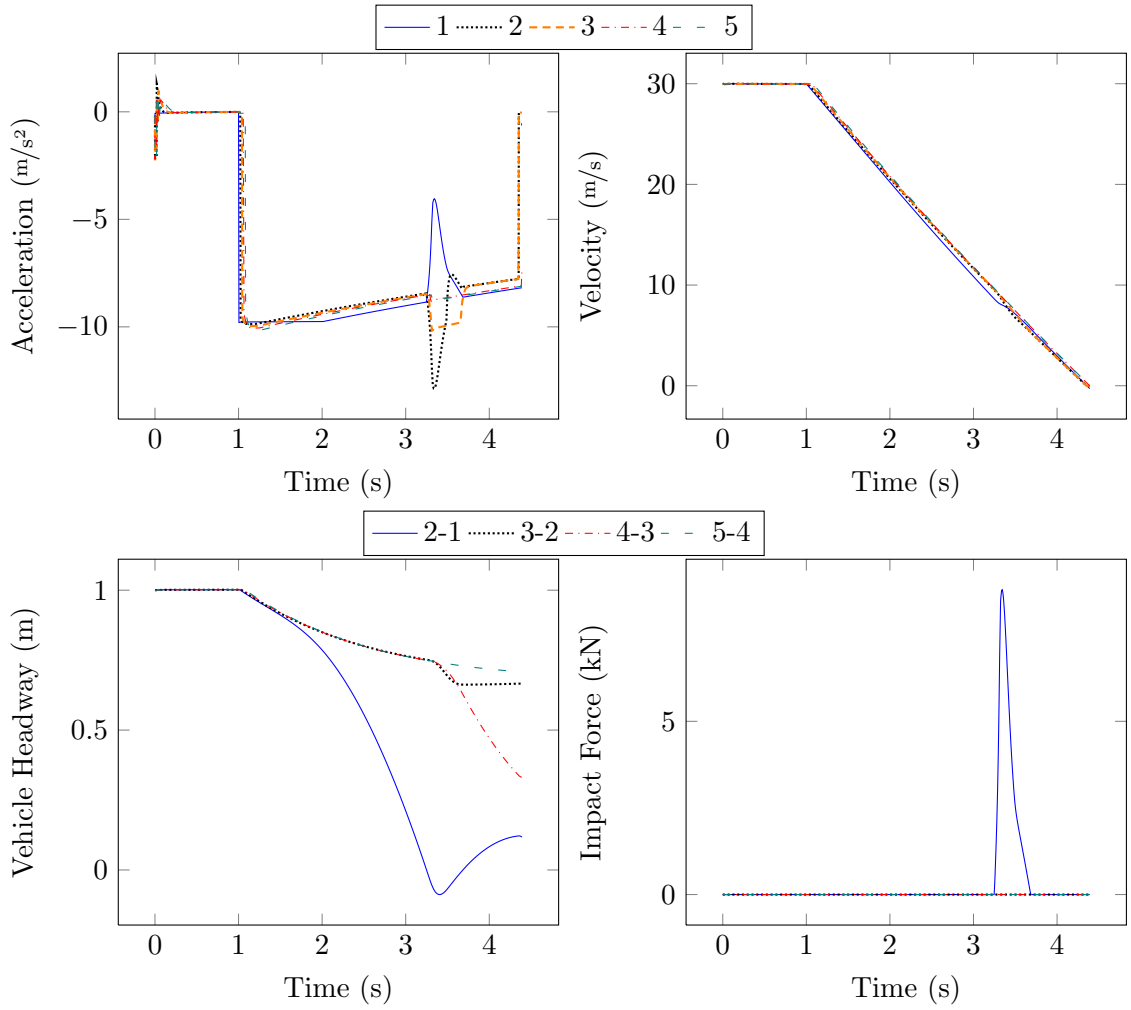

Fig. 4.2: Results of random-ordered platoon in emergency brake scenario using Choi controller.

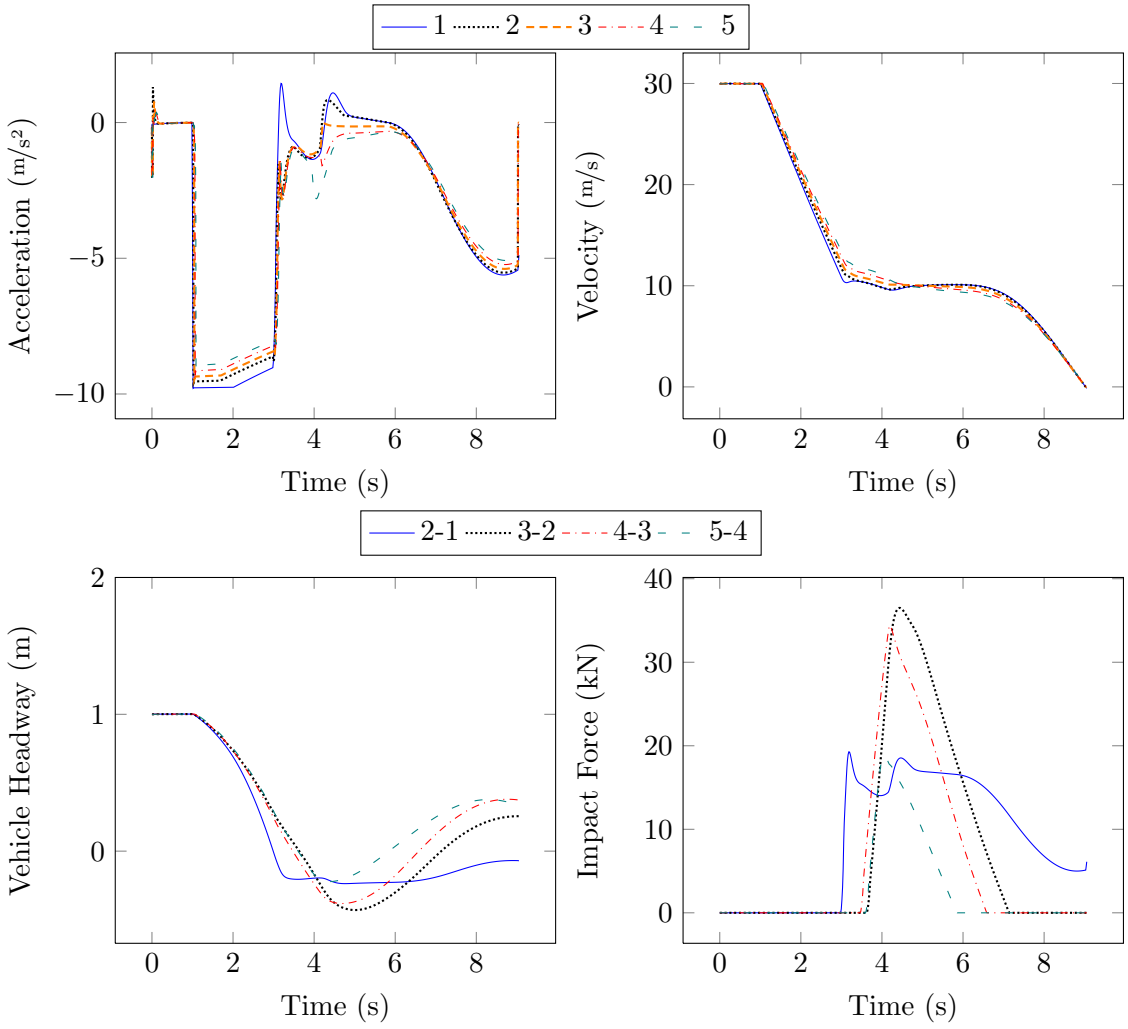

Fig. 4.3: Results of random-ordered platoon in emergency brake scenario using preceding acceleration controller.

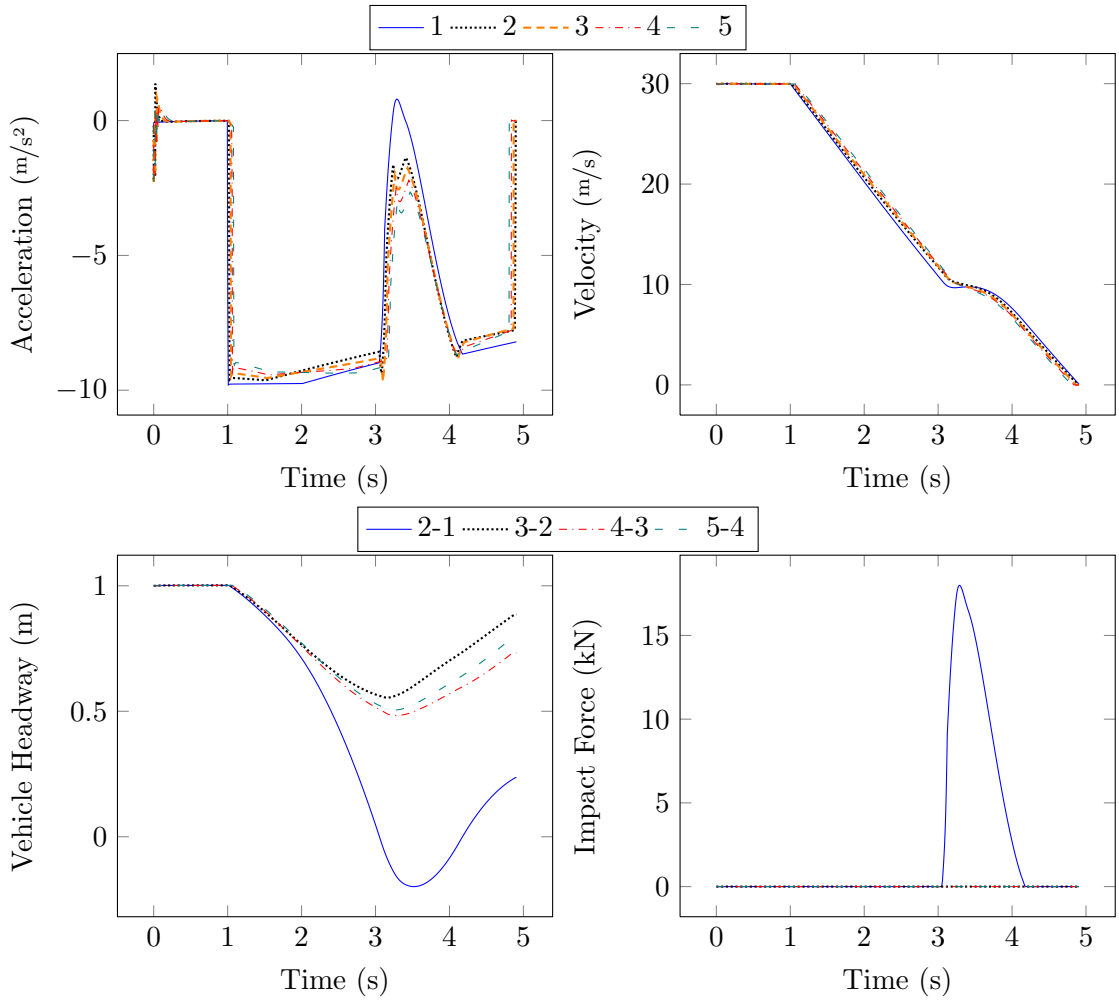

Fig. 4.4: Results of random-ordered platoon in emergency brake scenario using PAH controller.

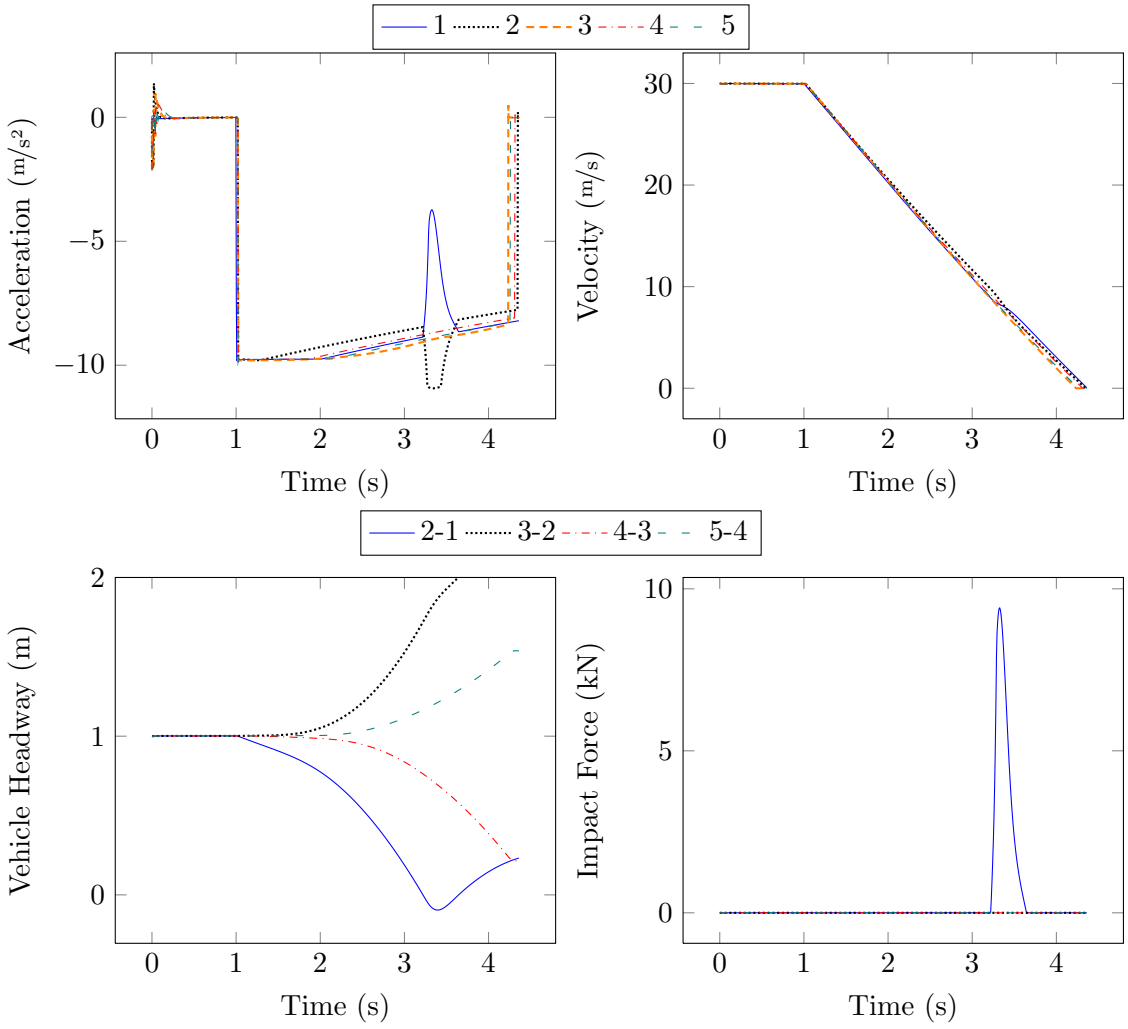

Fig. 4.5: Results of random-ordered platoon in emergency brake scenario using uncoordinated controller.

the lowest collision force and low stopping time.

Tables 4.4 through 4.6 illustrate clearly that the preceding acceleration method is not adequate. It is the only controller that caused multiple collisions and has the longest stop time. Figure 4.3 shows under this control there is significant jerk and the impact forces are the greatest, though the actual accelerations are not greater than those of the other controllers. This poor performance is because rear-end collisions accelerate a vehicle forward, causing the following vehicle to accelerate to match rather than brake harder, exacerbating the crash. That this controller does not work well is not surprising with consideration that it uses the least amount of information and the acceleration information it does use is delayed through the communication channel.

The PAH controller performs well in the stopping time, but has double the impact forces of the Rajamani and Choi controllers. Perhaps tuning with a gain for the spacing error term could improve performance, but other controllers already developed outperform it. The final controller is the uncoordinated controller. It is the fastest stopping overall, since all vehicles were attempting to brake at $a_{\text{emergency}}$ though the time difference is only 0.02s. The impact that occurs has slightly more force than that in the Rajamani and Choi control schemes. This indicates that the headway measurement is a larger contributer to safety than communicating acceleration as done by the PAH controller. This observation is weak however because of the assumptions made in the sensing and communication models. The headway measurement is perfect, continuous and instantaneous, whereas the communication is perfect, continuous, and delayed 20ms.

Table 4.4: Δv of impacts in random-ordered platoon under different control strategies.

	Δv (m/s)				
Vehicles	Rajamani	Choi	Prec. Acc.	PAH	Uncoord.
2-1	0.9	0.9	0.9	0.9	0.9
3-2	-	-	0.4	-	-
4-3	-	-	0.5	-	-
5-4	-	-	0.5	-	-

Table 4.5: Peak impact force in random-ordered platoon under different control strategies.

	F_C (N)				
Vehicles	Rajamani	Choi	Prec. Acc.	PAH	Uncoord.
2-1	8803	8800	19296	17992	09412
3-2	-	-	36509	-	0
4-3	-	-	34420	-	0
5-4	-	-	18791	-	0

Table 4.6: Time to stop a random-ordered platoon under different control strategies.

Controller	Stop Time (s)
Rajamani	4.39
Choi	4.39
Prec. Acc.	9.05
PAH	4.91
Uncoord.	4.37

4.4.3 Five Vehicle Platoon with Heaviest Vehicle in Rear

The order of the vehicles in the platoon is switched so that the most massive is the last vehicle in the platoon, the others remaining the same. This is generally the least desirable arrangement as the vehicles in front will surely have superior braking over the final vehicle, the absolute worst arrangement being monotonically increasing mass with each vehicle. The masses as now arranged are shown in Table 4.7. This arrangement is to provide additional insight to the performance of the controllers under poor platoon ordering.

The resulting curves are shown in Figures 4.6 through 4.10 in the same order as previously displayed. The Δv of the initial impacts are shown in Table 4.8, collision force peaks in Table 4.9, and the stopping time in Table 4.10.

Table 4.7: Masses of vehicles in heaviest-in-rear platoon.

Vehicle	Mass (Kg)
1	1750.0
2	1526.3
3	1776.0
4	1732.5
5	1853.7

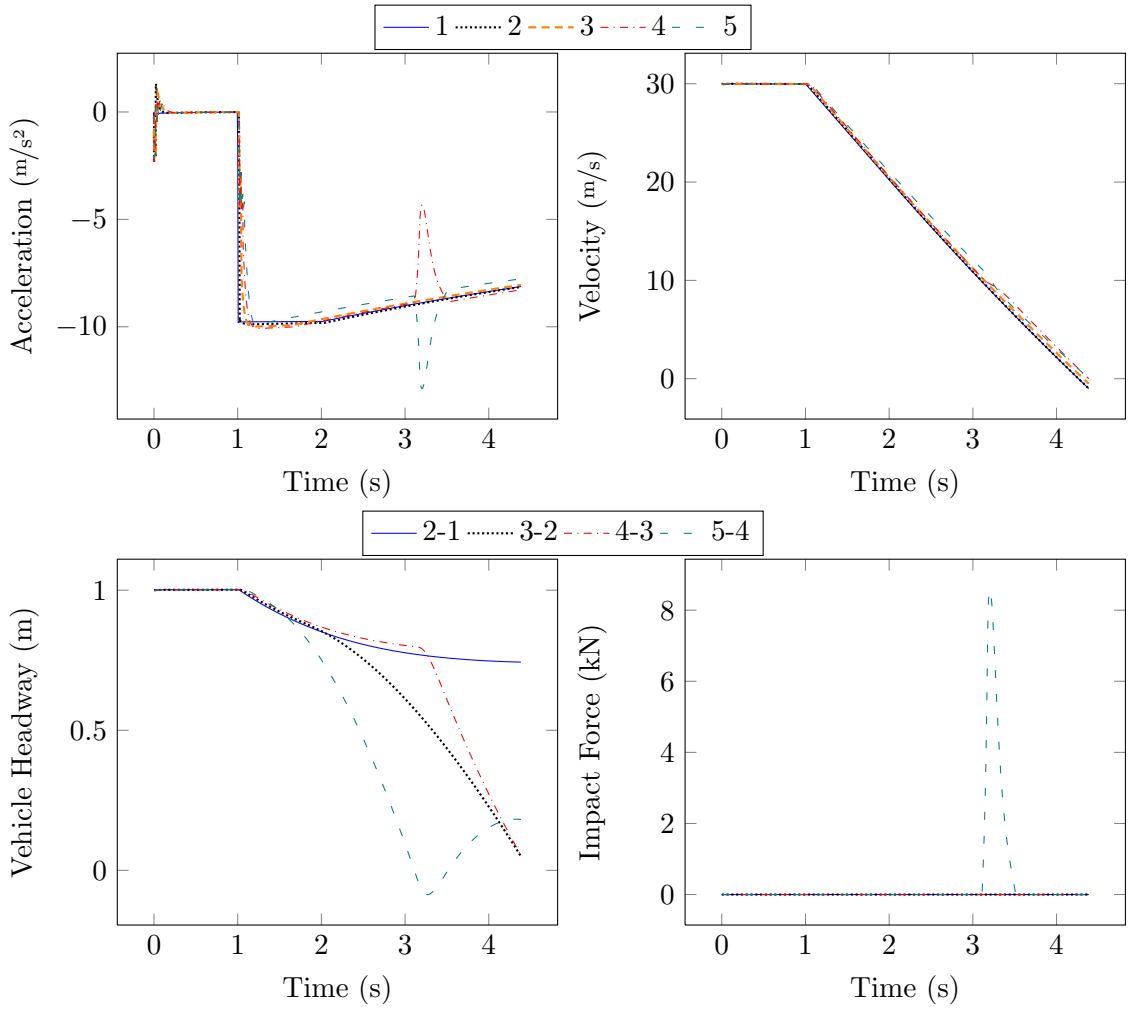

Fig. 4.6: Results of heaviest-in-rear platoon in emergency brake scenario using Rajamani controller.

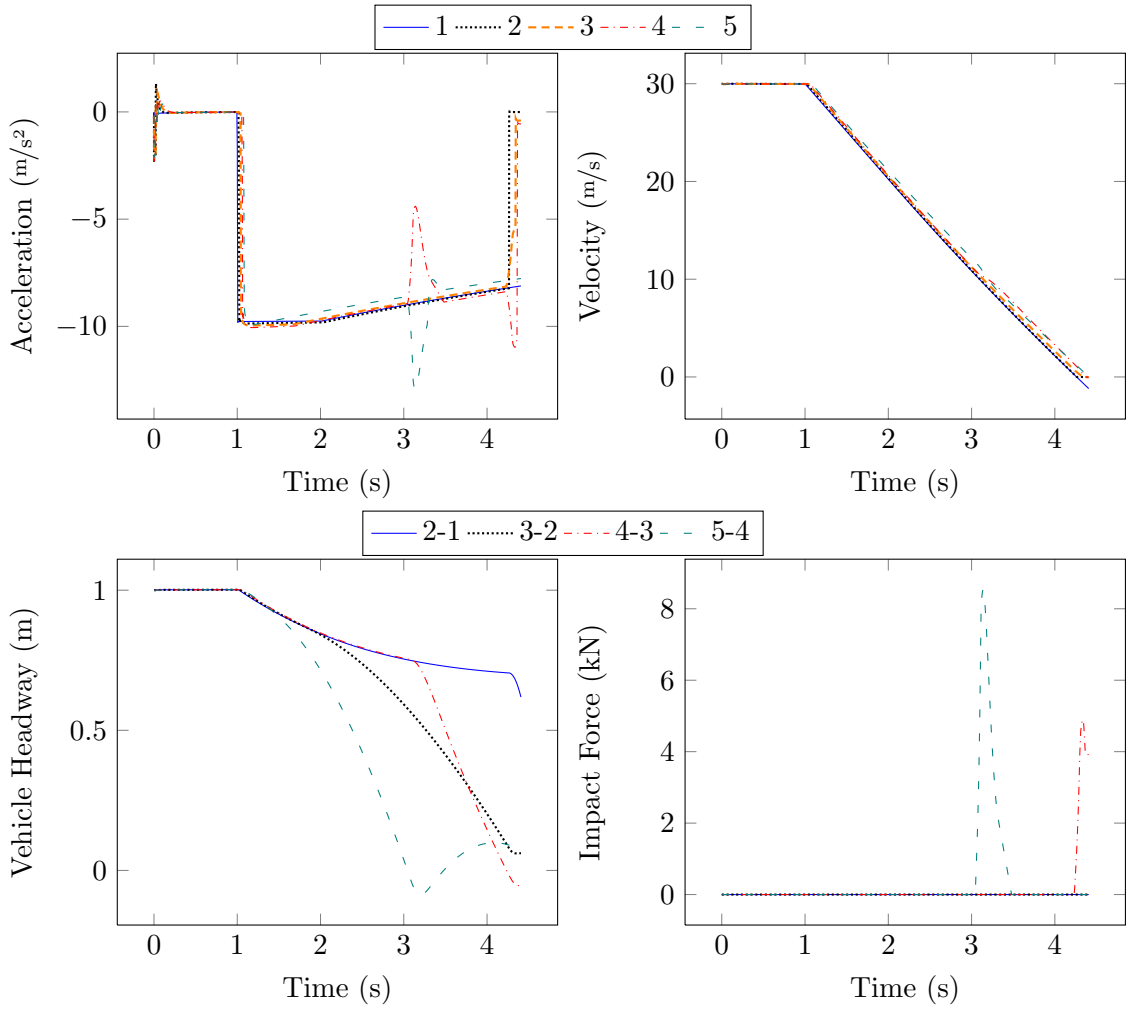

Fig. 4.7: Results of heaviest-in-rear platoon in emergency brake scenario using Choi controller.

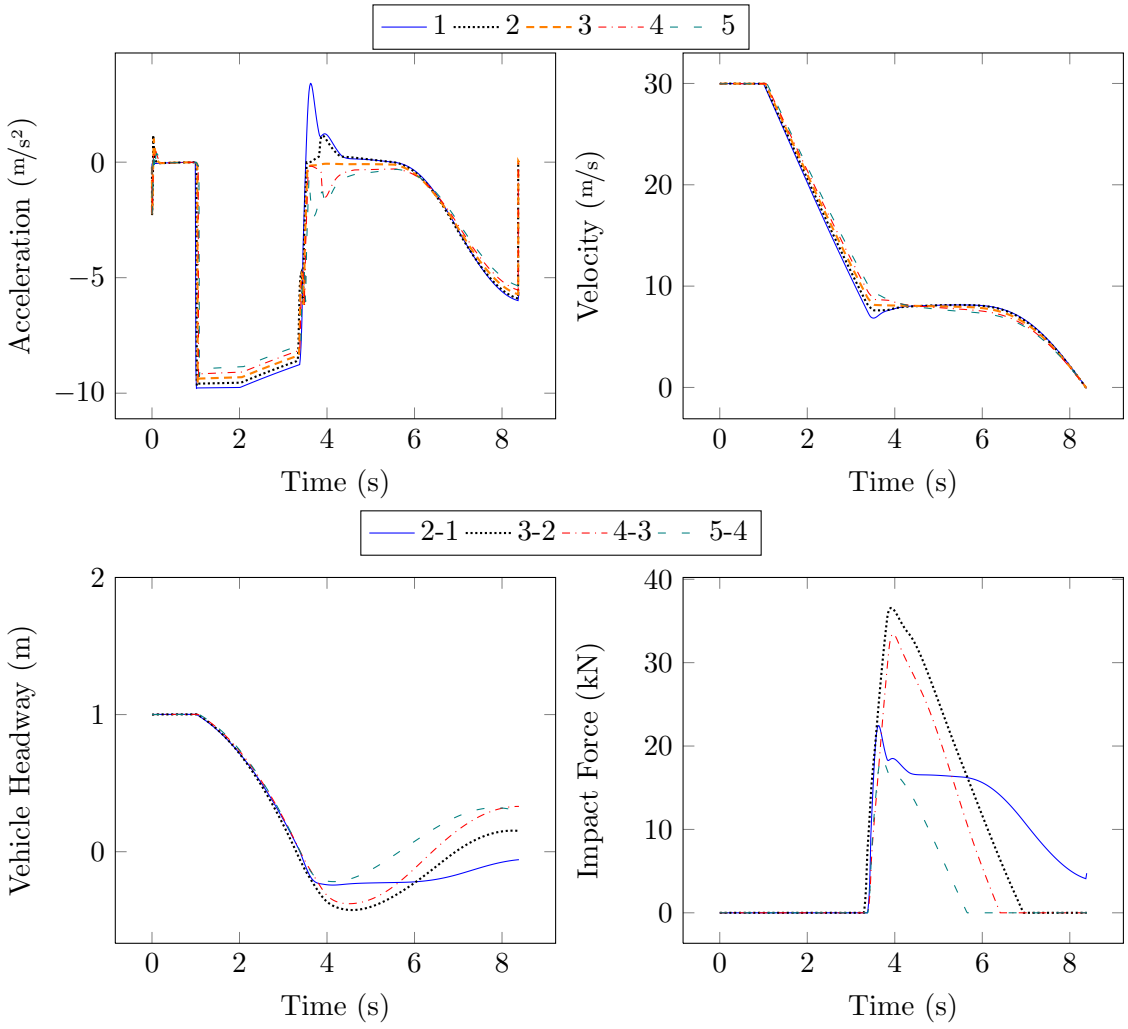

Fig. 4.8: Results of heaviest-in-rear platoon in emergency brake scenario using preceding acceleration controller.

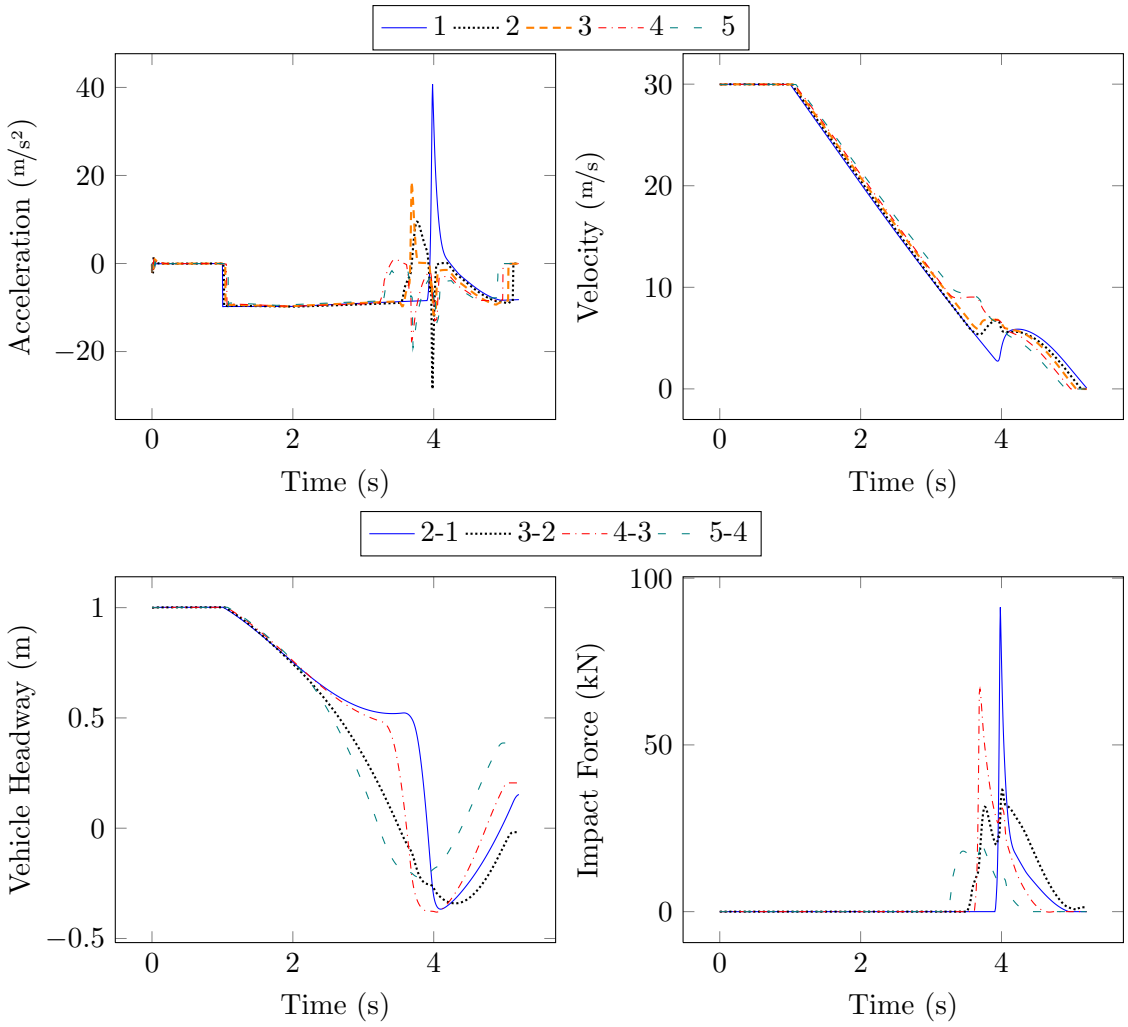

Fig. 4.9: Results of heaviest-in-rear platoon in emergency brake scenario using PAH controller.

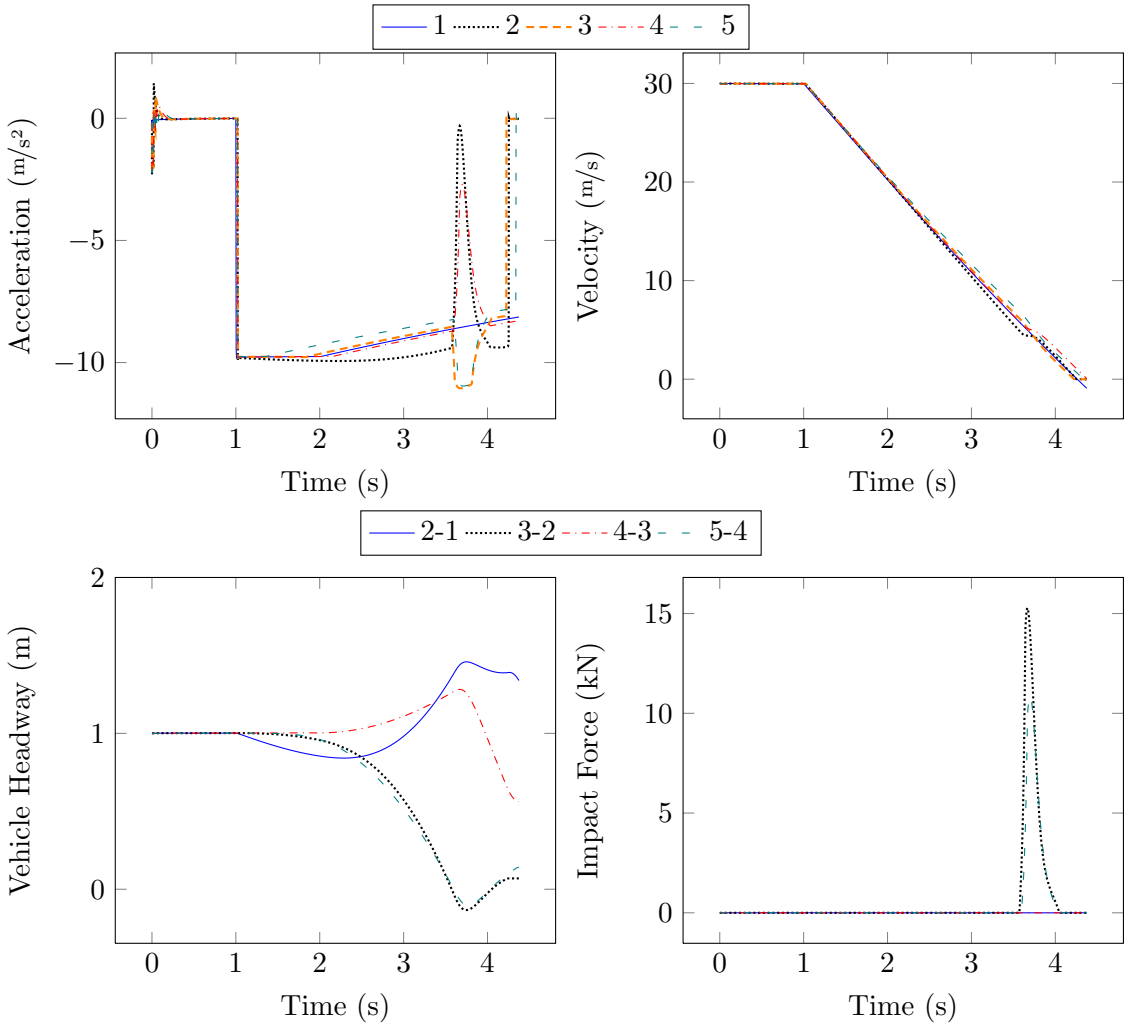

Fig. 4.10: Results of heaviest-in-rear platoon in emergency brake scenario using uncoordinated controller.

Once again the most massive vehicle consistently collides with the preceding vehicle, regardless of the controller used. In this case as Table 4.8 shows, the Δv for this vehicle are all very similar, attributable to the consistent one-meter spacing of the platoon. However, again the peak collision forces vary, especially in the preceding acceleration and PAH cases where pileups occur. In these results however, it is more clear that peak impact force is generally proportional to Δv when pileups do not occur.

The Rajamani controller had a faster stopping time than the Choi in this case, since under the Choi controller the fourth vehicle was effectively pushed into the third by the most massive fifth (see the headways in Figure 4.7). The difference in control that caused this behavior is the leader brake maneuver information that reaches the other vehicles earlier so they begin reacting earlier rather than waiting for only the vehicle ahead to begin reacting. The difference in velocity that results is very small (indeed, Figures 4.6 and 4.7 seem nearly identical, observe the headway between vehicles three and four to notice), but this difference is enough that the Rajamani controlled vehicles come to a complete stop before a second collision occurs. This indicates that under constraints of communication delay the benefits Choi suggests begin to degrade. Admittedly, the implementation here is not a full realization of the strategy posed by Choi, only one inspired by it. A proper implementation where subplatoon leader information is communicated is necessary to fully explore the merit of Choi's work.

The preceding acceleration controller actually improved in stopping time, but still pales in comparison with the others in all the metrics. The PAH controller was slower in stopping time than in the last scenario and had collisions between every vehicle, two of which are

Table 4.8: Δv of impacts in heaviest-in-rear platoon under different control strategies.

	Δv ($^{m}/_{s}$)				
Vehicles	Rajamani	Choi	Prec. Acc.	PAH	Uncoord.
2-1	-	-	0.7	3.8	-
3-2	-	-	0.7	0.7	1.3
4-3	-	0.6	0.6	2.9	-
5-4	0.9	0.9	0.7	0.9	1.0

Table 4.9: Peak impact force in heaviest-in-rear platoon under different control strategies.

	F_C (N)				
Vehicles	Rajamani	Choi	Prec. Acc.	PAH	Uncoord.
2-1	-	-	22466	92973	0
3-2	-	-	36564	36505	15282
4-3	-	4890	33449	66922	0
5-4	8577	8534	18470	21398	10890

Table 4.10: Time to stop a heaviest-in-rear platoon under different control strategies.

Controller	Stop Time (s)
Rajamani	4.39
Choi	4.41
Prec. Acc.	8.39
PAH	5.22
Uncoord.	4.38

over Δv_{safe}. The impact forces are the largest generated in all the experiments performed here, with large acceleration and jerk on the vehicle. This control scheme is clearly unsafe with the most massive vehicle in the back. This is because all the vehicles are braking at saturation and so the additional braking required to preserve headway is unavailable. In the random-ordered platoon case above, the most massive vehicle was in the second position and would saturate at greater acceleration and the vehicles behind could more easily achieve the acceleration required to follow.

Finally, the uncoordinated case has the shortest stopping time but shows a weakness that the Rajamani and Choi controllers are able to avoid through communication. Each vehicle that follows a less massive vehicle (vehicles three and five) collides, with Δv values still below Δv_{safe} but greater than those of the other controllers save the PAH. The larger collision forces correlate with Δv.

4.4.4 Five Vehicle Platoon with Heaviest Vehicle as Leader

Finally, the platoon is set into a safer ordering with the most massive vehicle being in front as indicated by the masses in Table 4.11. This is not as ideal as a perfectly ordered

platoon with monotonically decreasing mass between each vehicle.

Figures 4.11 through 4.15 show the resulting curves in the same order as previously displayed. The Δv of the initial impacts are shown in Table 4.12, collision forces in Table 4.13, and the stopping time in Table 4.14.

Comparing these results to the previous two cases make it clear why SARTRE is designing their platooning system such that large cargo trucks are always lead vehicles with passenger cars as followers [10]. Collisions did not occur under the Rajamani and Choi control schemes and stopping times were only affected by 0.7% of the random order.

The preceding acceleraton controller continued to prove the least of controllers tried, with longer stopping time, collisions between every vehicle with greater impact forces than the PAH or uncoordinated cases. The PAH shows significant improvement with only one collision with $\Delta v = 0.3^{\mathrm{m}}/_{\mathrm{s}}$ and collision force of only one fifth of the force that occurs in the random-ordered platoon case. The uncoordinated case again shows weakness with the largest Δv and impact force of the group save again the preceding acceleration control scheme.

Testing the five emergency controllers under these three cases, random-order, heaviest-in-rear, and heaviest-as-lead, shows several things. First is the performance comparisons of the control schema as already discussed. The Rajamani controller proved the safest overall through the three cases.

The second concept shown through these simulation results is the benefit of coordination. The uncoordinated controller performed well in all cases but was outperformed by the Rajamani with regard to collision force, especially in the heaviest-in-rear and heaviest-

Table 4.11: Masses of vehicles in heaviest-as-lead platoon.

Vehicle	Mass (Kg)
1	1853.7
2	1750.0
3	1526.3
4	1776.0
5	1732.5

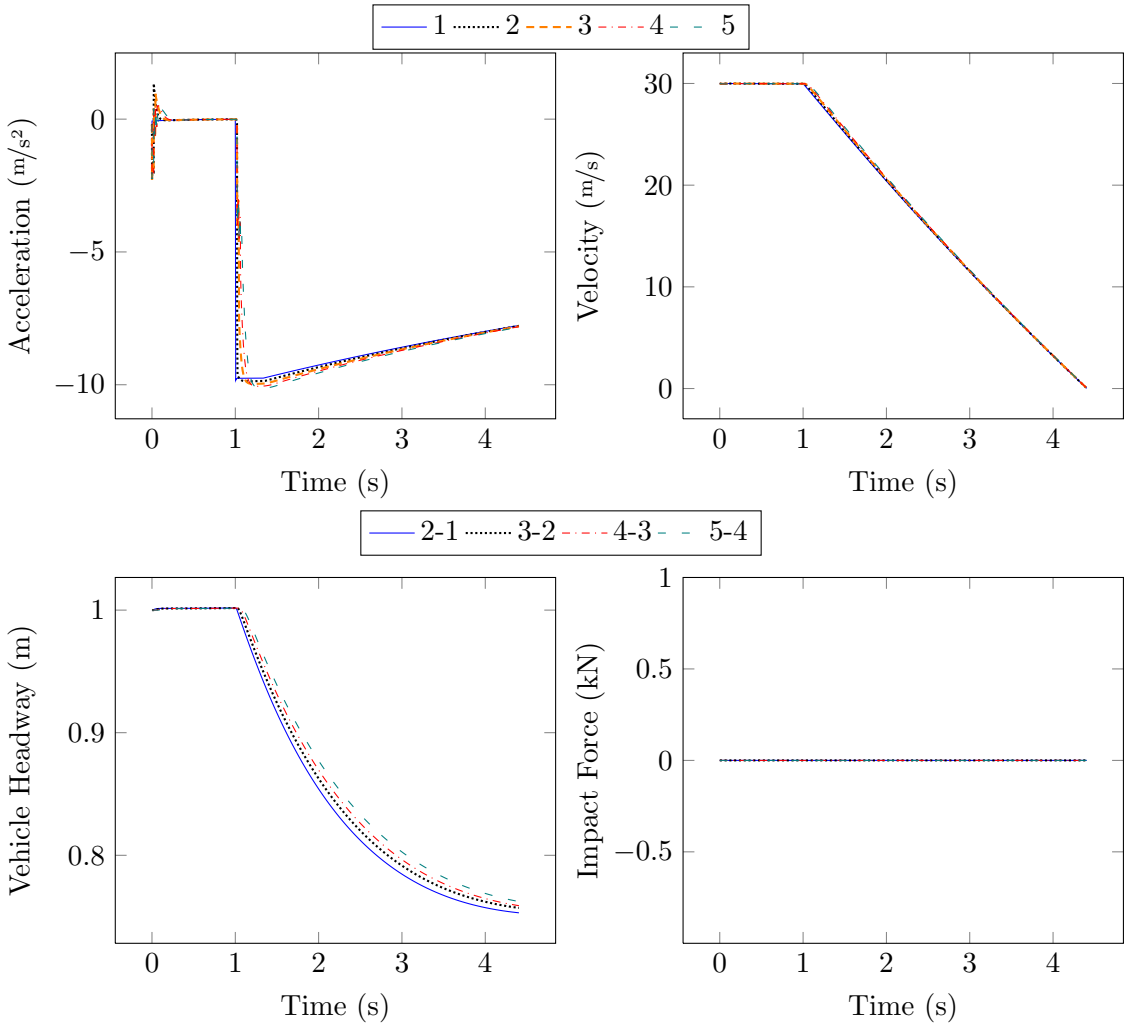

Fig. 4.11: Results of heaviest-as-lead platoon in emergency brake scenario using Rajamani controller.

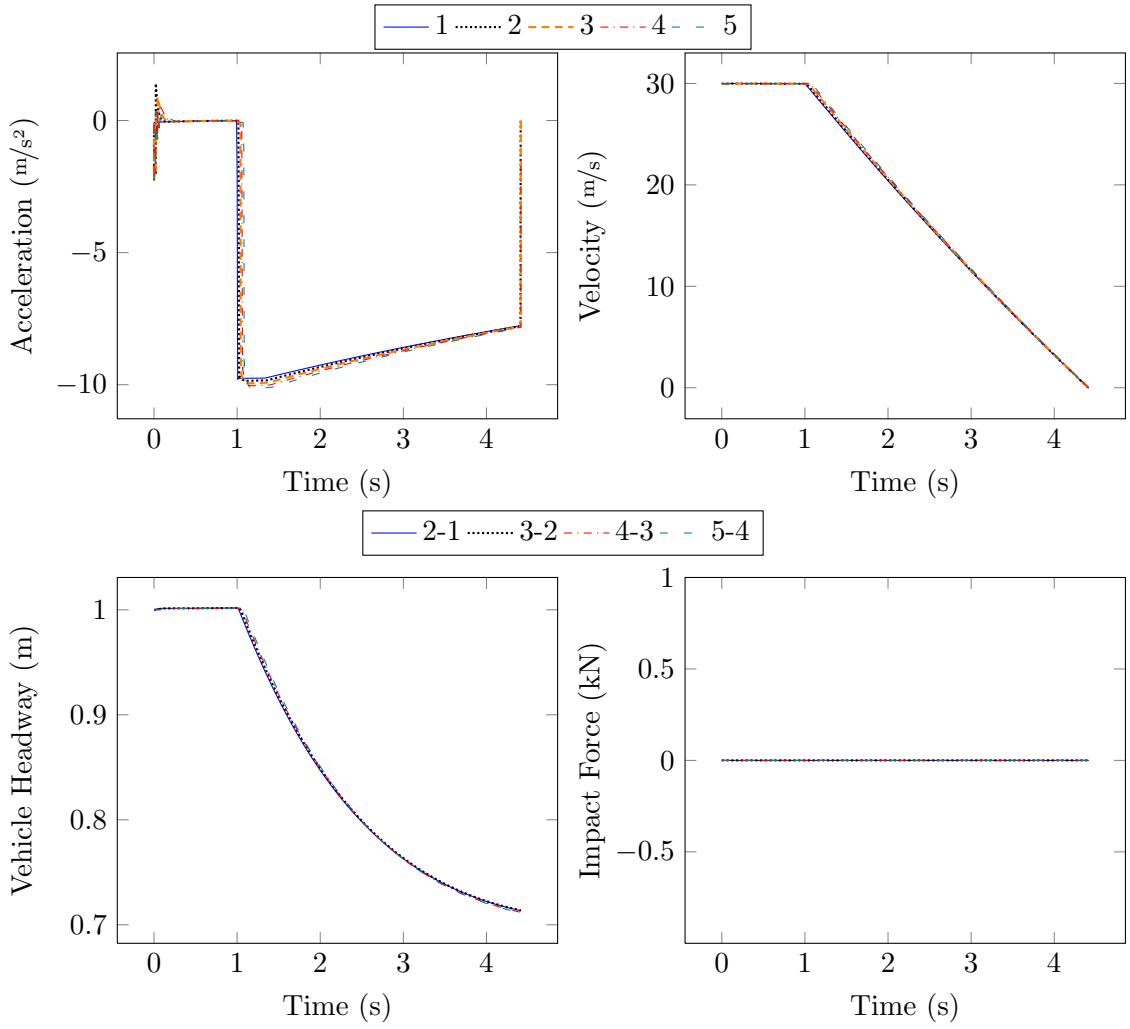

Fig. 4.12: Results of heaviest-as-lead platoon in emergency brake scenario using Choi controller.

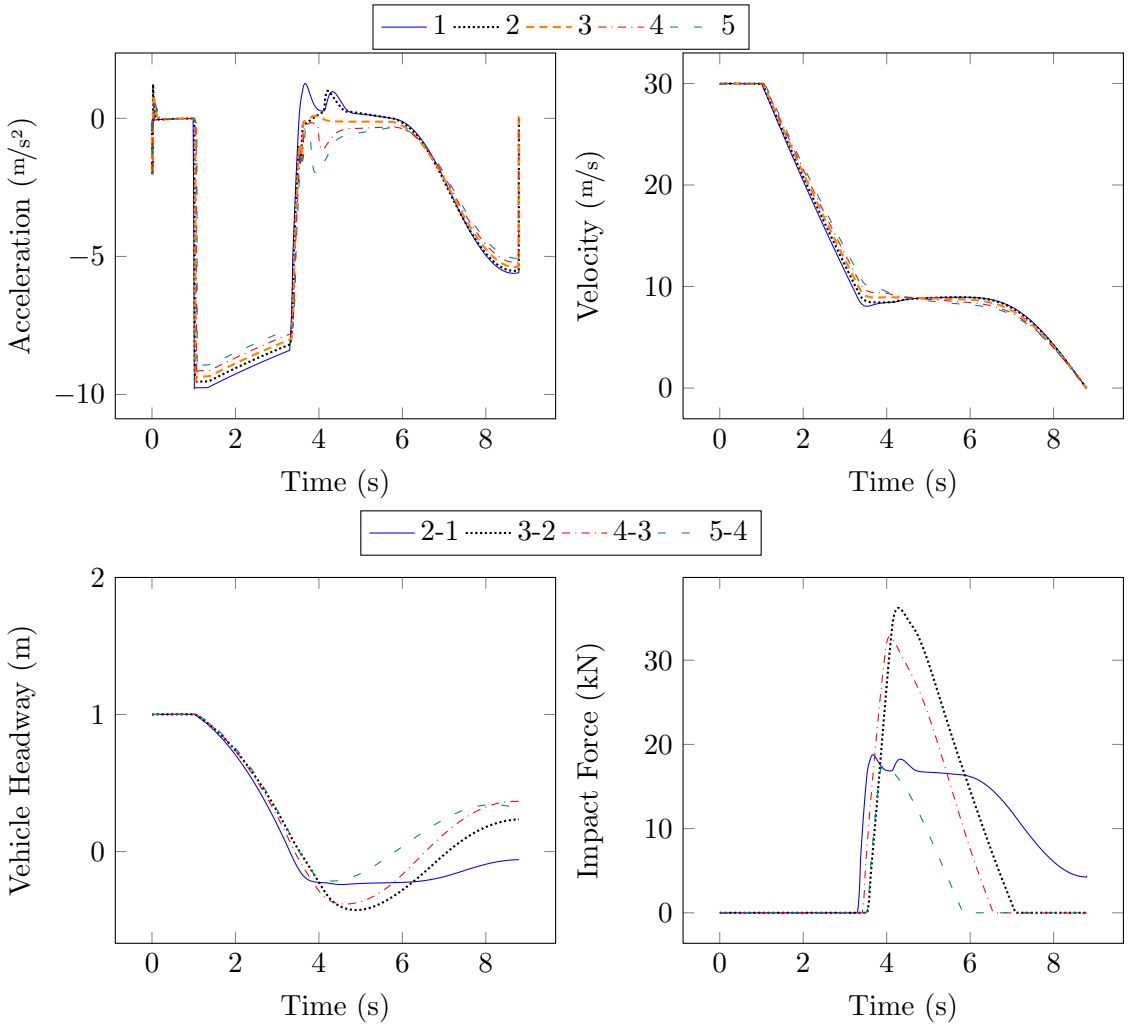

Fig. 4.13: Results of heaviest-as-lead platoon in emergency brake scenario using preceding acceleration controller.

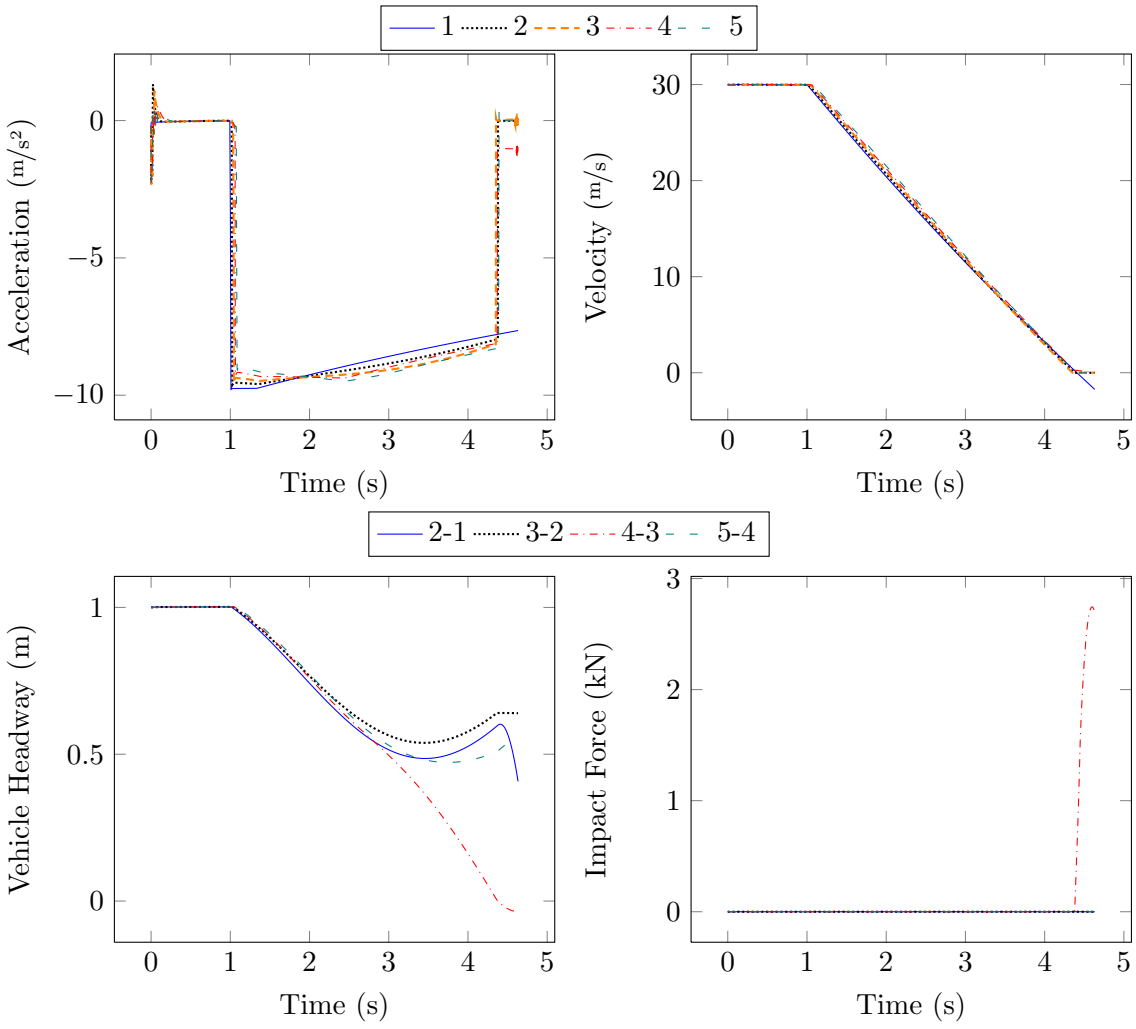

Fig. 4.14: Results of heaviest-as-lead platoon in emergency brake scenario using PAH controller.

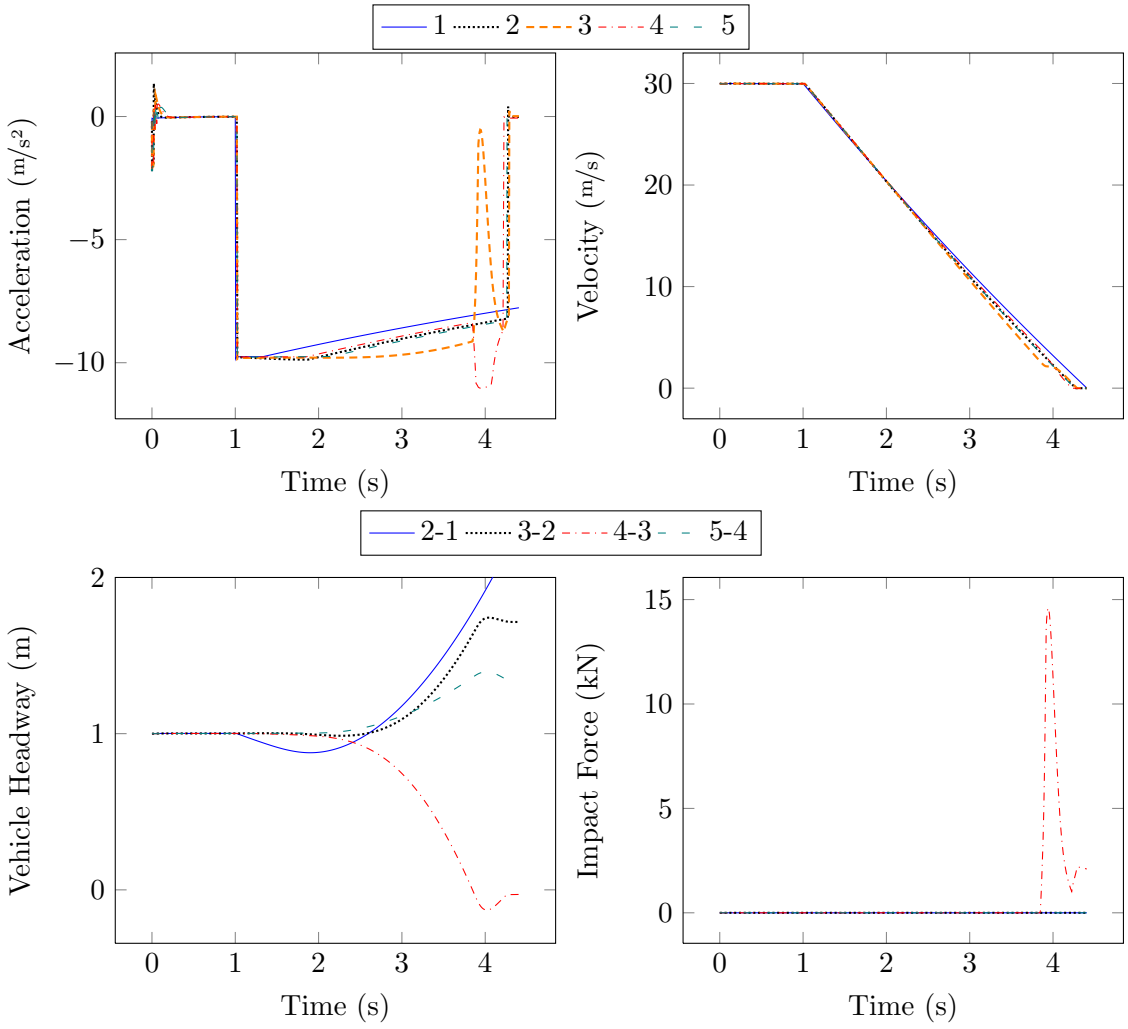

Fig. 4.15: Results of heaviest-as-lead platoon in emergency brake scenario using uncoordinated controller.

as-lead cases where additional collisions occurred. Even the subtle difference between the Rajamani and Choi control schemes appeared under the heaviest-in-rear case with the additional coordination through use of leader information giving the advantage.

The final concept illustrated is the safety gain of organizing the platoon by braking ability (represented here with mass). Under the Rajamani and Choi controllers collisions were avoided entirely with the most massive vehicle as leader, despite having other vehicles in the platoon following less massive ones. The number and severity of collisions is reduced under every controller when ordered this way. Conversely, with the most massive vehicle as the last, safety suffered under every control scheme. Keeping a platoon ordered with monotonically increasing braking ability is difficult if the UHZ is small enough that merging and splitting from the platoon must be restricted. If only the leader is required to be most massive, other vehicles occurring in random order, it eases this task some. This topic and the resulting effects on traffic flow warrants investigation as the benefits to safety are clear.

Table 4.12: Δv of impacts in heaviest-as-lead platoon under different control strategies.

	Δv ($^{m}/_{s}$)				
Vehicles	Rajamani	Choi	Prec. Acc.	PAH	Uncoord.
2-1	-	-	0.7	-	-
3-2	-	-	0.5	-	-
4-3	-	-	0.6	0.3	1.2
5-4	-	-	0.5	-	-

Table 4.13: Peak impact force in heaviest-as-lead platoon under different control strategies.

	F_C (N)				
Vehicles	Rajamani	Choi	Prec. Acc.	PAH	Uncoord.
2-1	-	-	18765	-	0
3-2	-	-	36208	-	0
4-3	-	-	32820	2855	14612
5-4	-	-	17425	-	0

Table 4.14: Time to stop a heaviest-as-lead platoon under different control strategies.

Controller	Stop Time (s)
Rajamani	4.41
Choi	4.41
Prec. Acc.	8.80
PAH	4.63
Uncoord.	4.41

4.5 Chapter Conclusions

The previously developed physical model of a vehicle is extended to a full platoon with sensing, communication, regulation layer control, and collision dynamics models added. Five different emergency control schemes are developed and compared in performance. The performance is tested with a five vehicle platoon with vehicle masses pulled from a normal distribution similar to the strict distribution discussed in Chapter 2. The tests are performed under three different vehicle orderings, random, heaviest-in-rear, and heaviest-as-lead. The results were compared with respect to the number of collisions, stopping time, vehicle acceleration and jerk, and impact force. The Rajamani controller used for normal operating conditions proved superior to the other five for emergency use.

The uncoordinated case performed interestingly well, never having collisions over Δv_{safe}. This controller is compelling because it removes the need for additional communication beyond the signal that an emergency scenario is occurring. While it was outperformed in all cases by the more communication intensive controllers, it is encouraging that if communication fails even in emergencies there is still possibility to maintain a moderate level of safety.

These results overall begin to show the gravity of these emergency scenarios, despite the strictness of the braking distribution and the relatively low relative velocities, large impact forces were generated. While no definite threshold of safety has been declared, the damage such forces are capable of is no small matter.

On the other hand, the significant safety improvement of proper ordering in a platoon is a welcome finding. This can come at almost no cost to system performance, simply if a

vehicle checking in has greater mass than any other in the platoon it will check into the front and become the new leader. Otherwise it will queue in the back. Other simple means might show to have great improvements to safety as models are refined and other configurations explored.

Chapter 5

Conclusions

Automated platooning is interesting because it offers large economic benefits if it can be achieved. AET is a form of highway automation that uses EVs for platooning. Safety is an important consideration for design decisions. In order to be successful the system must be safer than traditional highways in addition to higher capacity. It is also a fundamentally difficult problem, since inevitable delays and braking variations quickly cause emergency brake scenarios to generate unsafe differences in velocity within the platoon. If said delays and variations are not carefully controlled as much as possible, safe platooning is not possible in the emergency brake scenario.

Using Δv as a safety metric, platooning is justified through large improvements to highway density without significant compromise in safety. To avoid safety compromise, the vehicles must remain outside the UHZ, which is determined by vehicle and system design. Factors considered in the analysis include delays and braking ability, with consistency in ability showing to be more critical. Therefore, a homogeneous vehicle design is recommended. Some delay and variation in braking ability between vehicles is inevitable and can be tolerated as long as disparities are kept small.

To better understand how variation in braking ability can occur, a physical model of an AET vehicle is developed. This model shows that variation in the maximum voltage available to the motor and the vehicle mass are the greatest factors in braking ability. The results on the effects of tire condition were deemed inconclusive.

The variations in braking discussed in Chapter 2 are applied through variations in vehicle mass, subjecting a model of a five vehicles platoon to non-ideal emergency scenarios. Several longitudinal controllers are tested under the emergency brake scenario, the most effective proving that developed by Rajamani et al. [44]. These tests also show that better

safety is achieved when preceding vehicle and leader information is communicated and used. Another result is the importance of ordering vehicles in the platoon such that the most massive vehicle is the leader. While safety can be maintained through any ordering, safety is greatly improved through proper assignment of the most massive vehicle as the platoon leader. Therefore even if the distribution of braking is strict, appropriate measures must be applied to ensure that the platoon is well organized and controlled to maintain safety. Many such seemingly cursory system-level design decisions will have similarly large impacts on safety and performance.

Two main models result from this work which were implemented as Simulink models that can be run by Matlab script, the first order brake model, and the full platoon model. The former is more abstracted for system design, the latter more detailed for vehicle design. These models can be used for a variety of analyses that are beyond the scope of this work.

For future work that other investigators might pursue: the causes and probability of emergency brake scenarios occurring on an AET highway should be investigated. The results will provide a more clear context for the conclusions drawn here and indicate what threshold of probability of unsafe collision is acceptable for determining the safe headways. The effects of tire condition on braking ability needs more research and better representation in the model. More accurate models for communication and sensing may have important effects on these results as the controllers depend on the information received through these channels. Similarly, a better representation of the emergency control strategy suggested by Choi and Darbha [47] deserves a true implementation for comparison to the Rajamani controller. The simulations in Chapter 4 are limited to a very few cases. The effects of larger platoon size, larger communication delays, noise in the sensing, etc., are not addressed and may prove interesting at the least. A very important factor that could not be investigated more deeply in this work is the parameter distributions that would be appropriate for the model. Real world measurements and identification of the braking variance that occurs in an actual collection of homogeneous vehicles would help immensely to validate this work.

Altogether, safe platooning is an extremely challenging task. While many of these

results are discouraging, they do not prohibit safe platooning. They do indicate that a simplistic model is unlikely to yield a successful system, as most likely merging and splitting in a platoon will be constrained and vehicles will require very strict regulation. However, advances toward highway automation technology are likely to apply to current highways and vehicles with benefits of safety and efficiency for drivers and economies.

References

[1] A. Hitchcock, "Methods of analysis of ivhs safety," Partners for Advanced Transport and Highways, Technical Report, 1992-01-01. [Online]. Available: http://www.escholarship.org/uc/item/0xn46572

[2] M. Heron, "Deaths: leading causes for 2007." *National Vital Statistics Report*, vol. 59, no. 8, pp. 1–95, Aug. 2011.

[3] National Highway Traffic Safety Administration, "2007 traffic safety annual assessment highlights," National Highway Traffic Safety Administration, Washington, D.C., Technical Report, 2008.

[4] ——, "Summary of statistical findings: Highlights of 2009 motor vehicle crashes," National Highway Traffic Safety Administration, Washington, D.C., Technical Report, 2010.

[5] T. Golob, W. Recker, and V. Alvarez, "Freeway safety as a function of traffic flow," *Accident Analysis & Prevention*, vol. 36, no. 6, pp. 933–946, 2004.

[6] A. Kanaris, P. Ioannou, and F.-S. Ho, "Spacing and capacity evaluations for different ahs concepts," *Proceedings American Control Conference*, vol. 3, pp. 2036–2040, Jun. 1997. [Online]. Available: http://ieeexplore.ieee.org/stamp/stamp.jsp?tp=&arnumber=611047

[7] T. R. Board, "Special report 253: National automated highway system research program, a review," Washington, D.C., 1998.

[8] National Automated Highway System Consortium, "Technical feasibility demonstration summary report," National Automated Highway System Consortium, Troy, MI, Technical Report, Feb. 1998.

[9] ——, "Automated highway system (ahs) milestone 2 report, task c2: Downselect system configurations and workshop #3," California PATH, Troy, Michigan, Technical Report, 1997. [Online]. Available: http://www.path.berkeley.edu/nahsc/pdf/AHS-Milestone_2_Report_Task-C21.pdf

[10] A. Davila and M. Nombela, "Sartre: Safe road trains for the environment," in *Conference on Personal Rapid Transit*, 2010.

[11] M. Wille and M. Roewenstrunk, "Konvoi: Electronically coupled truck-convoy," in *HFES-EC Conference on Human Factors for Assistance and Automation*, 2007.

[12] Y. Choi, D. Kang, S. Lee, and Y. Kim, "The autonomous platoon driving system of the on line electric vehicle," *Proceedings ICCAS-SICE*, pp. 3423–3426, 2009. [Online]. Available: http://ieeexplore.ieee.org/stamp/stamp.jsp?tp=&arnumber=5335220

[13] M. Kees, K. J. Burnham, F. P. Lockett, J. H. Tabor, and R. A. Williams, "Hydraulic actuated brake and electromechanically actuated brake systems," *Proceedings ADAS Advanced Driver Assistance Systems International Conference (IEE Conf. Publ. No. 483)*, pp. 43–47, 2001.

[14] A. Hitchcock, "Intelligent vehicle/highway system safety: Multiple collisions in automated highway systems," Partners for Advanced Transport and Highways, Technical Report, 1995-01-01. [Online]. Available: http://www.escholarship.org/uc/item/6vm8z32v

[15] S. Shladover and United States Urban Mass Transportation Administration Office of Technology Development and Deployment, *Operation of automated guideway transit vehicles in dynamically reconfigured trains and platoons*. Dept. of Transportation, Urban Mass Transportation Administration, Office of Technology Development and Deployment, 1979. [Online]. Available: http://books.google.com/books?id=M4ZPAAAAMAAJ

[16] M. Krafft, A. Kullgren, A. Ydenius, and C. Tingvall, "Influence of crash pulse characteristics on whiplash associated disorders in rear impacts–crash recording in real life crashes," *Traffic Injury Prevention*, vol. 3, no. 2, pp. 141–149, 2002. [Online]. Available: http://www.tandfonline.com/doi/abs/10.1080/15389580212001

[17] A. Kullgren, L. Eriksson, O. Bostrom, and M. Krafft, "Validation of neck injury criteria using reconstructed real-life rear-end crashes with recorded crash pulses," in *Proceedings of 18th International Technical Conference on the Enhanced Safety of Vehicles*, May 2003.

[18] J. Hedrick, D. McMahon, V. Narendran, and D. Swaroop, "Longitudinal vehicle controller design for ivhs systems," in *Proceedings of American Control Conference*, June 1991, pp. 3107–3112. [Online]. Available: http://ieeexplore.ieee.org/xpls/abs_all.jsp?arnumber=4791980

[19] D. B. Maciuca, "Brake dynamics effect on ivhslane capacity," Partners for Advanced Transport and Highways, Technical Report, 1994-01-01. [Online]. Available: http://www.escholarship.org/uc/item/9dw3k3wk

[20] J. K. Hedrick, V. Garg, J. C. Gerdes, D. B. Maciuca, and D. Swaroop, "Longitudinal control development for ivhs fully automated and semi - automated system: Phase iii," Partners for Advanced Transport and Highways, Technical Report, 1997-01-01. [Online]. Available: http://www.escholarship.org/uc/item/6sv5m0kz

[21] J. C. Gerdes and J. K. Hedrick, "Brake System Rewuirements for Platooning on an Automated Highway," in *Proceedings of the American Control Conference*, Seattle,Washington, June 1995. [Online]. Available: http://ieeexplore.ieee.org/stamp/stamp.jsp?tp=&arnumber=529229

[22] T. A. Johansen, I. Petersen, J. Kalkkuhl, and J. Ludemann, "Gain-scheduled wheel slip control in automotive brake systems," *IEEE Transactions on Control System Technology*, vol. 11, no. 6, pp. 799–811, 2003.

[23] W.-y. Li, "Design and implementation of digital radio communications link for platoon control," Partners for Advanced Transport and Highways, Technical Report, 1995-01-01. [Online]. Available: http://www.escholarship.org/uc/item/27w805xq

[24] J. Hedrick, Y. Chen, and S. Mahal, "Optimized Vehicle Control/Communication Interaction in an Automated Highway System," UCB-ITS-PRR-2001-29, California Partners for Advanced Transit and Highways, Technical Report, Oct 2001. [Online]. Available: http://www.path.berkeley.edu/path/publications/pdf/PRR/2001/PRR-2001-29.pdf

[25] E. Ono, K. Asano, M. Sugai, S. Ito, M. Yamamoto, M. Sawada, and Y. Yasui, "Estimation of automotive tire force characteristics using wheel velocity," *Control Engineering Practice*, vol. 11, no. 12, pp. 1361–1370, 2003, ¡ce:title¿Award winning applications-2002 IFAC World Congress¡/ce:title¿. [Online]. Available: http://www.sciencedirect.com/science/article/pii/S096706610300073X

[26] C. Lee, K. Hedrick, and K. Yi, "Real-time slip-based estimation of maximum tire-road friction coefficient," *Mechatronics, IEEE/ASME Transactions*, vol. 9, no. 2, pp. 454 –458, June 2004.

[27] J. Harned, G. Scharpf, and L. Johnston, *Measurement of Tire Brake Force Characteristics as Related to Wheel Slip (anti-lock) Control System Design*, ser. Engineering publication. Society of Automotive Engineers, 1969. [Online]. Available: http://books.google.com/books?id=Ekm1HAAACAAJ

[28] C. Canudas de Wit and P. Tsiotras, "Dynamic tire friction models for vehicle traction control," *Decision and Control, Proceedings of the 38th IEEE Conference*, vol. 4, pp. 3746–3751, 1999.

[29] C. Canudas de Wit, H. Olsson, K. Astrom, and P. Lischinsky, "A new model for control of systems with friction," *Automatic Control, IEEE Transactions*, vol. 40, no. 3, pp. 419–425, Mar. 1995.

[30] C. Canudas de Wit, R. Horowitz, and P. Tsiotras, "Model-based observers for tire/road contact friction prediction," in *New Directions in Nonlinear Observer Design*, ser. Lecture Notes in Control and Information Sciences, H. Nijmeijer and T. Fossen, Eds. Springer Berlin / Heidelberg, 1999, vol. 244, pp. 23–42, 10.1007/BFb0109919. [Online]. Available: http://dx.doi.org/10.1007/BFb0109919

[31] T. Kenjō and S. Nagamori, *Permanent-magnet and Brushless DC Motors*, ser. Monographs in electrical and electronic engineering. Clarendon Press, 1985. [Online]. Available: http://books.google.com/books?id=2PJSAAAAMAAJ

[32] P. Waltermann, "Modelling and control of the longitudinal and lateral dynamics of a series hybrid vehicle," *Proceedings IEEE International Control Applications Conference*, pp. 191–198, 1996. [Online]. Available: http://ieeexplore.ieee.org/stamp/stamp.jsp?tp=&arnumber=558629

[33] M. Jain and S. S. Williamson, "Modeling and analysis of a 5-leg inverter for an electric vehicle in-wheel motor drive," *Proceedings 23rd Canadian Conference Electrical and Computer Engineering (CCECE)*, pp. 1–5, 2010.

[34] K. Kawashima, T. Uchida, and Y. Hori, "Rolling stability control of in-wheel electric vehicle based on two-degree-of-freedom control," *Proceedings 10th IEEE International Workshop Advanced Motion Control AMC*, pp. 751–756, 2008. [Online]. Available: http://ieeexplore.ieee.org/stamp/stamp.jsp?tp=&arnumber=4516161

[35] S. Sakai, H. Sado, and Y. Hori, "New skid avoidance method for electric vehicle with independently controlled 4 in-wheel motors," *Proceedings IEEE International Symposium Industrial Electronics*, vol. 2, pp. 934–939, 1999. [Online]. Available: http://ieeexplore.ieee.org/stamp/stamp.jsp?tp=&arnumber=798740

[36] G. Tao, Z. Ma, L. Zhou, and L. Li, "A novel driving and control system for direct-wheel-driven electric vehicle," *Magnetics, IEEE Transactions*, vol. 41, no. 1, pp. 497–500, 2005. [Online]. Available: http://ieeexplore.ieee.org/stamp/stamp.jsp?tp=&arnumber=1381598

[37] P. Xu, G. Guo, J. Cao, and B. Cao, "A novel fore axle whole-turning driving and control system for direct-wheel-driven electric vehicle," *Automation and Logistics, IEEE International Conference*, pp. 705–709, Sept. 2008. [Online]. Available: http://ieeexplore.ieee.org/stamp/stamp.jsp?tp=&arnumber=4636240

[38] Y.-P. Yang, J.-J. Liu, T.-J. Wang, K.-C. Kuo, and P.-E. Hsu, "An electric gearshift with ultracapacitors for the power train of an electric vehicle with a directly driven wheel motor," *Vehicle Technology, IEEE Transactions*, vol. 56, no. 5, pp. 2421–2431, 2007. [Online]. Available: http://ieeexplore.ieee.org/stamp/stamp.jsp?arnumber=04305551

[39] C. Canudas-de Wit and R. Horowitz, "Observers for tire/road contact friction using only wheel angular velocity information," *Decision and Control, Proceedings of the 38th IEEE Conference*, vol. 4, pp. 3932–3937, 1999.

[40] H. Lovatt, V. Ramsden, and B. Mecrow, "Design of an in-wheel motor for a solar-powered electric vehicle," *Electrical Machines and Drives, 1997 Eighth International Conference (Conf. Publ. No. 444)*, pp. 234–238, Sept. 1997.

[41] J. D. MacIsaac and W. R. Garrott, "Preliminary findings of the effect of tire inflation pressure on the peak and slide coefficients of friction," National Highway Traffic Safety Administration (NHTSA), Technical Report DOT 809428, June 2002.

[42] J. Yi, S. Suryanarayanan, A. Howell, R. Horowitz, M. Tomizuka, K. Hedrick, and L. Alvarez, "Development and implementation of a vehicle-centered fault diagnostic and management system for the extended path-ahs architecture: Part i," University of California, Berkeley, Technical Report, Nov. 2002. [Online]. Available: http://www.path.berkeley.edu/PATH/Publications/PDF/PRR/2002/PRR-2002-34.pdf

[43] U. of Michigan. Engineering Summer Conferences and U. of Michigan. College of Engineering, *Mechanics of Heavy-duty Trucks and Truck Combinations*. University

of Michigan, College of Engineering, 1984. [Online]. Available: http://books.google.com/books?id=hphTAAAAMAAJ

[44] R. Rajamani, H.-S. Tan, B. K. Law, and W.-B. Zhang, "Demonstration of integrated longitudinal and lateral control for the operation of automated vehicles in platoons," *Control System Technology, IEEE Transactions*, vol. 8, no. 4, pp. 695–708, 2000. [Online]. Available: http://ieeexplore.ieee.org/stamp/stamp.jsp?tp=&arnumber=852914

[45] D. Swaroop, "String stability of interconnected systems: An application to platooning in automated highway systems," in *Automatic Control, IEEE Transactions*, vol. 41, no. 3, Mar. 1996. [Online]. Available: http://escholarship.org/uc/item/86z6h1b1

[46] D. N. Godbole and J. Lygeros, "Longitudinal control of the lead car of a platoon," *Proceedings American Control Conference*, vol. 1, pp. 398–402, 1994. [Online]. Available: http://ieeexplore.ieee.org/xpls/abs_all.jsp?arnumber=4791980

[47] W. Choi and S. Darbha, "Assessing the benefits of coordination in automatically controlled vehicles," *Proceedings IEEE Intelligent Transportation Systems*, pp. 70–75, 2001.

[48] R. M. Brach, R. M. Brach, and S. of Automotive Engineers, *A review of impact models for vehicle collison*. Warrendale, PA: Society of Automotive Engineers, 1987.

[49] R. M. Brach, "Modeling of low-speed, front-to-rear vehicle impacts," *SAE Technical Paper*, no. 2003-01-0491, pp. 65–76, 2003.

[50] M. Krafft, A. Kullgren, S. Malm, and A. Ydenius, "Influence of crash severity on various whiplash injury symptoms: A study based on real-life rear-end crashes with recorded crash pulses," in *Proceedings - 19th International Technical Conference on the Enhanced Safety of Vehicles*, 2005.

[51] L. M. Hynes and J. P. Dickey, "The rate of change of acceleration: Implications to head kinematics during rear-end impacts," *Accident Analysis and Prevention*, vol. 40, no. 3, pp. 1063–1068, 2008. [Online]. Available: http://www.sciencedirect.com/science/article/pii/S0001457507002096

Appendices

Appendix A
Simulink Model of First Order Brake System and Associated Scripts

The Matlab scripts and Simulink models are included here so that subsequent investigators of AET are able to use for further research the models and methods of safety analysis developed in this work. The listings are complete and include all code written by the author for generating the plots found in Chapter 2. Understanding of these items may be useful for comprehension of the analysis in this document but is certainly not necessary.

A.1 Simulink Model

A screen-shot of the main model is displayed in Figure A.1, with screen-shots of the leader and follower subsystems in Figures A.2 and A.3, respectively.

Comparison of the leader and follower blocks shows that they are nearly identical, only differing in the leader having a source for the brake signal while the follower receives that signal through an input port. This allows for the addition of copies of the follower block if more than two vehicles are desired. For all the analysis in this document, two proved sufficient. These subsystems are a simple, first-order system with two additional integrations to find position. All the additional complexity is for switching between inputs when the vehicle has reached a complete stop (to prevent rolling backwards).

All the blocks have workspace variables for parameter values such that it can be entirely configured and run from the Matlab command line via script. The variables to be configured are shown in Table A.1.

The outputs of the simulation are the workspace structures `DeltaV` and `Headway`. Usage examples are found in the script in Section A.3.

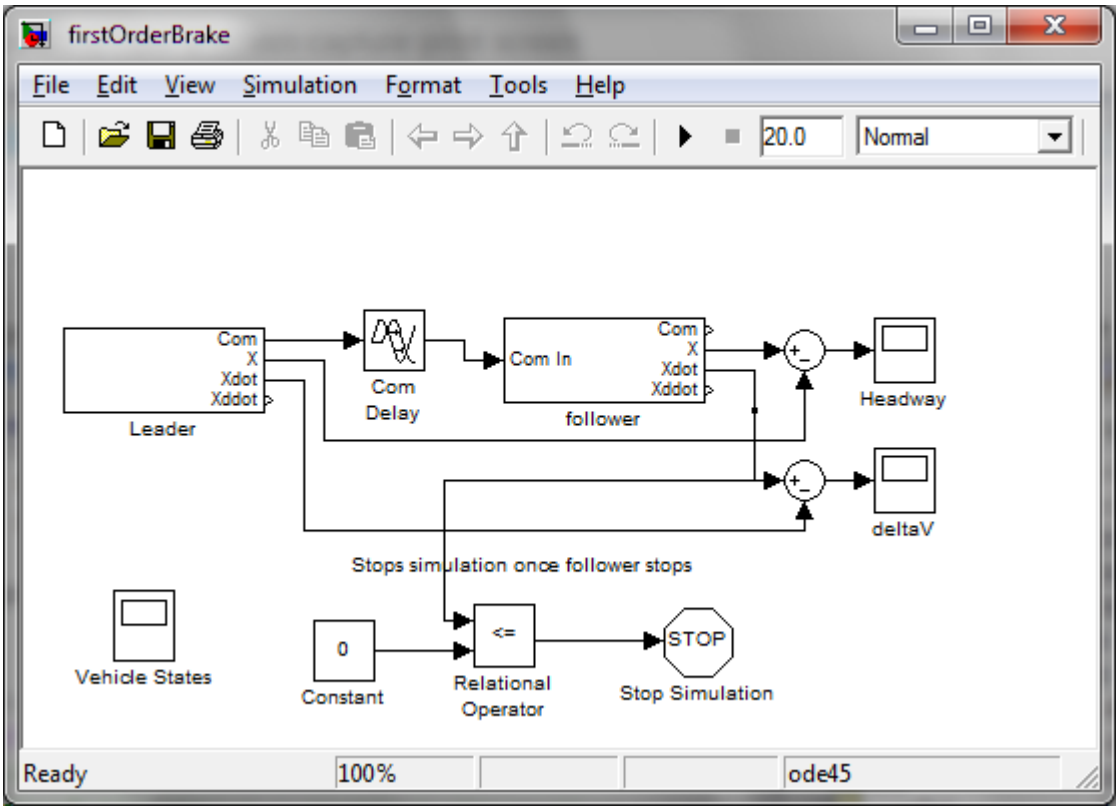

Fig. A.1: Simulink model.

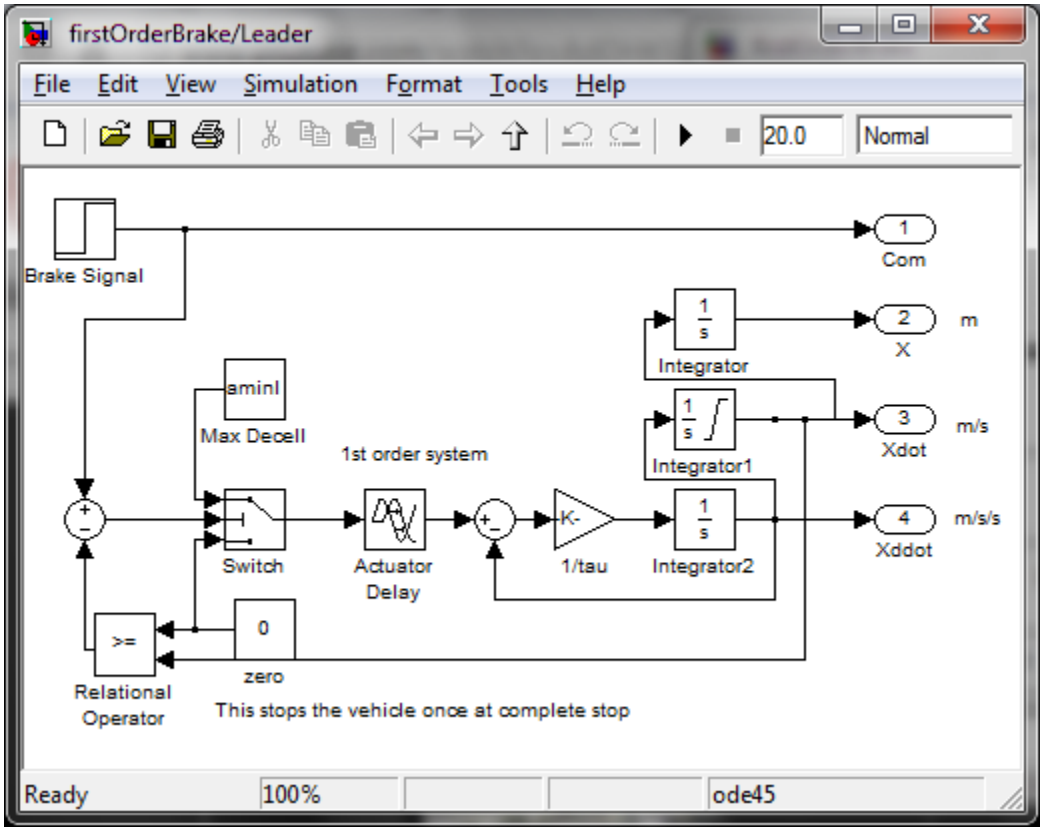

Fig. A.2: Leader subsystem.

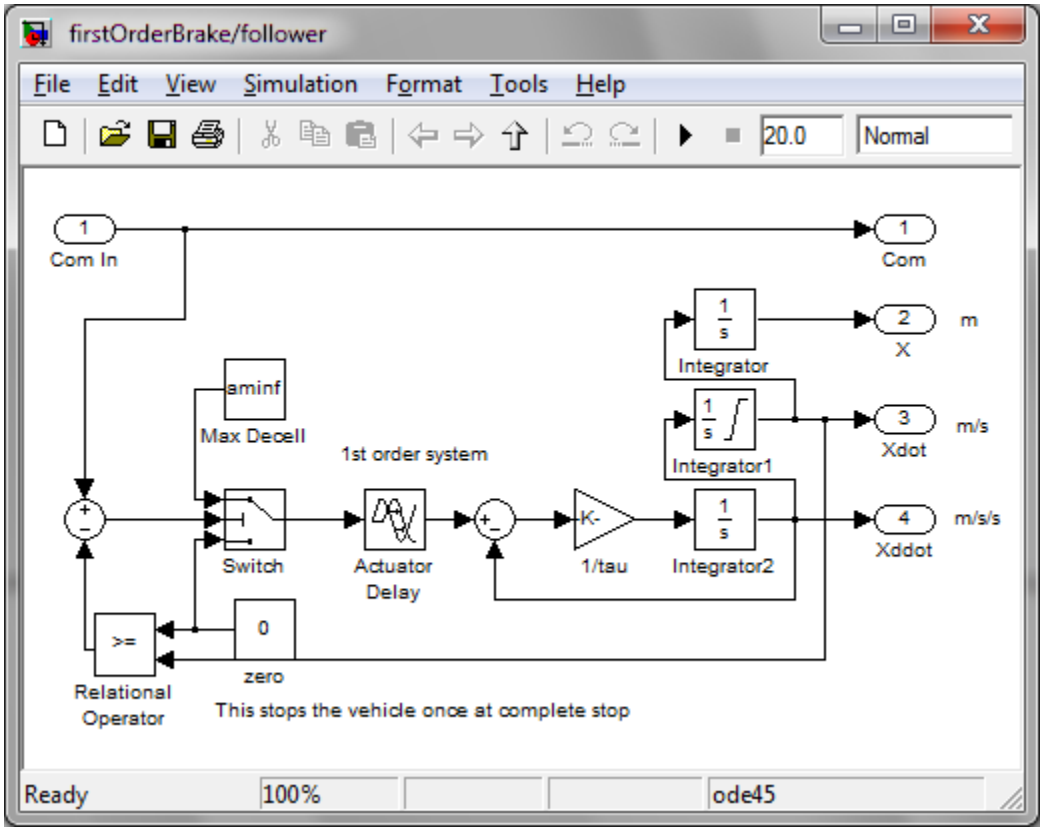

Fig. A.3: Follower subsystem.

A.2 Matlab Functions for Analyzing Data From the Model

The following functions are useful in interpreting the parametrically defined H-Δv curve found returned from the Simulink model. Usage is exemplified in these scripts used to generate the plots found in Chapter 2.

`success.m`

This function's task is to return the unit rect function corresponding to the unsafe headway zone. The return value is divided into headway bins of 0.1m, each containing a one if the safe Δv threshold is surpassed at that headway, zero otherwise.

```
1  %Spencer Jackson
2  function s = success(threshold, dV, H)
3    s = zeros(1,801);%cover from H=[0,80]meters
4    a=0;
5      b=0;
6    for i = 1:length(H)
7      if (dV(i)>=threshold)
8        if(a)
9                  b=H(i);
10               else
11                 a=H(i);
12                 b=a;
13       end
```

Table A.1: Inputs for first order brake system Simulink model.

Workspace Variable	Units	Description
`V0l`	m/s	Leader initial velocity
`V0f`	m/s	Follower initial velocity
`aminl`	m/s^2	Leader minimum acceleration
`aminf`	m/s^2	Follower minimum acceleration
`taul`	s	Leader time constant
`tauf`	s	Follower time constant
`actDell`	s	Leader actuatin delay
`actDelf`	s	Follower actuation delay
`comDel`	s	Communication delay

```
14      end
15      end
16
17    a = ceil(a*10)+1;%round to nearest .1m
18    b = ceil(b*10)+1;%+1 for index
19      if ~(a==1&&b==1)
20          for i=a:b
21              s(1,i)=1;
22          end
23      end
24      s = s(1,1:801);
25  end
```

`boundedrandn.m`

This function uses excised generation to pull outcomes from a bounded random normal distribution.

```
1  function x = boundedrandn(L, mu, sigma, lower, upper)
2  x = sigma*randn(1,L) + mu;
3  while (min(x)<lower)||(max(x)>upper)
4      indx = find(x<lower);
5      L = length(indx);
6      x(indx) = sigma*randn(1,L) + mu;
7      indx = find(x>upper);
8      L = length(indx);
9      x(indx) = sigma*randn(1,L) + mu;
10 end
```

A.3 Matlab Script for H-Δv Plots, HDV Plots, and Monte Carlo Plots in Chapter 2

Note that this script uses several functions, most of which are defined above in Section A.2. The exception is the `crossing` function as first referenced in line 92. This copywritten

function is available on the Matlab Central File Exchange at `http://www.mathworks.com/matlabcentral/fileexchange/2432`.

```
%Spencer Jackson
%This generates all the plots for the ITS paper
hdvcurves = 1;
uhzcurves =  1;
montecarlo =  1;
disthist = 1;

t1=clock;


%%%%%%%%%%%%%%%%%%%%%%%%%%%%%%%%%%%%%%%%%%%%%%%%%%%
%  HdV plots
%%%%%%%%%%%%%%%%%%%%%%%%%%%%%%%%%%%%%%%%%%%%%%%%%%%
if(hdvcurves)
        V0l = 30;%m/s
        V0f = 30;%m/s
        aminl = -10;%m/s^2
        aminf = -8;%m/s^2
        taul =.1;%s
        tauf = .1;%s
        actDell = .1;%s
        actDelf = .1;%s
        comDel = .060;%s

        sim('firstOrderBrake.mdl')
        H = Headway.signals.values;
        dv = max(0,deltaV.signals.values);
        data = [H dv];
        save hdvcurvesICV.tab data -ascii

        V0l = 30;%m/s
        V0f = 30;%m/s
        aminl = -10;%m/s^2
```

```
34          aminf = -8;%m/s^2
35          taul =.01;%s
36          tauf = .01;%s
37          actDell = 0;%s
38          actDelf = 0;%s
39          comDel = 0;%s
40          sim('firstOrderBrake.mdl')
41          H = Headway.signals.values;
42          dv = max(0,deltaV.signals.values);
43          data = [H dv];
44          save hdvcurvesEV.tab data -ascii
45          %fprintf(hdvcurve,'%f %f', H1, dv1);
46
47          %plot(H1,dv1,H2,dv2,'--');
48          %title('H- \Delta v');
49          %legend('ICV','EV');
50          %xlabel('Initial Headway (m)');
51          %ylabel('\Delta Velocity (m/s)');
52          %matlab2tikz('hdvcurve.tikz');
53          %disp('done')
54          %pause
55          clf
56          V0l = 30;%m/s
57          V0f = 30;%m/s
58          aminl = -10;%m/s^2
59          aminf = -9.5;%m/s^2
60          taul =.01;%s
61          tauf = .1;%s
62          actDell = 0;%s
63          actDelf = 0;%s
64          comDel = .2;%s
65          for aminf=[-9.5 -10 -10.5]
66          sim('firstOrderBrake.mdl')
67          H = Headway.signals.values;
68          dv = max(0,deltaV.signals.values);
```

```
69          data = [H dv];
70          hold on
71          plot (H,dv);
72          str = ['hdvcurves' num2str(-aminf) '.tab'];
73          save(str, 'data', '-ascii');
74          end
75          hold off
76  end%skip
77
78
79  %%%%%%%%%%%%%%%%%%%%%%%%%%%%%%%%%%%%%%%%%%%%%%%%%%%%%%%%%%%%%%%%%%%%%%%%
80  %  UHZ plots
81  %%%%%%%%%%%%%%%%%%%%%%%%%%%%%%%%%%%%%%%%%%%%%%%%%%%%%%%%%%%%%%%%%%%%%%%%
82  if(uhzcurves)
83          param = -10:.01:-7;
84          l = length(param);
85          V0l = 30;%m/s
86          V0f = 30;%m/s
87          aminl = -10;%m/s^2
88          aminf = -8;%m/s^2
89          taul =.01;%s
90          tauf = .01;%s
91          actDell = 0;%s
92          actDelf = 0;%s
93          comDel = .02;%s
94          vals = [.01 .02 .1];
95          z = zeros(6,l);
96          for j=1:3
97                  tauf = vals(j);
98                  for i = 1:l
99                      aminf = param(i);
100                     sim('firstOrderBrake.mdl')
101                     [int, tmp] = crossing(deltaV.signals.values,Headway.
                            signals.values,2.5);
102                     if (tmp)
```

```
103                         z(2*j-1:2*j,i) = tmp;
104                     end
105                 end
106             end
107             tauf = .01;
108             plot(param,z)
109             data = [param' z'];
110             save unsafeHeadwayTau.tab data -ascii
111
112             vals = [.02 .04 .2];
113             z = zeros(6,1);
114             for j=1:3
115                 comDel = vals(j);
116                 for i = 1:1
117                     aminf = param(i);
118                     sim('firstOrderBrake.mdl')
119                     [int, tmp] = crossing(deltaV.signals.values,Headway.
                            signals.values,2.5);
120                     if (tmp)
121                         z(2*j-1:2*j,i) = tmp;
122                     end
123                 end
124             end
125             comDel = .02;
126             plot(param,z)
127             data = [param' z'];
128             save unsafeHeadwayCom.tab data -ascii
129
130             vals = [.02 .04 .2];
131             vals2 = [.01 .02 .1];
132             z = zeros(6,1);
133             for j=1:3
134                 comDel = vals(j);
135                 tauf = vals2(j);
136                 for i = 1:1
```

```
137                         aminf = param(i);
138                         sim('firstOrderBrake.mdl')
139                         [int, tmp] = crossing(deltaV.signals.values,Headway.
                                signals.values,2.5);
140                         if (tmp)
141                             z(2*j-1:2*j,i) = tmp;
142                         end
143                     end
144             end
145             comDel = .02;
146             tauf = .01;
147             plot(param,z)
148             data = [param' z'];
149             save unsafeHeadwayBoth.tab data -ascii
150     end%skip
151
152     %%%%%%%%%%%%%%%%%%%%%%%%%%%%%%%%%%%%%%%%%%%%%%%%%%%%%%%%%%%%%%%%%%%%%%%
153     %  Monte Carlo
154     %%%%%%%%%%%%%%%%%%%%%%%%%%%%%%%%%%%%%%%%%%%%%%%%%%%%%%%%%%%%%%%%%%%%%%%
155     if(montecarlo)
156             nmc = 30;%number of monte carlo simulations
157             n = 1000;%number of runs/mc
158             dV = [0 2.5 5];%m/s
159
160             V0l = 30;%m/s
161             V0f = 30;%m/s
162             taul = .01;%s
163             tauf = .01;%s
164             actDell = 0;%s
165             actDelf = 0;%s
166             comDel = .02;%s
167
168             %taus = [.01 .1];
169             dels = .02:.02:.2;
170             amindev = [.2 .75];%std deviation
```

```
171         aminmean = [-9.75  -7.75];
172         aminboundu = aminmean+[1  3].*amindev;%upper bound
173         aminboundl = aminmean-[1  3].*amindev;%lower bound
174         m = length(dels);
175         l = length(amindev);
176         ldv = length(dV);
177         %distribution = zeros(ldv*l,801);
178         everything = zeros(m,l,ldv,nmc,801);
179         for h = 1:l %distributions
180         for i=1:nmc %monte carlo sims
181                 aminlarray = boundedrandn(n,aminmean(h),amindev(h),aminboundl(
                        h),aminboundu(h));
182                 aminfarray = boundedrandn(n,aminmean(h),amindev(h),aminboundl(
                        h),aminboundu(h));
183         for j = 1:m %delays
184                 %tauf = taus(j);
185                 comDel = dels(j);
186                 distribution = zeros(ldv,801);
187         for k = 1:n %runs
188                 aminl = aminlarray(k);
189                 aminf = aminfarray(k);
190                 sim('firstOrderBrakenodel.mdl');
191                 %s = success(dV(2),deltaV.signals.values,Headway.signals.
                        values);
192                 s1 = success(dV(1),deltaV.signals.values,Headway.signals.
                        values);
193                 s2 = success(dV(2),deltaV.signals.values,Headway.signals.
                        values);
194                 s3 = success(dV(3),deltaV.signals.values,Headway.signals.
                        values);
195
196                 %distribution(j,:) = distribution(j,:)+s/n;
197                 distribution(1,:) = distribution(1,:)+s1/n;
198                 distribution(2,:) = distribution(2,:)+s2/n;
199                 distribution(3,:) = distribution(3,:)+s3/n;
```

```
200
201         end %runs
202         everything(j,h,:,i,:) = distribution;
203         end %delays
204         end %monte carlos
205         %plot(0:.1:80, distribution)
206         end %distributions
207
208         data = 0:.1:80;
209         for i=1:ldv %dv
210         for h=1:l %dist
211         for j=1:m %del
212                 mat = squeeze(everything(j,h,i,:,:));
213                 data = [data;mean(mat);var(mat)];
214         end
215         end
216         end
217         data = data';
218         save newmontecarlodel.tab data -ascii
219
220         V0l = 30;%m/s
221         V0f = 30;%m/s
222         taul = .01;%s
223         tauf = .01;%s
224         actDell = 0;%s
225         actDelf = 0;%s
226         comDel = .02;%s
227
228         %taus = [.01 .1];
229         dels = [.02 .2];
230         amindev = .2:.055:.75;%std deviation
231         aminmean = -9.75:.2:-7.75;
232         aminboundu = aminmean+(1:.2:3).*amindev;%upper bound
233         aminboundl = aminmean-(1:.2:3).*amindev;%lower bound
234         m = length(dels);
```

```
235         l = length(amindev);
236         ldv = length(dV);
237         %distribution = zeros(ldv*l,801);
238         everything = zeros(m,l,ldv,nmc,801);
239         for h = 1:l %distributions
240         for i=1:nmc %monte carlo sims
241                 aminlarray = boundedrandn(n,aminmean(h),amindev(h),aminboundl(
                        h),aminboundu(h));
242                 aminfarray = boundedrandn(n,aminmean(h),amindev(h),aminboundl(
                        h),aminboundu(h));
243         for j = 1:m %delays
244                 %tauf = taus(j);
245                 comDel = dels(j);
246                 distribution = zeros(ldv,801);
247         for k = 1:n %runs
248                 aminl = aminlarray(k);
249                 aminf = aminfarray(k);
250                 sim('firstOrderBrakenodel.mdl');
251                 %s = success(dV(2),deltaV.signals.values,Headway.signals.
                        values);
252                 s1 = success(dV(1),deltaV.signals.values,Headway.signals.
                        values);
253                 s2 = success(dV(2),deltaV.signals.values,Headway.signals.
                        values);
254                 s3 = success(dV(3),deltaV.signals.values,Headway.signals.
                        values);
255
256                 %distribution(j,:) = distribution(j,:)+s/n;
257                 distribution(1,:) = distribution(1,:)+s1/n;
258                 distribution(2,:) = distribution(2,:)+s2/n;
259                 distribution(3,:) = distribution(3,:)+s3/n;
260
261         end %runs
262         everything(j,h,:,i,:) = distribution;
263         end %delays
```

```
264         end %monte carlos
265         %plot(0:.1:80,distribution)
266         end %distributions
267
268         data = 0:.1:80;
269         for i=1:ldv %dv
270         for h=1:l %dist
271         for j=1:m %del
272                 mat = squeeze(everything(j,h,i,:,:));
273                 data = [data;mean(mat);var(mat)];
274         end
275         end
276         end
277         data = data';
278         save newmontecarlodist.tab data -ascii
279 end%skip
280
281 if(disthist)
282         a = boundedrandn(n,-10,.25,-inf,-9.5);
283         b = boundedrandn(n,-10,1,-inf,-7);
284         r = ceil(10*(max(a)-min(a)));
285         [y,x] = hist(a,r);
286         data = [x' y'];
287         save distribution1.tab data -ascii
288         r = ceil(10*(max(b)-min(b)));
289         [y,x] = hist(b,r);
290         data = [x' y'];
291         save distribution2.tab data -ascii
292 end%skip
293
294 clock-t1
295 clock
```

Appendix B

Simulink Model of Full Platoon and Associated Scripts

The Matlab scripts and Simulink models are included here so that subsequent investigators of AET are able to use the models and methods of safety analysis developed here for further research. The listings are complete and include all code written by the author for generating the plots found in Chapter 4. Understanding of these items may be useful for comprehension of the analysis in this document but is certainly not necessary.

B.1 Simulink Model

Screen-shots of the model are found in Figures B.1 through B.6. The key to usage of this Simulink model is understanding that nearly every signal is or can be a vector with each element corresponding to a vehicle in the platoon. The first element of the vector is the leader, the second index the second vehicle, etc. This way the number of vehicles is easily configurable through Matlab scripts.

While this model has been used here almost exclusively for analysis of the emergency brake scenario, there is no inherent limitation to this application. This model can serve well for analyses of steady-state or less extreme emergency operations as well.

Screen-shots of Simulink Model

In the screen-shots several embedded Matlab functon blocks can be observed. The code contained in these blocks is listed in the sections that follow.

VehiclePlotter

This block is for the sole purpose of visualization. Its output is used by the script in Section B.2 to make plots that can be made into a movie by cycling through the plots like a slide show with each plot shown for 0.07s.

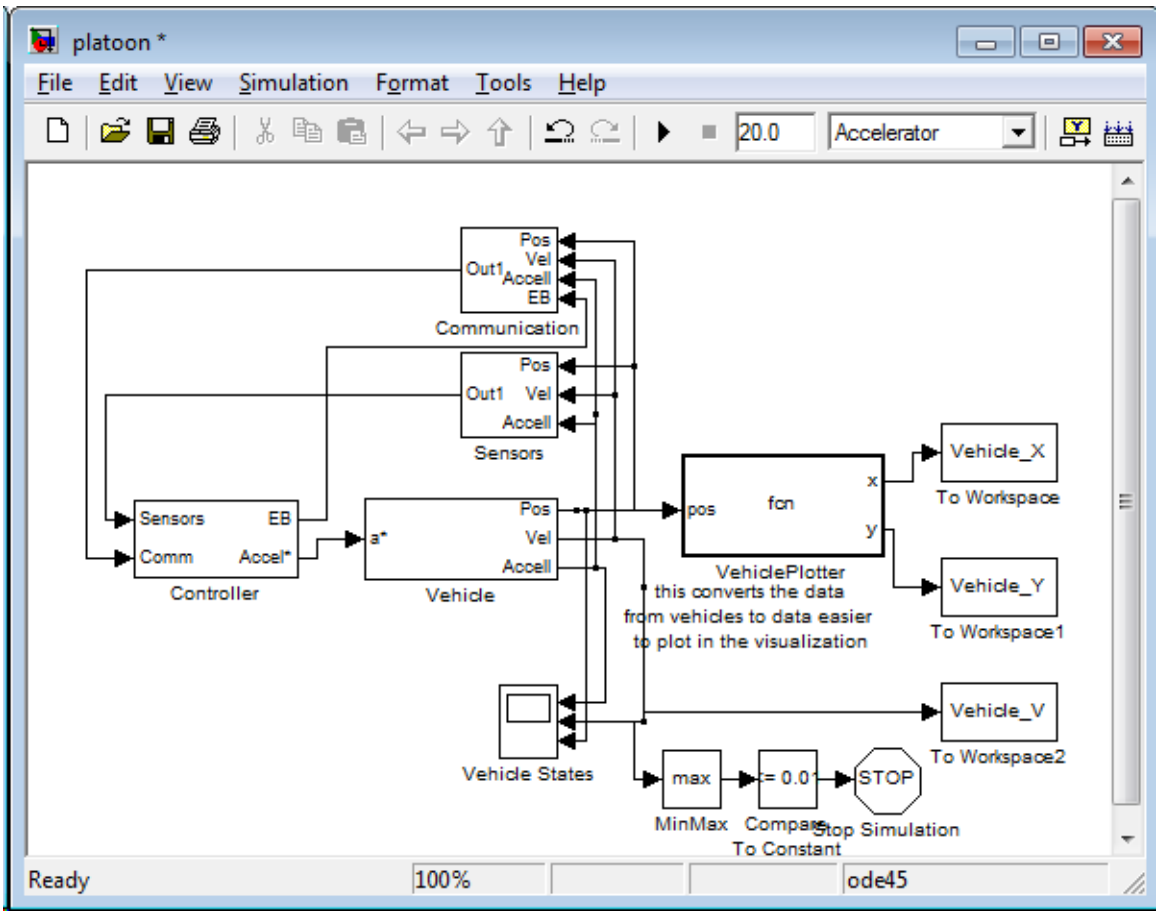

Fig. B.1: Full platoon model.

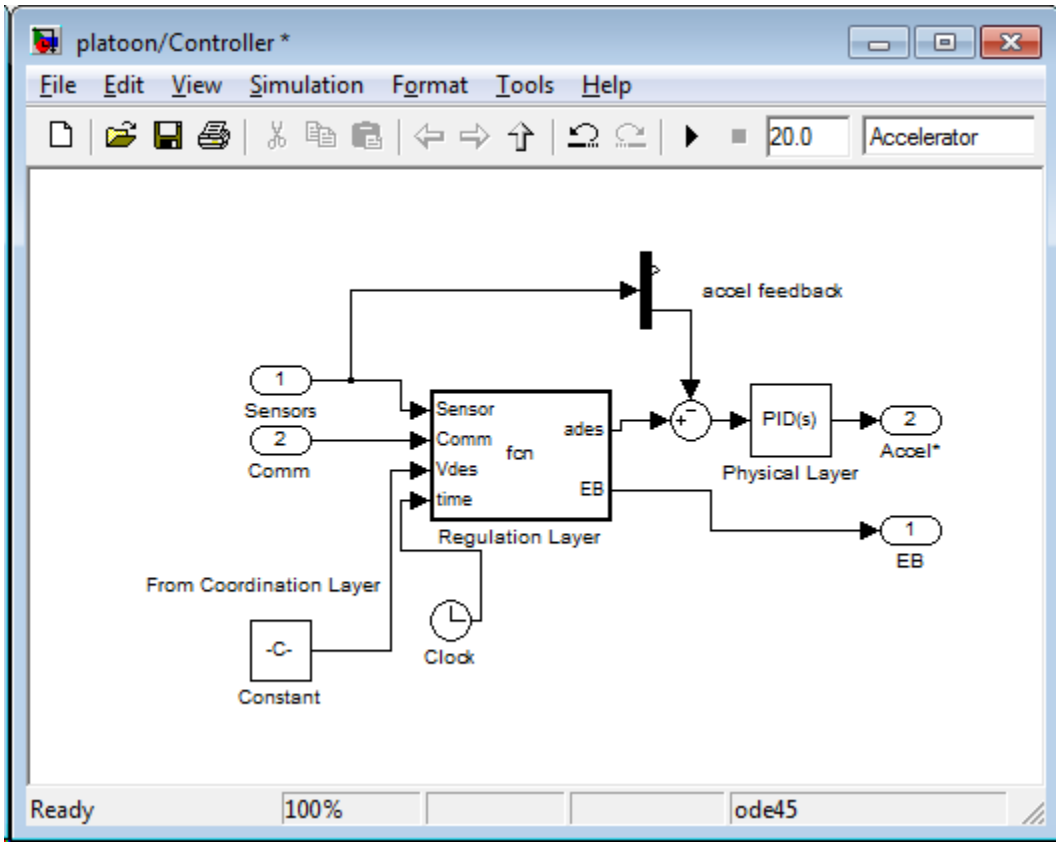

Fig. B.2: Controller subsystem.

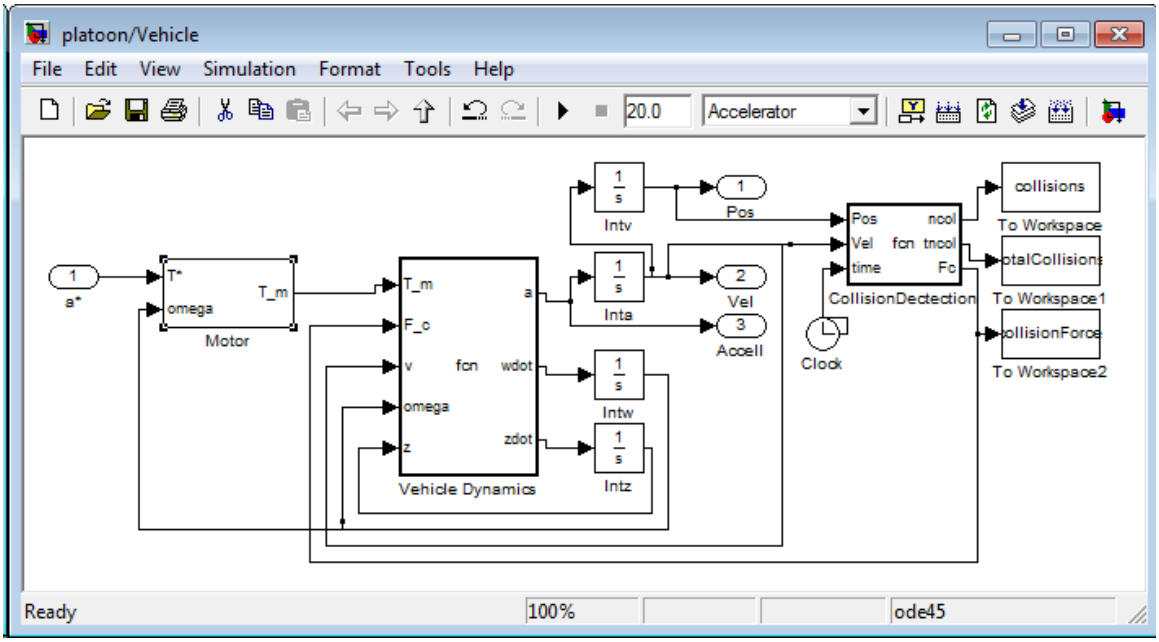

Fig. B.3: Vehicle subsystem.

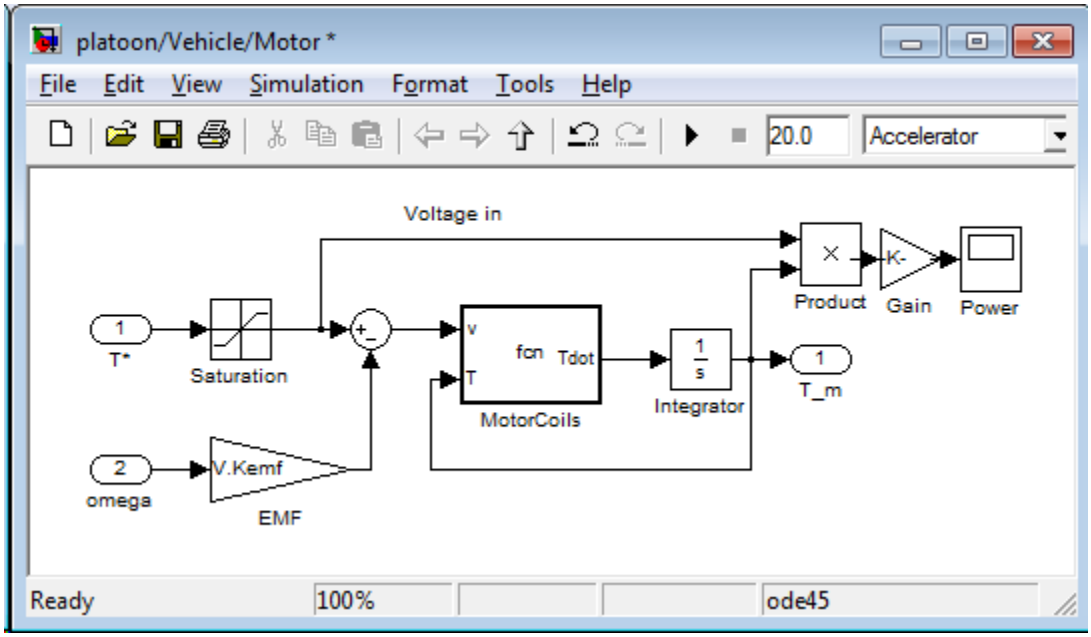

Fig. B.4: Vehicle motor subsubsystem.

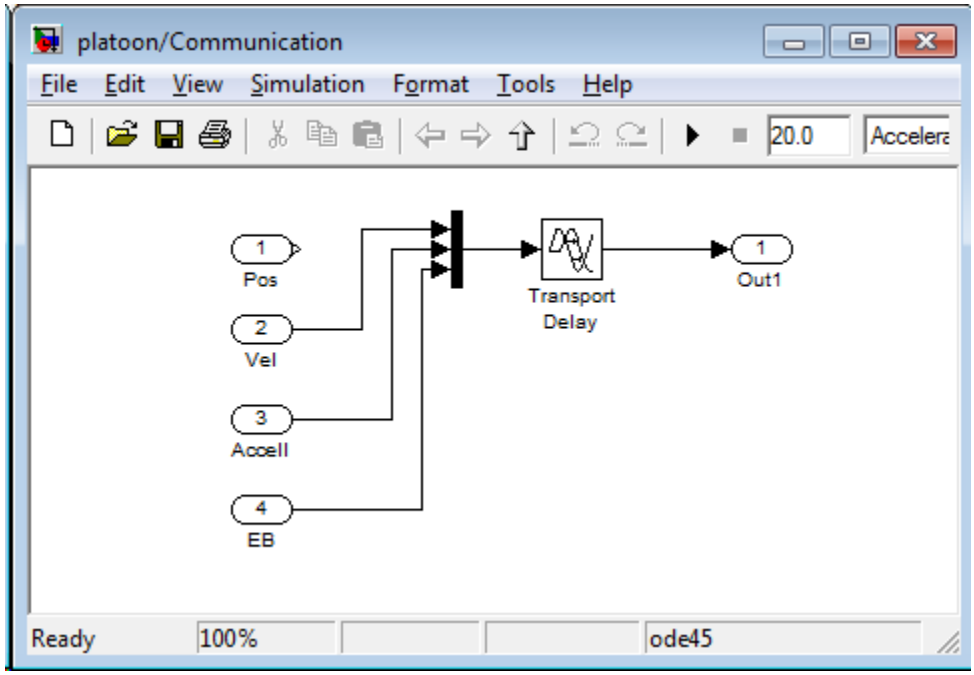

Fig. B.5: Vehicle communication subsystem.

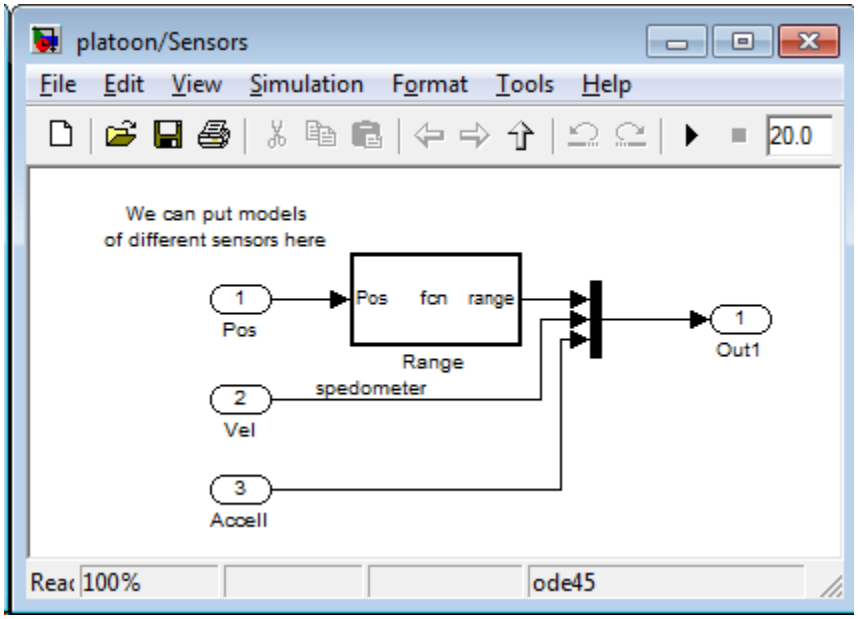

Fig. B.6: Vehicle sensors subsystem.

```
1 function [x,y] = fcn(pos, V)
2 %#eml
3 l = V.l/2;
4 w = V.w/2;
5 x = [pos+l pos+l pos-l pos-l pos+l];
6 y = [w -w -w w w];
```

Range

This sensor merely takes the vehicle positions and calculates the headway such as a laser range finder or ultrasonic sensor might report. Note the commented out code to add some noise to the measurement if desired.

```
1 function range = fcn(Pos, V)
2 %#eml
3
4 %sigma = .5;%st. dev.
5 H = -diff(Pos)-V.l;
6 %first car has no reading
7 range = [inf; H];% + sigma*randn(length(spacing),1)];
```

Regulation Layer

One of the more complicated function blocks, this takes the communicated, sensed, and predetermined data and calculates the desired acceleration for each vehicle. A switch-case function is used to determine which controller is employed during emergencies. Also in this function (at the end) the manner of emergency signal propagation is determined, with the serial type propagation (see Section 4.1.1 for description) commented out.

```
1  function [ades,EB] = fcn(Sensor,Comm, Vdes, time, Desired_Spacing,
       Emergency_accel, teb, Emergency_initiator,ctl)
2  %#eml
3
4  n = length(Sensor)/3;%Number_of_Vehicles;
5  H = Sensor(1:n);
6  vel = Sensor((n+1):2*n);
7  accel = Sensor((2*n+1):end);
8  precvel = Comm(1:(n-1));%preceding vehicle velocity
9  precacc = Comm((n+1):(2*n-1));%preceding vehicle acceleration
10 %EB =  Comm((2*n+1):end);%emergency signal see below
11 lvel = Comm(1);%leader velocity
12 lacc = Comm(n+1);%leader acceleration
13 err = H-Desired_Spacing;
14 errdot = vel-[Vdes; precvel];
15
16 %Rajamani's Controller
17 C1 = .5;%importance of leader info
18 zeta = 1;%dampint (1=critical)
19 wn = 5;%controller BW (small for comfort) (jerk<5m/s^3)
20 lades = -(zeta+sqrt(zeta^2-1))*wn*(vel(1)-Vdes);
21 ad1 = (1-C1).*precacc + C1*lacc...
22       -(2*zeta-C1*(zeta+sqrt(zeta^2-1)))*wn^2.*errdot(2:end)...
23       -(zeta+sqrt(zeta^2-1))*wn*C1.*(vel(2:end)-lvel) + wn^2.*err(2:end);
24 ad = max(-2,min(2,[lades; ad1]));%limit for passenger comfort
25
26 %in emergency
27 elad = Emergency_accel;%leader accel->0 once stopped
```

```
28 switch ctl
29     case 1 %%no change controller
30         ead = [elad; ad1];
31     case 2 %%choi
32         C1 = 0;%importance of leader info
33         zeta = 1;
34         wn = 5;
35         ead1 = (1-C1).*precacc + C1*lacc...
36             -(2*zeta-C1*(zeta+sqrt(zeta^2-1)))*wn^2.*errdot(2:end)...
37             -(zeta+sqrt(zeta^2-1))*wn*C1.*(vel(2:end)-lvel) + wn^2.*err(2:end)
                   ;
38         ead = min(0,[elad; ead1]).*(vel>0);
39     case 3%%preceding accel method
40         ead = [elad; min(0,precacc)].*(vel>0);%emergency desired acceleration
41     case 4%%mycontroller (PAH)
42         ead1 = precacc +err(2:n);
43         ead = min(0,[elad; ead1]).*(vel>0);
44     case 5 %%stay on target method (uncoordinated)
45          ead = [elad; elad+err(2:n)].*(vel>0);%emergency desired acceleration
46
47     otherwise
48         ead = -inf*ones(n,1);
49 end
50
51 EB =  Comm((2*n+1):end);%emergency signal
52 %EB = [EB(1); EB(1:n-1)|EB(2:n)];%1 vehicle at a time serial propagation
53 EB = min(cumsum(EB),1);%all following vehicles at the same time receive signal
54 ades = EB.*ead + (~EB).*ad;%EB vehicles use emergency controller
55 if(time>teb)
56     EB(Emergency_initiator) = 1;%initiator immediately begins braking
57     ades(Emergency_initiator) = elad;%initiator does not follow prec. vehicles
58 end
```

Motor Coils

A simple first order system based on the RC equivalent model of motor coils with the back electro-motive force.

```
function Tdot = fcn(v,T,V)
%#eml
Tdot = (V.Kt*v - V.Rm*T)/V.Lm;
```

Vehicle Dynamics

This function implements all the modeling from Chapter 3.

```
function [a,wdot,zdot] = fcn(T_m,F_c, v,omega,z,V)
%#eml

netFc = [F_c' 0] - [0 F_c'];%collision force is force on rear bumper, front
    bumper force= preceding vehicle rear
%relative velocity
v_r = V.h.*omega - v;
%normal force
F_n = 9.8*V.M';
%LuGre model
g = V.mu_c+(V.mu_st-V.mu_c).*exp(-sqrt(abs(v_r/V.v_s)));
zdot = v_r-V.theta.*V.sigma0.*abs(v_r)./g.*z;
%long. dynamics
F_tr = (V.sigma0.*z +V.sigma1.*zdot + V.sigma2.*v_r).*F_n;
F_adrag = V.c_adrag.*v.^2;
a = (4.*F_tr' -F_adrag' + netFc)./V.M;
%rot. dynamics
wdot = (T_m -V.h.*F_tr -V.B.*omega)./V.J;
```

Collision Detection

More than just detection, this block also calculates the force of collision between vehicles. This is perhaps the most complicated block shown. This is largely due to the requirement of knowing the time of initial impact. Thus persistent variables are used such

that the time of collision (`tci`) is remembered between calls to the function. This function also outputs the two vectors `totalCollisions` and `collisions` which should contain information about the number of impacts that occur between each vehicle and the number of vehicles that had collisions over Δv_{safe}. These outputs are not working correctly at the time of this writing due to switching chatter.

```
1  function [ncol, tncol, Fc] = fcn(Pos, Vel, V, time, dvsafe)
2  %#eml
3  persistent prevuCol prevCol tci totalCollisions collisions;
4  ldv = length(dvsafe);
5  H = -diff(Pos)-V.l;
6  n = length(H);%number of vehicles interactions (#vehicles-1)
7  dv = diff(Vel);
8  if isempty(prevuCol)%initialization
9      prevuCol = zeros(ldv,n);
10     prevCol = zeros(1,n);
11     tci = zeros(1,n);
12     totalCollisions = zeros(ldv,n);
13     collisions = zeros(ldv,n);
14 end
15 col = H<=0;%current collisions
16 %rst = double(~col);%reset collision time
17 tci = tci + (time-tci).*(col'-prevCol.*col');%initial collision time
18 prevCol = double(col');
19 unsafe = zeros(ldv,length(col));%collisions over dvsafe threshold
20 for i = 1:ldv
21     unsafe(i,:) = (dv>dvsafe(i))&col;
22 end
23 totalCollisions = totalCollisions + unsafe-prevuCol.*unsafe;%this shows how
       many collisions each vehicle had
24 collisions = min(1,collisions + unsafe);%this only shows what vehicles had
       unsafe collsions
25 prevuCol = unsafe;
26
27 tp = .07;%s
```

```
28 cd = 95800;%Ns/m^2
29 k = 73000;%N/m
30 tc = time - tci;
31 Fc1= cd.*min(1,tc'./tp).^3.*dv.*-H + k.*-H;
32 Fc = Fc1.*col;%force from each collision (non collisions set to 0)
33 ncol = collisions;
34 tncol = totalCollisions;
```

As has been mentioned in the main text, there is an infrastructure set up here such that much more sophisticated models can be easily implemented, specifically with communication and sensing.

All the blocks here can be configured through Matlab scripting. Comparison to Appendix A shows that this model is significantly more complicated with several times more variables. The variables used for input are shown in Table B.1. The structure `V` helps to organize the parameters that are representing vehicles directly instead of system or platoon characteristics. These parameters can be set to vectors of the same length as the platoon so that each vehicle has a unique value. These can also be set to scalars if homogeneity is desired in the platoon. Examples of both types of assignment are found in the script in Section B.3.

All the Matlab workspace variables in Table B.1 must be assigned for the Simulink model to run properly, so it is recommended to always use a script such as found below.

There are several model outputs, nearly all in the form of workspace structure variables. The vehicle states of acceleration, velocity, and position are output to the structure `VehicleStates`. The collision force between each vehicle is found in the structure `collisonForce`. These are the primary outputs used for the analysis. Another important output is the `VehiclePower` structure which contains in Watts the power used by the motor. The outputs `collisions` and `totalCollisions` are not currently functional.

B.2 Matlab Functions for Analyzing Data From the Full Platoon Model

The Matlab functions that follow are useful for analyzing and visualizing the outputs

Table B.1: Inputs for full platoon Simulink model.

Workspace Variable	Units	Description
V.w	m	width
V.l	l	length
V.M	kg	mass
V.h	m	wheel effective radius
V.J	Kgm^2	wheel moment of inertia
V.B	$\mathrm{Kgm}^2/\mathrm{s}$	rotational damping
V.c_adrag	-	aerodynamic drag coefficient
V.Kemf	Vs/rad	motor back EMF constant
V.Kt	Nm/a	motor torque/amp constant
V.Rm	Ω	motor resistance
V.Lm	H	motor inducance
V.sat	V	battery maximum voltage
V.comDel	s	Communication delay
V.Kp	-	physical layer controller proportional gain
V.Ki	-	physical layer controller integral gain
V.Kd	-	physical layer controller derivative gain
V.theta	-	tire/road condition
V.mu_c	-	Coulomb friction coefficient
V.mu_st	-	static friction coefficient
V.sigma0	$1/\mathrm{m}$	spring factor
V.sigma1	s/m	damping factor
V.sigma2	s/m	viscus friction factor
V.v_s	m/s	Stribeck velocity
V.v0	m/s	initial velocity
V.x0	m	initial position
Desired_Velocity	m/s	platoon desired velocity
Desired_Spacing	m	desired headway
teb	s	time emergency brake initiates
Emergency_initiator	-	index of vehicle that begins emergency signal
Emergency_accel	m/s^2	desired acceleration of platoon in emergency
dvsafe	m/s	acceptable Δv of collision

from the model. Some of the dependencies of these functions are already discussed in Appendix A.

`findDv.m`

This function uses the impact force output of the model to find the time of impact, with which the difference of vehicles' velocities can be easily found. In the event of multiple impacts the first is reported.

```
1  %Spencer Jackson
2  function Dv = findDv(states,forces)
3  [r c] = size(forces);
4  n=c;
5  Dv = zeros(1,n-1);
6  for i=1:n-1
7      indx = crossing(forces(:,i+1),forces(:,1),.001);
8      %for j=1:length(indx)
9      if(indx)
10         Dv(i) = states(indx(1),n+2+i) - states(indx(1),n+1+i);
11     end
12 end
```

`make500.m`

This function is only useful if using the output data in LaTeX plots created by the pgfplots package. Very large data sets are easily generated by this model, and the full resolution plots showed tendencies to exceed the limited memory of TeX. A resolution of about 500 points proved perfectly appropriate for this document, so the outputs were down sampled to approximately this size.

```
1  %Spencer Jackson
2  %this function takes a table and makes it more manageable (500ish points) for
       pgfplots
3  function smalldata =  make500(data)
4  [r c] = size(data);
5  if(r>600)
```

```
6       step = floor(r/500);
7       smalldata = data(1:step:end,:);
8   else
9       smalldata = data;
10  end
```

`makevid.m`

This visualization function can be run after the model to both display a video in the Matlab figure and save each plot created so that they can be made into other format videos using simple video editors available for free on the Internet. The images are numbered and need only be imported in order and set so that each displays for one fifteenth of a second (about 0.07s). It is recommended that a separate directory be used to contain all the files generated as they can number in the hundreds for even short videos.

```
1   %Spencer Jackson
2   %Aug 2012
3   %this function only works after running platoon.mdl
4   function makevid(dir)
5   mkdir(dir);
6   Vstr = ['V = '];
7   VX = evalin('base','Vehicle_X');
8   VY = evalin('base','Vehicle_Y');
9   VV = evalin('base','Vehicle_V');
10  V = evalin('base','V');
11  n = size(VX.signals.values,1)
12  for i=1:n-1
13      Vstr = [Vstr;'V = '];
14  end
15  figure(1);
16  clf;
17  handle = plot([0 0],[-1 2]);
18  texthandle = text(1,1,'.');
19  for t = 1:size(VX.signals.values,3)
20      delete(handle);
```

```
21      delete(texthandle);
22      handle = plot(VX.signals.values(:,:,t)',VY.signals.values(:,:,t)');
23      axis equal;
24      texthandle = text(VX.signals.values(1,3,t),V.w,['V = ' num2str(VV.signals.
            values(1,1,t)',2)]);
25      print('-dpng',[dir '/' num2str(t) '.png']);
26      %pause(.06);%uncomment for in figure movie
27  end
28  end
```

B.3 Matlab Script for Setting Up and Running the Full Platoon Model with Emergency Brake Scenario, and Analyzing the Results

This script runs the Simulink model and generates the data for plots such as shown in Chapter 4. The model is run once for each of the five controllers.

```
1  %Spencer Jackson
2  %July 2012
3
4  %controllers
5  nctl=5;
6  ctlname = cell(nctl,1);
7  ctlname{1} = 'none';
8  ctlname{2} = 'choi';
9  ctlname{3} = 'precacc';
10 ctlname{4} = 'mine';
11 ctlname{5} = 'sot';
12
13 %Vehicle/platoon characteristics
14 Number_of_Vehicles = 5;
15 V.w = 2;%m width
16 V.l = 5;%m length
17 V.M = 1707+80*randn(1,Number_of_Vehicles);%kg mass
18 V.h = .323;%m wheel effective radius
19 V.J = 2.603; %rotational inertia (wheel + motor)
```

```
20 V.B = 1.2257; %rotational damping
21 V.c_adrag = .3693; %aerodynamic drag coeff
22 V.Kemf = .47;%vs/rad Motor back emf gain
23 V.Kt = .49;%nm/a motor torque/amp gain
24 V.Rm = .1;%ohm motor resistance
25 V.Lm = .000022;%h armature inductance
26 V.sat = 250; %v saturation (battery max V)
27 V.comDel = .02;%s communication delay
28
29 %physical layer pid controller gains
30 V.Kp = 1000; %vcontroller
31 V.Ki = 10; %vcontroller
32 V.Kd = 0; %vcontroller
33
34 %tire and road characteristics
35 V.theta = 1; %road condition
36 V.mu_c = .35; %Coulomb friction coeff
37 V.mu_st = .5; %static friction coeff
38 V.sigma0 = 100; %spring factor
39 V.sigma1 = .7; %damping factor
40 V.sigma2 = .011; %viscous fric. factor
41 V.v_s = 10; %Stribeck velocity
42
43 %set points
44 Desired_Velocity = 30;%m/s
45 Desired_Spacing = 1;%m, bumper to bumper dist.
46 teb = 1;%s time of emergency brake start
47 Emergency_initiator = 1;%vehicle # in platoon that starts EBS
48 Emergency_accel = -10;%m/s^2 desired acceleration in EBS
49 dvsafe = [0 2.5 5];%m/s allowable delta V in collision
50
51 %initial conditions: (lead vehicle is index 1);
52 V.v0 = 30*ones(1,Number_of_Vehicles);%m/s
53 %you probably don't need to change anything below this point
54 if(length(V.l)==1)
```

```
55      step = (V.l+1);%1 is initial headway
56      V.x0 = step*Number_of_Vehicles:-step:step;
57  else
58      V.x0 = (Number_of_Vehicles:-1:1) + fliplr(cumsum(fliplr(V.l)));
59  end
60
61  %everything after this is simulation stuff
62  Dv = zeros(nctl,Number_of_Vehicles-1);%closing speed of initial impacts
63  tstop = zeros(1,nctl);%time to stop
64  for(ctl=1:nctl) %ctl selects the controller (1 rajamani, recommended)
65          sim('platoon.mdl');
66          data = [VehicleStates.time squeeze(VehicleStates.signals(1).values
                (1,:,:))' squeeze(VehicleStates.signals(2).values(1,:,:))' squeeze
                (VehicleStates.signals(3).values(1,:,:))'];
67          data2 = [collisionForce.time collisionForce.signals.values];
68          Dv(ctl,:) = findDv(data,data2);
69          tstop(ctl) = max(collisionForce.time);
70          d = make500(data);
71          d2 = make500(data2);
72          s = ['Vstates' ctlname{ctl} '3.tab'];
73          save(s,'d','-ascii');
74          s = ['cf' ctlname{ctl} '3.tab'];
75          save(s,'d2','-ascii');
76  end%skip sim
77  Dv = Dv
78  tstop = tstop
```